

٢٠٠٢/٥/١٥
٢٠٠٢/٥/١٥

BEHAVIOR OF LIGHTWEIGHT CONCRETE-ENCASED COMPOSITE COLUMNS

تتعمد كلية الدراسات العليا
هذه النسخة من الرسالة
التوقيع التاريخ: ٢٠٠٢/٥/١٥

By

Abbas Mohammed Ali Al-Shahari

Supervisor

Professor Bassam Abu Ghazaleh

٢٨
٢
٧
عالية
صفحة
علاء

Submitted in Partial Fulfillment of the Requirements for the
Degree of Doctor of Philosophy in
Civil Engineering

Faculty of Graduate Studies
University of Jordan

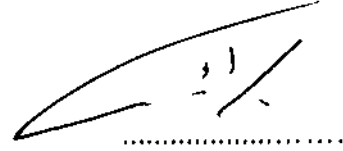
May 2002

This thesis was successfully defended and approved on 5/ 5/ 2002

Examination Committee

Signature

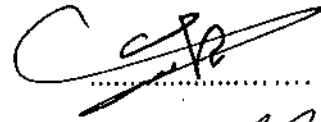
Dr. Bassam Abu Ghazaleh, Chairman
Prof. of Structural Engineering



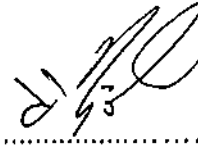
Dr. Samih Qaqish, Member
Prof. of Structural Engineering



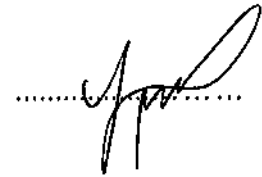
Dr. Yasser Hunaiti, Member
Prof. of Structural Engineering



Dr. Raed Samra, Member
Prof. of Structural Engineering



Dr. Yahia A. Jawad, Member
Assoc. Prof. of Structural Engineering



Dedication

**To my father, my mother, to my wife, my sons
& daughters, to my brothers & sisters
with my sincere love**

Acknowledgement

I would like to express my deepest gratitude and appreciation to my supervisor, chairman of the examination committee Professor Bassam Abu Ghazaleh for his guidance and suggestions throughout this study. Special thanks are due to Professors, Samih Qaqish, Yasser Hunaiti, Raed Samra, and Yahia A. Jawad, members of the examination committee, for reviewing this thesis and for their helpful suggestions.

I would also like to express my deep sorrow over the passing away of my previous advisor, Dr. Adel Tayem, who was a source of inspiration for his students and provided me with excellent suggestions in this work. May god rest his soul in peace, and may his children grow to be the example their father was, Amen.

I wish to thank the Faculty of Engineering & Technology, especially the staff of Civil Engineering Department for their help. Special thanks are due to Mr. Nader Yousif, Mr. Abdel-Hadi Mohammed, and Mr. Daoud Hasan at the welding section for their work in fabricating the column specimens. I also wish to thank Mr. Zohair Shaker and Mr. Mousa Al-Sharief for their help.

I would like to express my appreciation to my sons Ossama and Mohammed, my brother Majed, Eng. Zakria Al-Sharafi, Eng. Mahmoud Abu Abed, Eng. Nabil Falah, Eng. Ahmad Al-Wathaf, Dr. Fuad Balkam, Dr. Shehdeh Ghannam, and Eng. Hani Qa'adan for their valuable assistance in the experimental work.

The financial support of Sana'a University provided to me during my study is also gratefully acknowledged.

Last, but not least, I would like to express my gratitude and sincere appreciation to all members of my family for their endless love, continuous encouragement, sacrifice, and fruitful care.

List of Contents

	<u>Page</u>
Committee Decision	ii
Dedication	iii
Acknowledgement	iv
List of Contents	v
List of Tables	x
List of Figures	xi
Abstract	xv
Notation	xvii
CHAPTER ONE: INTRODUCTION	1
1.1 General	1
1.2 Types of Composite Columns	2
1.2.1 Concrete-encased composite columns	3
1.2.2 Concrete-filled composite columns	4
1.3 Advantages and Disadvantages of Composite Columns	4
1.4 Literature Review	6
1.5 Objectives and Scope of the Research	18
CHAPTER TWO: LIGHTWEIGHT CONCRETE	21
2.1 Introduction.....	21
2.2 History	22
2.3 Use of Lightweight Concrete	25
2.4 Classification of Lightweight Concrete.....	25
2.5 Properties of Lightweight Aggregate Concrete	27
2.5.1 Density	27

	<u>Page</u>
2.5.2 Water absorption	28
2.5.3 Workability	28
2.5.4 Compressive strength	28
2.5.5 Flexural and tensile strength	29
2.5.6 Modulus of elasticity	30
2.5.7 Bond	31
2.5.8 Drying shrinkage	32
2.5.9 Creep	32
2.5.10 Freeze-thaw resistance	32
2.5.11 Thermal expansion	33
2.5.12 Thermal insulation	33
2.5.13 Fire resistance	33
2.5.14 Durability	34
CHAPTER THREE: DESIGN METHODS OF CONCRETE- ENCASED COMPOSITE COLUMNS	35
3.1 Load and Resistance Factor Design Method (LRFD, 1993) .	35
3.1.1 General	35
3.1.2 Design assumptions and limitations	36
3.1.3 Axial design strength of composite columns	39
3.1.4 Flexural design strength of composite columns	41
3.1.5 Axial load and bending	42
3.1.5.1 Calculations of flexural strength, M_u ..	46
3.1.5.2 Moment magnification factors B_1 and B_2	47
3.1.6 Design procedure of composite columns	50
3.1.7 LRFD design tables	51

	<u>Page</u>
3.2 Bridge Code Method (BS 5400: PART 5: 1979)	52
3.2.1 Materials	52
3.2.1.1 Steel	52
3.2.1.2 Concrete	53
3.2.1.3 Reinforcement	53
3.2.2 Analysis of column cross section	53
3.2.2.1 General	53
3.2.2.1.1 Squash load	54
3.2.2.1.2 Concrete contribution factor	55
3.2.2.1.3 Slenderness function	55
3.2.2.2 Axially loaded columns	56
3.2.2.2.1 Short columns	57
3.2.2.2.2 Slender columns	58
3.2.2.3 Columns with end moments	59
3.2.2.3.1 Columns under uniaxial bending	60
3.2.2.3.2 Columns under biaxial bending	64
3.2.2.4 Ultimate moment of resistance	65
3.2.2.4.1 Equations for calculating ultimate moment of resistance	65
 CHAPTER FOUR: EXPERIMENTAL PROGRAM TEST	72
4.1 General	72
4.2 Testing Machine	73
4.3 Test Specimens	75
4.3.1 Column geometry	76
4.3.2 Fabrication of test specimens	79
4.3.3 Orientation of column in test machine	81

	<u>Page</u>
4.3.4 Materials	81
4.3.4.1 Lightweight aggregate concrete and normal concrete	83
4.3.4.2 Structural steel and reinforcing bars	85
4.4 Instrumentation and Experimental Data Acquisition	88
4.4.1 Load measurements	88
4.4.2 Deflection measurements	89
4.4.3 Strain Measurements	90
4.4.3 Observation of cracks and separation	91
4.5 Experimental Procedure	92
 CHAPTER FIVE: TEST RESULTS AND DISCUSSION	94
5.1 Behavior of Column Specimens	94
5.2 Failure Mode of Column Specimens	96
5.3 Load Bearing Capacity	101
5.4 Strains	106
5.5 Deflections	117
5.5.1 Lateral deflections	117
5.5.2 Axial shortening	122
5.6 Moment-Thrust-Curvature Relationship	125
5.7 Separation and Bond	129
5.8 Cracks	130
5.9 Tensile Cracking of Concrete (BS 5400)	131
5.10 Remarks on the Test Results	132
5.10.1 Casting of columns	132
5.10.2 Local spalling of concrete at the column ends	132

	<u>Page</u>
CHAPTER SIX: SUMMARY, CONCLUSIONS, AND RECOMMENDATIONS	134
7.1 Summary	134
7.2 Conclusions	135
7.3 Recommendations	138
REFERENCES	140
APPENDIX A: Illustrative Example.....	149
ABSTRACT IN ARABIC	161

List of Tables

			<u>Page</u>
Table	2.1	Approximate Relations between Strength of Lightweight Aggregate Concrete and Cement Content.	29
Table	3.1	Terms and Specifications Used in the Two Codes of Practice for Composite Columns	70
Table	4.1	Details and Properties of Column Specimens	78
Table	4.2	Material Properties	83
Table	4.3	Details of Concrete Mix	84
Table	4.4	Details of Structural Steel and Reinforcing Bars	86
Table	5.1	Test Results of Columns	102

List of Figures

		<u>Page</u>
Figure 1.1	Concrete-Encased Composite Columns	3
Figure 1.2	Concrete-Filled Composite Columns	3
Figure 2.1	Typical Ranges of Air-Dry Densities of Concrete Made with Various Lightweight Aggregate Concrete ...	27
Figure 3.1	Plastic Stress Distributions	43
Figure 3.2	Beam-Column Interaction Equations	45
Figure 3.3	a. Moment Amplification of a Column that is Braced against Sidesway	46
	b. Column in an Unbraced Frame	46
Figure 3.4	Typical Interaction Graphs for Composite Column	60
Figure 3.5	Force Diagram for Calculating M_u , Plastic Neutral Axis outside the Steel Section /Major Axis Bending ...	66
Figure 3.6	Force Diagram for Calculating M_u , Plastic Neutral Axis within Top Flange/Major Axis Bending	68
Figure 3.7	Force Diagram for Calculation M_u , Plastic Neutral Axis in Web/Major Axis Bending	69
Figure 3.8	Force Diagram for Calculating M_u , Plastic Neutral Axis in Flange/Minor Axis Bending	70
Figure 4.1	General View of the Testing Machine	74
Figure 4.2	Test Specimen Placed in Testing Machine	75
Figure 4.3	Column Geometry and Cross-Section Properties	77
Figure 4.4	End Plates Welding to Column Specimen	80

	<u>Page</u>
Figure 4.5	Fabrication of Test Specimens 81
Figure 4.6	Casting of Column Specimens 82
Figure 4.7	Compression and Tension Test Machine 85
Figure 4.8	Concrete Stress-Strain Curves 86
Figure 4.9	Stub Column Test 88
Figure 4.10	Dial Gauges and LVDTs on Column Specimens 89
Figure 4.11	Electrical Strain Gauges Attached on the Flange Tips of the H Steel Section For Column 16 (a) Before Coating (b) After Coating 90
Figure 4.12	Electrical Strain Gauges Attached on the Flange Center of the H Steel Section for Columns 1-15 (after coating) 91
Figure 4.13	Locations of Electrical Strains Gauges and LVDTs 92
Figure 4.14	Location of the LVDT on Column Specimen 92
Figure 5.1	Failure Mode of Column No. 16 97
Figure 5.2	Failure Mode of Column No. 11 98
Figure 5.3	Failure Mode of Column No. 12 99
Figure 5.4	Failure Mode of Column No. 4 100
Figure 5.5	Strains in Steel and Concrete at Mid-height of Column No. 1 108
Figure 5.6	Strains in Steel and Concrete at Mid-height of Column No. 2 108
Figure 5.7	Strains in Steel at Mid-height of Column No.3 109
Figure 5.8	Strains in Steel and Concrete at Mid-height of Column No. 4 109
Figure 5.9	Strains in Steel and Concrete at Mid-height of Column No. 5 110

	<u>Page</u>
Figure 5.10	Strains in Steel at Mid-height of Column No. 6 110
Figure 5.11	Strains in Steel and Concrete at Mid-height of Column No. 7 111
Figure 5.12	Strains in Steel and Concrete at Mid-height of Column No. 8 111
Figure 5.13	Strains in Steel at Mid-height of Column No.9 112
Figure 5.14	Strains in Steel and Concrete at Mid-height of Column No. 10 112
Figure 5.15	Strains in Steel and Concrete at Mid-height of Column No. 11 113
Figure 5.16	Strains in Steel at Mid-height of Column No. 12 113
Figure 5.17	Strains in Steel and Concrete at Mid-height of Column No.13 114
Figure 5.18	Strains in Steel and Concrete at Mid-height of Column No. 14 114
Figure 5.19	Strains in Steel and Concrete at Mid-height of Column No. 15 115
Figure 5.20	Strains in Steel at Mid-height of Column No. 16 115
Figure 5.21	Mid-Height Strain Distribution Across the Section at Different N/N_u Ratios for Columns 1, 6, And 11 116
Figure 5.22	Load-Lateral Deflection Curves about Major and Minor Axes at Mid-height of Columns 1, 2, and 3 119
Figure 5.23	Load-Lateral Deflection Curves about Major and Minor Axes at Mid-height of Columns 4, 5, and 6 120
Figure 5.24	Load-Lateral Deflection Curves about Major and Minor Axes at Mid-height of Columns 7, 8, and 9 120
Figure 5.25	Load-Lateral Deflection Curves about Major and Minor Axes at Mid-height of Columns 10, 11, and 12 121

	<u>Page</u>
Figure 5.26	Load-Lateral Deflection Curves about Major and Minor Axes at Mid-height of Columns 13, 14, 15, and 16 121
Figure 5.27	Load Versus Axial Shortening of Columns 1, 2, and 3 122
Figure 5.28	Load Versus Axial Shortening of Columns 4, 5, and 6 123
Figure 5.29	Load Versus Axial Shortening of Columns 7, 8, and 9 123
Figure 5.30	Load Versus Axial Shortening of Columns 10, 11, and 12 124
Figure 5.31	Load Versus Axial Shortening of Columns 13, 14, 15, and 16 124
Figure 5.32	Moment-Thrust-Curvature Relationship about Major Axis at Mid-height for Columns 1, 2, and 3 127
Figure 5.33	Moment-Thrust-Curvature Relationship about Major Axis at Mid-height for Columns 4, 5, and 6 127
Figure 5.34	Moment-Thrust-Curvature Relationship about Major Axis at Mid-height for Columns 7, 8, and 9 128
Figure 5.35	Moment-Thrust-Curvature Relationship about Major Axis at Mid-height for Columns 10, 11, and 12..... 128
Figure 5.36	Moment-Thrust-Curvature Relationship about Major Axis at Mid-height for Columns 13, 14, 15, and 16 129
Figure 5.37	Mid-span Region of Column 16, with Part of Concrete Encasement Removed 130
Figure A.1	Column Cross-Section of the Example (Column No. 16) 149

Abstract

Behavior of Lightweight Concrete-Encased Composite Columns

By

Abbas Mohammed Ali Al-Shahari

Supervisor

Professor Bassam Abu Ghazaleh

One of the common patterns of composite columns is the encased steel profile. This system combines the rigidity and formability of reinforced concrete with the strength and speed of construction associated with structural steel to produce an economic structure. Concrete encased composite columns have not received the same level of attention as steel or reinforced concrete columns. Notwithstanding their popularity, only very few experimental studies have been reported on lightweight concrete encased composite columns. Moreover, some codes have special provisions on using lightweight concrete.

An experimental study was conducted to investigate the behavior of eccentric lightweight aggregate concrete encased composite columns. This study aims at verifying the validity of such type of concrete in composite construction and checking the adequacy of the AISC-LRFD and the British Bridge Code BS 5400 Codes in predicting the column strength. To achieve this sixteen full-scale pin ended columns subjected to uniaxial bending about the major axis in symmetrical single curvature were tested to failure. Nine of the columns were encased in lightweight aggregate concrete, three in normal concrete, while four were tested as bare steel columns for comparison

purposes. The effect of slenderness ratio, the eccentricity of the applied load, the concrete compressive strength, and the structural steel ratios on the load carrying capacity and on the column behavior were examined. Emphasis was placed on the load-deflection and moment-thrust-curvature relationships as well as bond characteristics, slippage, failure modes, and cracks in concrete.

The test results have shown that, lightweight concrete encasement significantly enhances the load carrying capacity of the steel sections but its ductility is decreased. Furthermore, lightweight concrete columns of small load eccentricity, reached between 63% and 73% of the load carrying capacity of normal concrete columns, while for large eccentricity, the capacities are almost identical. Moreover, lightweight concrete can provide perfect bond to steel sections up to failure. The structural steel ratio to gross column area has also a significant effect on the load carrying capacity of the composite column. A 2% increase in steel ratio causes an increase in the load carrying capacity that reached 47%. It is also demonstrated that, the design provisions of the present code procedures; LRFD as well as BS 5400 are found to be adequate to predict the strength of lightweight concrete encased composite columns. Column strength predictions using the two methods are on the conservative side and are in reasonable agreement with the test results. Although quality control of lightweight aggregate concrete is somewhat difficult, it is still valuable in certain cases to replace ordinary concrete by lightweight aggregate concrete due to its good performance and distinct advantages.

Notation

The following is a list of the symbols that are used in this thesis.

A_c	area of concrete in cross section;
A_f	area of the top flange of the steel section;
A_g	gross area of the steel section;
A_r	area of longitudinal reinforcement;
A_s	area of the steel shape;
A_w	web area of the encased steel shapes;
b	least dimension of the composite column cross section;
B_1, B_2	factors used in determining M_u for combined bending and axial forces when first order analysis is employed;
b_f	breadth of steel flange of H-section;
c_1, c_2, c_3	numerical coefficients consider the influence of reinforcement, concrete confinement, and creep respectively LRFD;
C_4	constant for columns designed to BS 5400 curves;
c_r	average distance from face of the member to the longitudinal reinforcement;
D	outer diameter of circular hollow steel sections;
d_c	depth of neutral axis of composite column;
d_r	distance between symmetrically placed reinforcing bars measured perpendicular to the axis of bending;
d_s	thickness of concrete core to encased steel section;
E	modulus of elasticity of steel shape (LRFD);
E_c	modulus of elasticity of concrete = $(0.043) w_c^{1.5} \sqrt{f'_c}$, MPa (LRFD);
E_c	modulus of elasticity of concrete = $450 f_{cu}$ (BS 5400);

E_m	modified modulus of elasticity of composite section;
E_r	modulus of elasticity of reinforcement;
e_x	eccentricity of the applied load about the major axis;
e_y	eccentricity of the applied load about the minor axis;
f'_c	concrete cylinder compressive strength;
f_{ck}	characteristic strength of concrete;
F_{cr}	critical stress (LRFD);
f_{cu}	Characteristic 28-day cube compressive strength of concrete;
F_e	Euler stress;
F_{my}	modified yield stress of composite section;
f_{rk}	characteristic strength of reinforcement;
f_{ry}	nominal yield strength of reinforcement;
f_{sk}	characteristic strength of structural steel;
f_y	yield strength of steel shape (BS 5400);
F_y	yield strength of steel shape (LRFD);
F_{yr}	specified minimum yield stress of the longitudinal reinforcing bars, (LRFD);
h	column overall depth;
h_1	width of the composite member perpendicular to the plane of bending;
h_2	width of the composite member parallel to the plane of bending;
I_c	moment of inertia of the uncracked concrete cross-section;
I_r	moment of inertia of the reinforcement;
I_s	moment of inertia of the steel section;
K	effective length factor;

- k_1, k_2, k_3 non-dimensional design coefficients describing the approximate interaction curves (BS 5400);
- k_1 intercept on N/N_u axis;
- k_2 magnitude of N/N_u at $Pe/M_u = 1$;
- k_{20} k_2 for short columns ($L = 0$)
- k_3 maximum deviation of interaction curve from a straight line;
- L unbraced length of the column;
- l_e effective length of the actual column in the plane of bending considered (BS 5400);
- l_E length of the column for which the Euler load equals the squash load;
- M maximum applied moment acting about the appropriate axis, and should not be taken less than $0.03bN_u$;
- M_{lt} required flexural strength in member as a result of lateral translation of the member (LRFD);
- M_n nominal flexural strength determined in accordance with section F1-LRFD;
- M_{nt} required flexural strength in member assuming no translation;
- M_p plastic bending moment;
- M_u ultimate moment of resistance of the column section about the appropriate axis, neglecting the buckling effects (BS 5400);
- M_u required flexural strength determined in accordance with section C1-LRFD;
- M_{ux}, M_{uy} design ultimate moment of resistance about the x and y axes respectively, in the absence of axial load;
- M_{uxe} experimental mid-height moment about the major axis at failure;
- M_{xe} experimental mid-height moment about the major axis;

N_{ax}, N_{ay}	axial failure loads;
N_{BS}	ultimate load predicted by BS 5400;
N_e	experimental failure load;
P_{LRFD}	ultimate load predicted by LRFD;
N_u	squash load;
N_x, N_y	design failure loads of the column under uniaxial bending about the major and the minor axis, respectively;
N_{xy}	design failure load of the column under biaxial bending;
P_{e1}, P_{e2}	elastic Euler buckling load for braced and unbraced frame respectively, kN;
P_n	nominal axial strength of the column, kN, (LRFD);
P_{no}	nominal axial strength of stub column, kN, (LRFD);
P_u	factored axial compressive load;
r	radius of gyration of the steel shapes;
r_m	modified radius of gyration of composite section $r_m = \max. (r, 0.3h_1)$;
t_f	average thickness of the flange of a steel section;
u	experimental mid-height deflection about the major axis;
w_c	unit weight of concrete, kg/m^3 ;
x	subscript relating symbol to strong axis bending;
y	subscript relating symbol to weak axis bending, or the distance from extreme fiber to the neutral axis;
Z	plastic section modulus of the steel section, mm^3 ;
ψ	factor depends on an effective breadth of the steel section (BS 5400);
η	imperfection constant for composite column (BS 5400);

CHAPTER ONE

INTRODUCTION

1.1 General

During the past few decades, several composite columns of different ingredients have been used particularly in the construction of tall buildings. One of the common and popular patterns of such columns is the encased steel profile. This system combines the rigidity and formability of reinforced concrete with the strength and speed of construction associated with structural steel to produce an economic structure (Griffis, 1986). The reason for such sound performance is the mutual resistance of both the concrete and the steel section in the composite columns (Hunaiti, 1993). The concrete used for encasing the structural steel section not only increases its strength and stiffness, but also it acts as fireproofing. In recognition of the practicality of such construction technique, most international codes provide provisions for determining the capacity of such columns (Mirza *et al.* 1996). Moreover, the ductility and energy absorption capacities as well as the high impact resistance were behind the extensive use of such member in seismic zones (Hunaiti, 1994).

Concrete encased composite columns have not received the same level of attention as steel or reinforced concrete columns. Past studies on composite columns have mostly concentrated on short specimens and this

lead to methods for calculating their ultimate loads, which may seriously overestimate the load carrying capacity. In recent years, research on composite columns with steel shapes encased in normal concrete has dealt with the behavior of both short and long columns. Consequently, the physical tests on lightweight concrete seem to be rare in the literature reviewed. On the relevant theoretical level, most of the existing codes provide empirical formulas for assessing the behavior of composite columns subjected to axial and flexural actions. The Load and Resistance Factor Design, LRFD (1993), provides an empirical formula for determining the axial load capacity of concentric composite columns. The formula is based on limiting concrete strain to only 0.0018. It is believed that the concrete strain can easily exceed 0.003 when adequate lateral confinement is provided.

1.2 Types of Composite Columns

A composite column is any concrete column reinforced with steel other than reinforcing bars, and can be regarded as a natural development of the original reinforced concrete column (Furlong, 1988). The choice of the cross-section of the column is restricted in practice by current experience in design and construction. There are two main types of composite columns, namely the concrete-encased steel sections and concrete-filled tubes, examples of which are shown in Figures 1.1 and 1.2 respectively (Shakir-Khalil, 1988).

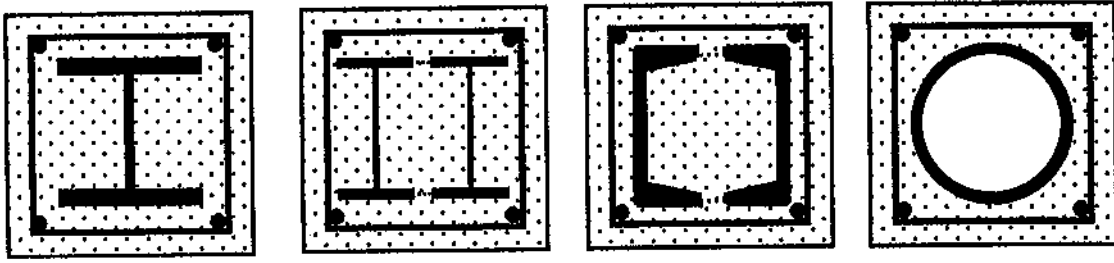


Figure 1.1 Concrete-Encased Composite Columns

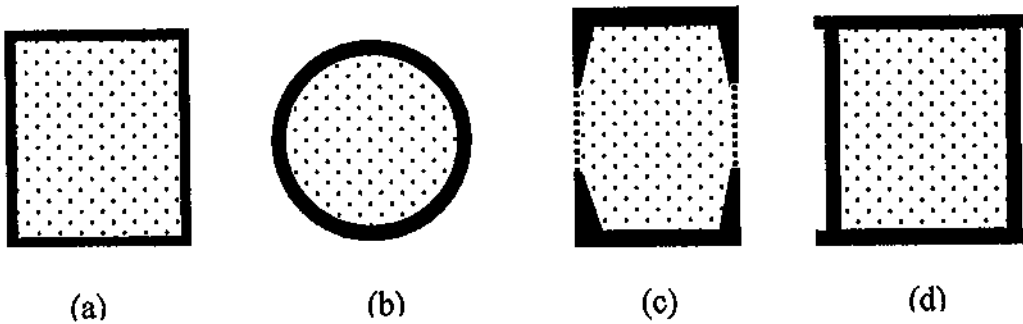


Figure 1.2 Concrete-Filled Composite Columns

1.2.1 Concrete-encased composite columns

One of the common and popular columns is the encased steel profile (Fig. 1.1) where a steel W section is encased in concrete. Some times, structural pipe, tube, or built up section is placed instead of the W section. In addition to supporting a proportion of the load acting on the column, the concrete encasement enhances the behavior of the structural steel core by stiffening it, and so making it more effective against both local and overall buckling. The load-bearing concrete encasement performs the additional function of fireproofing the steel core. The cross sections, which usually are square or rectangular, must have one or more longitudinal bars placed

in each corner and these must be surrounded by lateral ties at frequent vertical intervals in the manner of a reinforced concrete column. Ties are effective in increasing column strength, confinement and ductility. Furthermore, they prevent the longitudinal bars from being displaced during construction and they resist the tendency of these same bars to buckle outward under load, which would cause breaking or spalling of the outer concrete cover at low load levels, especially in the case of eccentrically loaded columns. It will be noted that these ties will be open and U-shaped. Otherwise, they could not be installed, because the steel column shapes will have always been erected at an earlier time.

1.2.2 Concrete-filled composite columns

In this type of composite columns, a steel pipe, steel tubing, or built up section is filled with concrete. Four types of concrete filled composite columns are shown in Figure 1.2, namely rectangular (a), circular (b), battened (c), and box type composite column (d). The most common steel sections used are the hollow rectangular and circular tubes. In the later case, the strength of concrete is enhanced due to being triaxially contained within the circular tube.

1.3 Advantages and Disadvantages of Composite Columns

For quite a few decades, structural steel shapes have been used in combination with plain or reinforced concrete. Originally, the encasing

concrete was used to provide only fire and corrosion protection for the steel, with no consideration given to its strengthening effects. During the last 30 years, however, the development and increasing popularity of composite frame construction has encouraged designers to include the strength of concrete in their calculations. Composite columns may be practically used for low-rise and high-rise buildings.

Composite columns have gained acceptance for high-rise buildings as an alternative to pure reinforced concrete during the past decades (Saw and Liew, 2000). The advantages of using composite columns are:

- 1- This system combines the rigidity and formability of reinforced concrete.
- 2- Smaller cross-section and higher strength-to-weight ratio than a conventional reinforced concrete members.
- 3- Significant savings in material and construction time.
- 4- Inherent ductility, toughness, and energy absorption for use in cases of repeated and reversal loading.
- 5- Enhanced fire resistance characteristics when compared to plain steel.
- 6- Higher load carrying capacity due to the composite action of steel and concrete.
- 7- The concrete can be used to limit global and local buckling problems in the thinner steel elements.

557056

- 8- The steel in tubular and round sections can be used to increase the confinement of the concrete and thus help to maintain its strength in the post-peak region.
- 9- High rigidity for use in lateral-load resisting systems.
- 10- The concrete filled composite columns require no formwork and no reinforcement.

The disadvantages of using composite columns are:

- 1- For concrete encased type, it requires a complete formwork.
- 2- For concrete filled type, the concrete does not provide protection to the steel against fire and corrosion.
- 3- The difficulty of effective connections in the case of concrete filled type.
- 4- The difficulty of controlling their rates and amounts of shortening in relation to shear walls and perhaps adjacent plain steel columns in high-rise buildings.
- 5- Creep in the composite sections can be a problem if composite columns are used around the outside of high-rise buildings and plain steel section are used in the building core.

1.4 Literature Review

Encasing structural steel columns in concrete to increase their resistance became a widespread practice early in the USA, but the

increased column stiffness and strength resulting from encasement was not taken into consideration until much later.

Burr (1912) made the first tests of encased latticed steel section in 1908. He conducted a set of systematic tests of composite columns in Columbia University, New York, and observed that concrete encasement caused a considerable increase in strength. These tests, as well as other early tests on built-up sections, were referred to by Stevens and were summarized by Laredo and Bard. Steven's tests done on relatively short, axially loaded rolled columns, he indicated that the load capacity of an encased column was equal to the sum of strengths of the steel section and the effective concrete section. None of the tests was made on eccentrically loaded columns and this was reflected by in the code provisions (Walter, 1988).

The 1948 edition of British Standard BS449 was the first to recognize the increased column stiffness by permitting an increase in the least radius of gyration for an encased column. The 1959 edition recognized the increased strength of encased columns by permitting the design assumption that the concrete carries load over its entire cross section.

The beginnings of modern research on encased columns may be traced to Stevens (1965), where he summarized the results of tests of axially and eccentrically loaded encased columns made at the Building Research Station. Some of the 35 axially loaded columns were encased in

lightweight concrete. Steven concluded that the behavior of axially loaded encased columns is similar to that of reinforced concrete columns. The type of concrete, whether normal or lightweight, had no effect on the column strength. Twenty-four encased columns were eccentrically loaded in such a way as to cause bending about the minor axis. The behavior and failure modes of these columns were again similar to those observed for reinforced concrete columns. Based on these tests, Stevens suggested formulas and rules for the design of encased columns, and compared his proposed formulas with the procedures prescribed by the British Codes BS 449 for steel and CP 114 for concrete. Additional British tests of encased columns were reported by Jones and Rizk (1963), who investigated the effect of longitudinal and lateral reinforcement in the concrete encasement and the effect of slenderness on the behavior and strength of axially loaded columns. Moreover, Proctor (1967) investigated the possibility of lateral-torsional failure in eccentrically loaded columns. Watanabe in Japan, and Laredo and Brad in France studied the question of bond between the steel section and the encasement and found that bond strength in encased columns is not a problem (Viest, 1974).

Further studies were concerned primarily with analytical developments. Bondale (1966) presented a rigorous treatment of column stability. He compared the load predicted from his analytical solution with the results of tests of 16 encased columns and found good correlation between the experiments and the theory. Basu (1967) at the Imperial

College reported the development of a computer program for calculating the ultimate loads of eccentrically loaded rectangular columns based on classic inelastic column buckling theory. Good agreement was observed between the failure loads predicted by the computer program and the results of tests of encased columns made at the Building Research Station and at the Imperial College. One year later, Basu and Hill (1968) reported the development of a new computer program based on the actual equilibrium shape of the deflected column rather than on the assumed cosine wave shape used in the earlier program. Furthermore, the new program was applicable to columns with unequal end eccentricities. The differences between the loads computed with those two programs were found to be small, and it was concluded that the earlier, simpler program was sufficiently accurate for practical purposes. Another computer program for calculating the ultimate load-carrying capacity of axially and eccentrically loaded columns was developed by Roderick and Rodgers (1969). They compared their solutions with the results of full-size column tests reported by Stevens and small-scale column tests made by Loke at the university of Sydney. Roderick (1972) reported the results of tests of concrete encased columns bent about both principal axes. The theoretical collapse loads were lower than the actual collapse loads for eccentricities of up to 0.8 in. about any centroidal axis.

Furthermore, fundamental research by Basu and Sommerville (1969), and further work by Viridi and Dowling (1973), led to the present design method of composite columns in the new British Standard (BS 5400, 1979). This design method covers both cased-strut and concrete-filled steel tubes, and takes into account uniaxial as well as biaxial bending. Furlong (1974) tabulated both the strength and slenderness properties of A36 steel composite columns, to be available to the design. The tables are for encasement consisting of lightweight concrete with cylinder compressive strength equals 21 MPa ($f'_c = 21$ MPa). A research by Furlong (1978), and Furlong et al (1976) was reviewed by Task Group 20 of the Structural Stability Research Council, chaired by Furlong. This SSRC Task Group Report (SSRC, 1979) recommended design rules of composite column that forms the basis for design of composite columns under LRFD-I2, (Salmon, 1996).

Bridge (1979) developed a theoretical treatment and a computer solution as an extension of the analysis for short-term loading to account for the effects of creep and shrinkage on the behavior of eccentrically loaded composite columns under sustained load using the rate of creep method. He compared the analytical predictions of deformations with values measured from tests and observed that creep deflections were predicted to within 10 %. Even under sustained loads, the function of

transmitting shear between the components of the steel core can be performed by the concrete encasement.

Later on, Johnson and Smith (1980) presented a new design method of composite columns that provides a combination of simplicity and economy. This method was devised and checked against both the Bridge Code and the Cased Strut methods. It consists of 'reduced squash load' expressions of wide applicability to short braced columns, and a general method for columns resisting significant bending moments that is applicable to normal concrete-encased universal column (H) sections. Furthermore, this method gave too conservative results, especially, for columns loaded at large minor-axis eccentricities. Smith (1980) developed design methods for composite columns with lightweight concrete casings as a sequel to a comparison of slenderness effects in reinforced concrete and composite construction. The proposed methods modified both the Bridge Code BS 5400 and the Building Code methods, which are available for the design of composite columns with concrete casings of normal density aggregates, to be adapted to lightweight concrete casing.

Litzner and Crisinel (1981) investigated the effect of residual stresses in steel sections on the carrying capacity of composite columns. The results were compared with that obtained for bare steel columns. Lachance (1982) developed a theory for the non-linear or linear analysis of arbitrary composite sections subjected to biaxial bending. He concluded that the

factor that most influences ultimate biaxial bending strength and curvature is the allowable concrete compressive strain. The shape of concrete stress distribution has little effect on the section behavior. Robert and Yam (1983) reported some recent methods, which are progressively given covering the design of short and slender pin-ended composite steel-concrete columns when subjected to axial load only and to uniaxial and biaxial bending. Simplified design methods are described for the last two cases. Furlong (1983) carried out a comparison between the three different sets of regulations; ACI, Structural Specifications Liaison Committee (SSLC), and LRFD, on the design philosophies of composite columns. Results from the three-design documents highlight some of the differences in design philosophies. Shakir-Khalil (1988) reviewed briefly the recommended procedure for the design of both concrete-encased and concrete-filled composite columns in accordance with British and Europe standards.

Sharif R. (1988) made different lightweight concrete mixes of pozzolan aggregate which is lighter than average limestone concrete by about 25%, but their slump was zero in some mixes although w/c ratio was 0.89. He found that the addition of 10-14% Suweileh sand by volume of aggregates, increased slump, workability, compressive and flexural strengths, as well as unit weight of finished concrete. Sabalieish (1988) studied the feasibility of producing and developing lightweight concrete

from local Jordanian raw materials. He suggested proportions to produce the lightweight concrete. Odeh (1993) studied the behavior of lightweight concrete structure with pumice and perlite. He concluded that there is saving in the total cost of building between 30-35% by using lightweight concrete.

As part of a general investigation of the behavior of composite columns, theoretical and experimental works were carried out at the university of Jordan by Al-Ryalat (1990), Irshedat (1990), Hunaiti (1991), and Hamdan & Hunaiti (1991), to compute the failure loads and bond strength of pin-ended columns under uniaxial bending. In their calculations of failure loads, Newmark's method of numerical integration and the column deflection curve method were used. Bazlamit (1993), Hunaiti (1993), and Hunaiti & Abdel Fattah (1994) investigated experimentally, the load-carrying capacity of partially encased composite columns subjected to eccentric load. They concluded that the behavior of the columns under load proved that the partially encased composite column is a simple and reliable form of composite construction.

Armin, Hongqiang and Fengyang (1991) provided the calculating formulae of encased composite columns, which can be used for structural design by the use of stability theory and the ultimate strength. Mirza and Skrabek conducted a study to simulate the statistical properties of the short-time ultimate strength of short composite beam columns in which $l/r < 22$

(Mirza, 1991) and slender composite beam columns where $l/r > 22$ (Mirza, 1992) in which steel shapes are encased in cast-in-place concrete. The results of this study indicated that: for short columns, the specified concrete strength, the structural steel ratio, and the end eccentricity ratio influence the strength. The end eccentricity ratios of 0.5 or less are critical. While for slender columns the ratio of theoretical strength to nominal strength was influenced most significantly by the slenderness ratio, the structural steel ratio, and the end eccentricity ratio, whereas the effect of specified concrete strength seems to be significant only for beam-columns with a few slenderness ratios ($l/r < 33$). The results also indicated that the effect of structural steel grade and strain hardening of steel could be neglected.

Mirza and Hyttinen (1996) studied the behavior of slender tied composite steel-concrete beam-columns in which steel shapes are encased in concrete and second-order effects are significant from 16 specimens loaded to failure. Loading included combinations of axial and transverse forces producing a wide range of different external eccentricities. They also examined the applicability of American Concrete Institute code (ACI-318, 1999), Eurocode 4 (1992), and nonlinear finite-element modeling procedures for such beam-columns. They observed from the physical tests that for static loads the bonding condition at the interface of steel rib connectors and the surrounding concrete has a small effect on the ultimate strength. The tests also show that the ACI code assumption of maximum

usable strain of 0.003 at concrete extreme fibers near the ultimate load is valid for such beam-columns.

Hunaiti (1997) conducted an experimental study on steel tubes of square and circular sections filled with foamed and lightweight aggregate concrete. He concluded that the foamed concrete contribution to the squash load of composite section is negligible while its contribution to the bending strength is quite significant. On the other hand, the contribution of lightweight aggregate concrete to the squash load and bending capacity is shown to be considerable.

Munoz and Hsu (1997a) reported the experimental test results of four small-scale concrete-encased I-shape steel columns subjected to biaxial bending moments and axial compressive load in single curvature. The analytical and experimental results of biaxially loaded composite columns indicated that the factors that most influence the strength and curvature of a particular composite column are the ultimate compressive strength of concrete and its corresponding maximum compressive strain. The shape of the concrete stress distribution had minor effect on the ultimate strength and the behavior of the columns under study. Munoz and Hsu (1997b) also proposed interaction equation defines a design approach that is based on a continuous mathematical function to present the load-moment interaction diagrams, providing a more accurate representation of the actual behavior of a biaxially loaded composite column. The proposed

design equation satisfies the basic analysis and design parameters of both the ACI and the AISC.

El-Tawil and Deierlein (1999) reviewed and evaluated concrete encased composite column design provisions of the American Concrete Institute Code (ACI), AISC-LRFD specification, and the AISC Seismic Provisions based on fiber section analysis that account for the inelastic behavior of steel and concrete, including the effects of strength and confinement on the concrete's stress-strain properties. They concluded that, the ACI 318 are slightly unconservative, particularly at higher axial loads and for higher-strength concrete ($f'_c=110$ MPa) while the AISC-LRFD provisions are shown to be overly conservative at intermediate to high axial load levels, particularly for columns with small steel sections encased in higher-strength concrete. Moreover, ductility improved significantly, when confinement steel was provided by the transverse hoop reinforcement specified in the AISC-LRFD Seismic Provisions. The presence of a large steel core provides a beneficial residual strength following concrete crushing that leads to improved ductility.

Saw and Liew (2000) presented the design assessment of encased I-sections and concrete-filled composite columns based on the approaches given in Eurocode 4, BS 5400, and AISC-LRFD. They found that, in some cases, results obtained from the above three codes may vary considerably. This is because of the different design considerations adopted in these

codes. For encased composite sections, the axial capacity obtained by LRFD is higher than Eurocode 4 and BS 5400. This may be due to the strut curve used in LRFD, which is above that of Eurocode 4 and BS 5400. In addition, the predicted column strengths using the three design methods are on the conservative side and are in reasonable agreement with the available test results. They recommended the method of Eurocode 4 because it covers a wide scope of the latest research findings influencing the resistance of composite columns. Moreover, the development of M-N interaction curve is direct and this enables hand calculation to be done. Barbero (2000) predicted buckling-mode interaction in composite columns of intermediate length, for which the global and local buckling loads are close. A relationship between column imperfection and the interaction constant is established. Experimental results are presented to support the analysis. Videla and López (2000) developed a general proportioning methodology for structural sand-lightweight concrete (SLC) where an extensive experimental program was carried out, including 47 trial mixtures. The study considers lightweight aggregate concrete as a two-phase material. The first phase, composed of cement, water, and siliceous or calcareous natural sand, is called the resistance phase, and contributes to the structural strength. The second phase is the lightweight phase constituted by coarse lightweight aggregate such as pumice and leca, and is

meant to decrease the concrete density. The concrete strength will depend on strength and proportion of each one of the phases.

Recently, Ghannam (2001) studied experimentally the behavior of lightweight aggregate concrete-filled steel tubular columns subjected to axial load. A comparison between the test results and results predicted by codes, from USA, UK, Australia, Finland, Japan, China, Germany and Belarus as well as Euro code, was carried out. He concluded that the lightweight concrete-filled steel tubular column exhibited much more ductility than the bare steel sections and it is valuable to replace ordinary concrete by lightweight concrete due to its distinct advantages.

In conclusion, it seems that very little experimental research has been conducted on the use of lightweight concrete-encased composite section. In addition, theoretical modeling of this promising constructional material is not available in this regard.

1.5 Objectives and Scope of the Research

Reducing the self-weight of a structure is undoubtedly considered an advantage if not a necessity in some cases. Using lightweight concrete is one way of achieving such reduction. In addition to reducing stresses through the lifetime of the structure, due to using smaller elements, the total weight of materials to be handled during construction is also reduced, which consequently increase productivity. Furthermore, lightweight

concrete offers better thermal insulation and better fire protection than ordinary concrete. The Load and Resistance Factor Design (LRFD, 93) permit using structural lightweight concrete for encasing steel profile, but with a characteristic cylinder compressive strength, f'_c , of not less than 28 MPa. Other codes such as the British Standard code of practice for design of composite bridges (BS 5400, 79) does not permit the use of concrete other than ordinary concrete of a density less than 2300 kg/m^3 with a 28-day cube compressive strength, f_{cu} , of not less 25 MPa for concrete encased sections.

This study is aimed at investigating experimentally the behavior of eccentric lightweight aggregate concrete-encased columns in order to verify the validity of such type of concrete in composite construction and to check the adequacy of the applicable provisions such as the LRFD, and the Bridge Code BS 5400 in predicting the strength of lightweight aggregate concrete-encased composite columns.

The study was carried out on sixteen full-scale pin-ended columns subjected to uniaxial bending about the major axis and axial compressive load in symmetrical single curvature. With the aim of comparison, nine of the columns were encased in lightweight aggregate concrete, three in normal concrete, while four were tested as bare steel columns. Emphasis have been placed on investigating the following parameters:

- 1- Failure modes.

- 2- The load carrying capacity of the specimen.
- 3- The load-deflection relationship.
- 4- Strains in steel and concrete.
- 5- Moment-thrust-curvature relationship.
- 6- Bond characteristics and slippage criterion.
- 7- Crack development in concrete.

Comparisons between experimental and design results obtained by LRFD, and Bridge Code BS 5400 provisions will be conducted.

CHAPTER TWO

LIGHTWEIGHT CONCRETE

2.1 Introduction

The self-weight of concrete elements is high and can represent a large proportion of the total load on a structure, and there are clearly considerable advantages in reducing the density of concrete. The chief of these are the use of smaller cross-sections and the corresponding reduction in the size of foundations. Furthermore, with lighter concrete, the formwork and the total mass of materials to be handled are reduced with a consequent increase in productivity. Concrete which has a lower density also gives better thermal insulation than ordinary concrete. On the other hand, lightweight concrete has higher cement content than normal weight concrete. This represent additional cost, and so does the more expensive lightweight aggregate. A meaningful comparison of cost, however, cannot be limited to the cost of materials but should be made on the basis of the design of the structure using lightweight concrete. The practical range of densities of lightweight concrete is between about 300 and 1850 kg/m³ (Neville, 2000).

Structural lightweight aggregate concrete (SLC) has been used in many applications since the second half of the twentieth century, and has become a very convenient alternative when compared with conventional

concrete. More recently the execution of high-rise buildings and large-span concrete structures has required concrete with higher strength and low weight, and this encourages the use of lightweight concrete, especially for construction in seismic areas (Campione, 2001). Concrete with compressive strength up to 60 MPa and densities under 1900 kg/m^3 have been obtained using artificial lightweight aggregate (Videla, 2000). The SLC may be conceived as a two-phase material: a resistance phase constituted by mortar (cement, water, and siliceous or calcareous natural sand) and a lightweight phase defined by the lightweight coarse aggregate. The concrete strength will depend on strength and proportion of each one of the phases.

This chapter deals with history, use, classifications of lightweight concrete, and some important properties of lightweight aggregate concrete; more details are presented in several references (Neville, 2000), (Videla, 2000), (PCA, 1975), (Short, 1978), and (Spratt, 1974).

2.2 History

One of the earliest uses of reinforced lightweight concrete was in the construction of ships and barges by the Emergency Fleet Building Corporation of World War I. Investigation of various aggregates for this program led to the selection of the type of aggregate developed by Stephen J. Hayde in 1917. Hayde had observed that certain raw shales and clays

would expand into a tough, hard, lightweight aggregate when treated with heat under controlled conditions in a rotary kiln. Eight plants were subsequently licensed under the Hayde patent to produce an expanded shale aggregate called "Haydite."

About the same time, F. J. Straub developed the use of cinders as an aggregate for concrete masonry units. Following World War I, the leading lightweight aggregate was coal cinder, and the major use was in Mr. Straub's "cinder block." In 1923, expanded slag was produced commercially, and it has since been used extensively in the manufacture of concrete masonry units, in precast structural concrete products, and in cast-in-place concrete.

Haydite, together with cinders, pumice, scoria, and expanded slag, was used extensively by the concrete masonry industry and in occasional structural applications. The Park Plaza Hotel in St. Louis, built during the 1920s, is a fine example of the early use of reinforced lightweight concrete.

Early in the 1930s, the San Francisco-Oakland Bay Bridge became a reality, and lightweight concrete for the upper roadway of the double deck structure was one of the keys to its economic feasibility. Structural lightweight aggregate concrete was selected for the deck, which is still in service today with only a minimum of maintenance to the roadway.

In World War II, history repeated it self with construction of concrete ships to conserve steel and, once again expanded shale and clay aggregates

were used.

After World War II, in 1948, the first commercial expanded shale aggregate was developed in eastern Pennsylvania. A coal-bearing shale was used, which produced a highly satisfactory lightweight aggregate in conjunction with the operation of a heating plant.

Shortly after World War II, a National Housing Agency survey of potential lightweight aggregate for home building use was conducted. Attention was directed to the fact that structural concrete could be made from certain types of lightweight aggregate: the rotary kiln expanded shales, clays and slates, the sintered clays and shales, and the expanded slags.

In early 1950s, several structural application of lightweight concrete attracted the interest of the construction industry to the economy of the lightweight concrete. It was used extensively in steel frame buildings for floors and interior walls and was used later in suspension bridges.

These and other structural application stimulated research by several organization in order to develop more information on the properties and potential economics of structural lightweight concrete. As a result of these developments, aggregate plants were built in various parts of the United State and Canada. High-grade, structural lightweight aggregate concrete is now available in most countries (PCA, 1975).

2.3 Use of Lightweight Concrete

Structural lightweight aggregate concrete (SLC) has been used in many applications since the second half of the twentieth century, and has become a very convenient alternative when compared with conventional concrete. Some outstanding projects built with High-strength, structural, lightweight concrete are:

1. The thin-shell roof of the TWA terminal building at Kennedy International Airport, New York.
2. Floor slabs and beams of Marina Towers and Lake Point Tower, Chicago.
3. The Broadmoor Hotel's International Center, Colorado Springs.
4. The Assembly Hall at the University of Illinois, Urbana.
5. One Shell Plaza, Houston.

Lightweight concrete is used in prestressed members, hyperbolic paraboloid roofs, multistory frame, and floor joists designed by either elastic or ultimate-strength methods, long span folded plates or barrel shells, floating docks, barges, bridge decks, and many other projects (PCA, 1975).

2.4 Classification of Lightweight Concrete

The density of concrete can be reduced by replacing some of the solid material in the mix by air voids. There are three possible locations of the air: in the aggregate particles, which are known as *lightweight aggregate*;

in the cement paste; and between the coarse aggregate particles, the fine aggregate being omitted. Accordingly, the resulting concrete being known as:

- a) Lightweight aggregate concrete
- b) Cellular concrete
- c) No-Fines Concrete

Lightweight aggregate concrete is a particular category of lightweight concrete and will be discussed in details in the next section. The practical range of densities of lightweight concrete is between 300 and 1850 kg/m³ (see Fig. 2.1).

ACI 213R-87 used density to categorize concrete according to its application as follow:

- a) ***Structural lightweight concrete*** has a density between 1350 and 1900 kg/m³, this concrete is used for structural purposes, and has minimum compression strength of 17 MPa.
- b) ***Moderate strength concrete*** has compressive strength between 7 and 17 MPa.
- c) ***Low density concrete*** has a density between 300 and 800 kg/m³, this concrete is used for non-structural, mainly for thermal insulation, purposes.

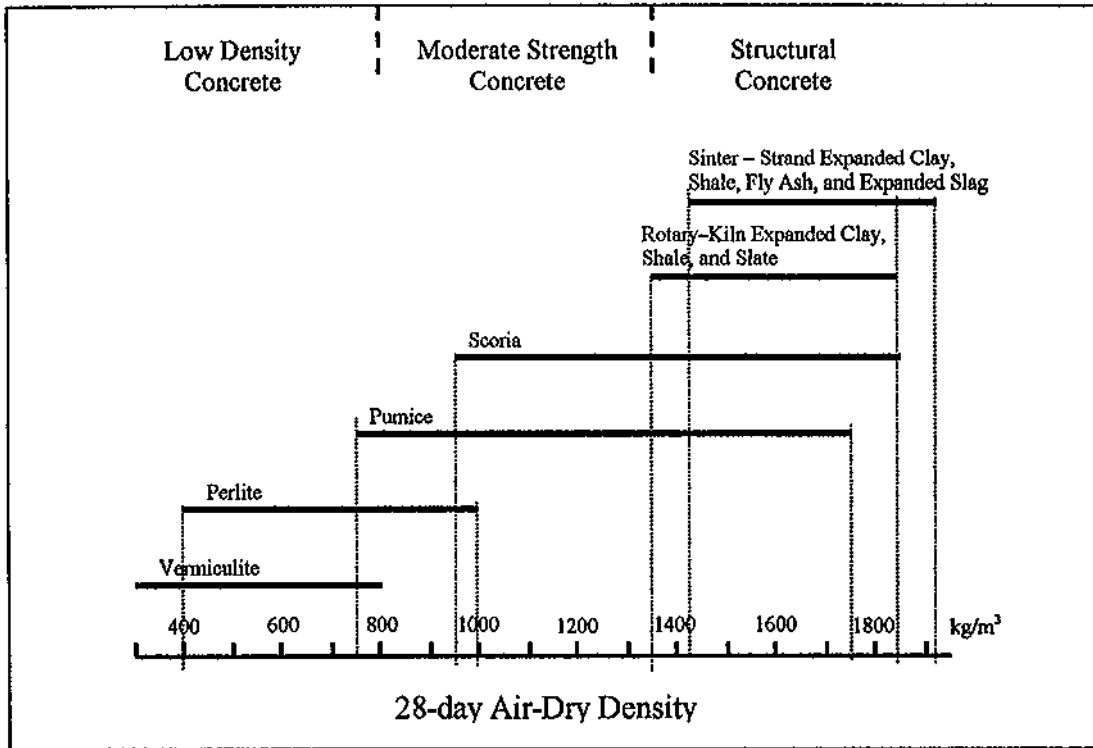


Figure 2.1 Typical Ranges of Air-Dry Densities of Concrete Made with Various Lightweight Aggregate Concrete (ACI 213R-87)

2.5 Properties of Lightweight Aggregate Concrete

Lightweight aggregate concrete has been used successfully for structural purposes for many years. The various physical properties of lightweight aggregate concrete were considered in this section.

2.5.1 Density

It is clear that lightweight aggregate concrete covers an extremely wide field: using appropriate materials and methods, the air-dry density of concrete can be between little over 300 and about 1850 kg/m³ and the corresponding strength range is between 0.3 and 70 MPa, and some times even 90 MPa (Neville, 2000). This wide range of composition is reflected

in various properties of lightweight aggregate concrete. For structural applications of lightweight aggregate concrete, the density of the concrete is often more important than the strength. A decreased density for the same strength level permits a saving in dead load for structural design and foundation. The density depends primarily on the density of the aggregates and their proportions, also influenced by cement, water, and air content.

2.5.2 Water absorption

The majority of lightweight aggregates have a high and rapid absorption; this will cause an increase in concrete density. The absorbed water may represent as much as 25% of aggregates weight but it does not contribute to the mix workability.

2.5.3 Workability

Slump test is a good indication for concrete workability. For equal workability, normal weight concrete has a higher slump than lightweight concrete. In order to improve workability, fine aggregates of ordinary weight are preferred instead of fine lightweight aggregates. Based on the property of high absorption of lightweight aggregate, workability will be quickly reduced if the aggregates used were dry, so it is desirable to use aggregates in a damp condition.

2.5.4 Compressive strength

Lightweight aggregate concrete with 28-day compressive strength of

20 MPa can generally be produced with cement content of 260 to 330 kg/m³; the corresponding range for 40 MPa concrete is 420 to 500 kg/m³, depending on the particular lightweight aggregates being used (Neville, 2000). Certain lightweight aggregates can be used to make concretes with strengths of 48 to 62 MPa, with cement content of 340 to 560 kg/m³. Some values quoted in ACI 213R-87 are shown in Table 2.1, but these are not meant to be more than indicative.

Table 2.1 Approximate Relations between Strength of Lightweight Aggregate Concrete and Cement Content (ACI 213R-87)

Compressive strength of standard cylinders		Cement content			
		With lightweight fine aggregate		With normal weight fine aggregate	
MPa	psi	kg/m ³	lb/yd ³	kg/m ³	lb/yd ³
17	2500	240-300	400-510	240-300	400-510
21	3000	260-330	440-560	250-330	420-560
28	4000	310-390	530-660	290-390	490-660
34	5000	370-450	630-750	360-450	600-750
41	6000	440-500	740-840	420-500	700-840

The limitation on strength of lightweight aggregate concrete imposed by the strength of the coarse aggregate particles can be alleviated by the use of a smaller maximum size of aggregate. Higher compressive strengths require very high cement contents; a strength of 70 MPa may require a cementitious material content of 630 kg/m³.

2.5.5 Flexural and tensile strength

Moist-cured specimens of lightweight and normal-weight concrete of

equal compressive strength have approximately equal flexural and tensile strengths.

In one test series using commercial aggregates, the split-cylinder tensile strength of air-dried lightweight concrete varied from about 70 to 100% of that of normal weight concrete of equal compressive strength (PCA, 1980).

The addition of natural sand fines to the mix will in most cases improve both the compressive and tensile strength as well as workability of lightweight concrete. However, it must be borne in mind that this may be to the detriment of other worthwhile properties of the concrete.

2.5.6 Modulus of elasticity

The modulus of elasticity of lightweight aggregate concrete can be expressed as a function of its density as well as of its compressive strength.

For strength up to 41 MPa, ACI 318-99 express the modulus of elasticity of concrete, E_c , in MPa as:

$$E_c = w_c^{1.5} 0.043 \sqrt{f'_c}$$

where f'_c standard cylinder strength in MPa, and

w_c density of concrete in kg/m^3 .

This expression is meant to be valid for values of density between 1500 and 2500 kg/m^3 but the actual modulus of elasticity may well deviate from the calculated value by up to 20 percent (ACI 213R-87).

As far as lightweight aggregate concrete with a compressive strength in the range of 60 to 100 MPa is concerned, the relation of the modulus of elasticity to the compressive strength seems to be best described by a Norwegian standard expression (Neville, 2000) as:

$$E_c = 9.5 f_c^{0.3} \times \left(\frac{\rho}{2400} \right)^{1.5}$$

where E_c modulus of elasticity in GPa,
 f_c compressive strength of 100 by 200 mm cylinders in MPa, and
 ρ density of concrete in kg/m^3 .

2.5.7 Bond

Bond arises primarily from friction and adhesion between concrete and steel, and from mechanical interlocking in the case of deformed bars. Bond may also be beneficially affected by the shrinkage of concrete relative to the steel.

The strength of the bond between concrete and deformed steel reinforcement is principally a function of the compressive strength of the concrete.

A rise in temperature reduces the bond strength of concrete: at 200-300°C there may be a loss of one-half of the bond strength at room temperature, (Neville, 2000).

2.5.8 Drying shrinkage

Drying shrinkage of lightweight concrete made and cured at normal temperatures is slightly greater than that of normal weight concrete because of the higher water and air contents. The difference in shrinkage is usually less than about 30% and, in some cases, there is little or no difference. High-strength lightweight concrete (48 to 62 MPa) has about the same shrinkage when compared to normal weight concrete.

2.5.9 Creep

As with ordinary dense concrete, lightweight aggregate concrete creeps under sustained loading. The range of creep of lightweight concrete is about the same as the range of creep of normal weight concrete. The average ultimate creep of lightweight concrete, however, is generally slightly greater than that of normal weight concrete. Creep is dependent upon magnitude of stress, strength of concrete, age at loading, time after loading, method of curing, and moisture condition of concrete. When precise knowledge of creep is required, tests should be performed on the concrete in question.

2.5.10 Freeze-thaw resistance

The resistance of lightweight concrete to the action of freezing and thawing is dependent upon the same factors that affect freeze-thaw resistance of normal weight concrete. These factors include: sand fines,

entrained air, water-cement ratio, and moisture condition of the concrete.

2.5.11 Thermal expansion

Few studies have been conducted to investigate the linear thermal expansion coefficients of concrete. Spratt (1974) gives values for lightweight concrete of $7-11 \times 10^{-6}/^{\circ}\text{C}$, depending upon the amount of sand used. Values for dense gravel concrete are $9-13 \times 10^{-6}/^{\circ}\text{C}$ and those for limestone concrete are $6-9 \times 10^{-6}/^{\circ}\text{C}$.

2.5.12 Thermal insulation

Because thermal insulation varies inversely with unit weight, lightweight aggregate concrete has better thermal insulation properties than normal weight concrete.

It should be noted, however, that as the water content of a lightweight aggregate increase and air content decrease, the thermal conductivity increase because heat passes through water 25 times as fast as through stationary air.

2.5.13 Fire resistance

Since most lightweight aggregates are made or processed at a temperature in excess of 1000°C , these aggregates have a high percentage of voids and a low coefficient of thermal expansion, it follows that lightweight concrete has a higher fire resistance than normal concrete.

Lightweight concrete retain much of their strength when heated to high temperature. Some lightweight concrete, when heated to 650°C, retain as much as 85% of their original strength, whereas dense concretes retain only 35% to 75%, depending upon the type of aggregates.

2.5.14 Durability

Because of the relative newness of lightweight aggregates, little information is available on the long-term durability of lightweight concrete. However, a well-compacted high-strength lightweight concrete with low water content will be as durable as an ordinary dense concrete when subjected to natural weathering and atmospheric industrial pollution. Sand fines and entrained air increase durability and thus porous aggregates with high moisture content reduce durability, while, reducing the water-cement ratio results in an improvement in durability.

As an indication of long-term durability in marine conditions, the case of the concrete ship 'Selma' may be quoted. Reinforcement embedded in an expanded shale lightweight concrete was still in excellent condition after some forty years, despite the fact that it had only 10 mm of cover. This is believed to be due to the low water/cement ratio, high cement content and good compaction of the concrete.

CHAPTER THREE
**DESIGN METHODS OF CONCRETE-ENCASED
COMPOSITE COLUMNS**

A large number of design approaches have been proposed for composite columns over the years. Several design codes that address the design of encased-composite columns are now available; these include AISC-LRFD (1993), ACI (1999), Eurocode 4 (1994), and BS 5400 (1979). Each code has its essential characteristics based on the historical background of their own design method.

The design of composite columns by the AISC-LRFD (1993) is based on the work of Furlong (1974) and the statistical studies of the SSRC Task Group 20 (1979). The recommendations given in the BS 5400 were developed by Basu and Somerville (1969) and modified by Viridi and Dowling (1973). Eurocode4 (1994) procedure is based primarily on the work of Roik and Bergman (1989, 1992). The Japanese provisions are based on the work of Wakabayashi (1980).

Load and Resistance Factor Design Code (AISC-LRFD) and Bridge Code (BS 5400) design recommendations for concrete-encased composite columns will be presented in this chapter.

3.1 Load and Resistance Factor Design Method (AISC-LRFD, 1993)

3.1.1 General

Load and Resistance Factor Design (LRFD) specifications were the

- b. Lateral ties must be used: spacing of ties may not be exceeding $2/3$ of least lateral column dimension.
 - c. Area of lateral ties and longitudinal reinforcement each must be at least $0.178 \text{ mm}^2/\text{mm}$ ($0.007 \text{ in}^2/\text{in}$) of bar spacing.
 - d. Clear cover of at least 1.5 in. is required.
3. Concrete strength f'_c :
- a. Normal weight-concrete: 21 MPa (3 ksi) $\leq f'_c \leq 55$ (8 ksi).
 - b. Structural lightweight concrete $f'_c \geq 28 \text{ MPa}$ (4 ksi).
4. Maximum yield stress of steel used in strength computations is 380 MPa (55 ksi) for either structural steel or reinforcing bars. This means that the failure condition for composite cross-section under uniform axial stress is limited to a strain of 0.0018.
5. When the elastic stress distribution is required, strains in steel and concrete shall be assumed directly proportional to the distance from the neutral axis. The stress equals the strain times the modulus of elasticity for steel, E , or modulus of elasticity of concrete, E_c . Maximum stress in steel shall not exceed F_y and the compressive stress in concrete shall not exceed $0.85 f'_c$.
6. Minimum wall thickness, t , for concrete-filled pipe or tubing:
- a. For each face width, b , in rectangular sections: $t \geq b\sqrt{F_y/3E}$
 - b. For outside diameter, D , in circular sections: $t \geq D\sqrt{F_y/8E}$

These provisions are intended to insure that the steel section yields before the concrete crushes or significant local buckling occurs.

3.1.3 Axial design strength of composite columns

The contribution of each component of a composite column to its overall strength is difficult, if not impossible, to determine. One reason for such difficulty is that the amount of flexural concrete cracking varies throughout the height of the column. In addition, the concrete is not nearly homogeneous as is the steel, and the modulus of elasticity of concrete varies with time and under the action of long-term or sustained loads. Moreover, the effective lengths of composite columns in the rigid monolithic structures in which they are frequently used cannot be determined exactly. The contribution of the concrete to the total stiffness of a composite column varies depending on whether it is placed inside a tube or whether it is on the outside of a steel section where its stiffness contribution is less (SSRC, 1979).

It can be seen from the preceding paragraph that it is difficult to develop an exact theoretical formula for the design of composite columns. As a result, a set of empirical formulas are presented in the LRFD specifications for the design of composite columns (McCormac, 1995).

The design axial compressive strength of steel columns is given as:

$$P_u = \phi_c P_n \quad (3.1)$$

where $\phi_c = 0.85$, and $P_n = A_g F_{cr}$. For bare steel columns, the critical stress, F_{cr} , can be determined as follows:

$$\text{If } \lambda_c \leq 1.5 \quad F_{cr} = (0.658^{\lambda_c^2}) F_y \quad (3.2)$$

$$\text{If } \lambda_c \geq 1.5 \quad F_{cr} = \left(\frac{0.877}{\lambda_c^2} \right) F_y \quad (3.3)$$

$$\text{in which} \quad \lambda_c = \sqrt{\frac{F_y}{F_e}} = \frac{KL}{r\pi} \sqrt{\frac{F_y}{E}} \quad (3.4)$$

$$\text{and} \quad F_e = \frac{\pi^2 E}{(KL/r)^2}$$

where

A_g gross area of the steel member.

E modulus of elasticity of steel.

F_{cr} critical stress.

F_e Euler stress.

λ_c the slender parameter.

F_y yield stress of the steel shape, pipe, or tube.

K the effective length factor.

L unbraced length of the column

P_n nominal axial capacity of the column, kN

r radius of gyration of the steel shape, mm

ϕ_c resistance factor for axially loaded composite columns = 0.85

The formulas to be used for composite columns for, critical stress,

F_{cr} are the same as for plain steel column, except that the areas, radii of gyration, yield stress, and moduli of elasticity are modified in an attempt to account for composite behavior (AISC-LRFD, 1993). The modifications made in these formulas are as follows:

1. Replace A_g with A_s :
2. Replace r with the modified radius of gyration r_m :

$$r_m = \max. (r, 0.3h_I)$$

3. Replace F_y with the modified yield stress F_{my} :

$$F_{my} = F_y + c_1 F_{yr} \frac{A_r}{A_s} + c_2 f'_c \frac{A_c}{A_s} \quad (3.5)$$

4. Replace E with the modified modulus E_m :

$$E_m = E + c_3 E_c \frac{A_c}{A_s} \quad (3.6)$$

where

A_c area of concrete in the cross section.

A_r area of longitudinal reinforcing bars.

A_s area of steel section.

E modulus of elasticity of steel.

E_c modulus of elasticity of concrete = $(0.043) w_c^{1.5} \sqrt{f'_c}$, where w_c is the unit weight of concrete in kg/m^3 and f'_c in MPa.

F_y specified minimum yield stress of the steel shape, pipe, or tube.

F_{yr} specified minimum yield stress of the longitudinal reinforcing

bars.

f'_c specified compressive strength of concrete cylinder.

h_l overall thickness of entire composite cross section in the plane of buckling.

r radius of gyration of the steel shape.

c_1, c_2, c_3 numerical coefficients consider the influence of reinforcement, concrete confinement, and creep, respectively.

For concrete-encased shapes $c_1 = 0.7$, $c_2 = 0.6$, and $c_3 = 0.2$. For concrete-filled tubing and pipes $c_1 = 1.0$, $c_2 = 0.85$, and $c_3 = 0.4$ (LRFD, 1993).

3.1.4 Flexural design strength of composite columns

The AISC states that, the nominal beam-column flexural strength, M_n , should be determined from the plastic stress distribution on the composite section. The plastic neutral axis (PNA), can be located by equating the tensile forces on one side of the member to the compression forces on the other side. On the tensile side, there will be reinforcing bars and part of the embedded steel section stressed to their yield stresses. On the compression side, there will be a compression force equal to $0.85 f'_c$ times the area of an equivalent stress block. The equivalent stress block will have a width equal to the column width and a depth equal to β_1 times the distance to the plastic neutral axis. The value of β_1 is provided by the ACI code (ACI 318M, 1999). The nominal flexural strength, M_n , then

equals the sum of the moments of the axial force about PNA. Such method of analysis is time consuming, and only recently has design aids become available for the case of encased sections (SSRC, 1998).

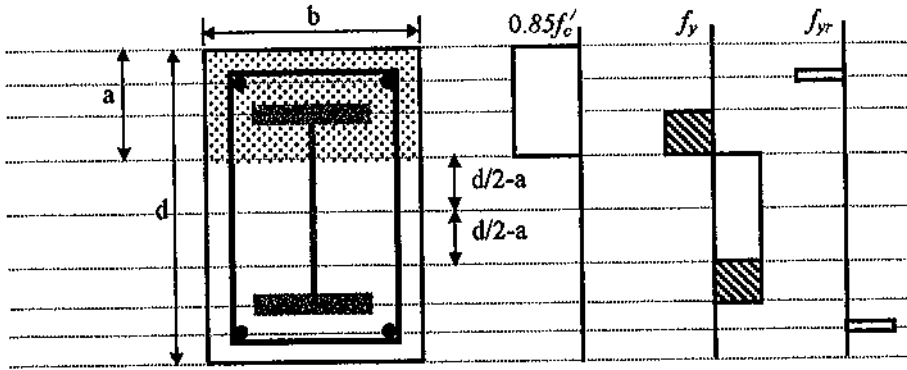


Figure 3.1 Plastic Stress Distributions (SSRC, 1998)

The AISC specifications, in its commentary, also give an approximate formula for the flexural capacity, M_n , at zero axial load as follows:

$$M_n = M_p = ZF_y + \frac{1}{3}(h_2 - 2c_r)A_rF_{yr} + \left(\frac{h_2}{2} - \frac{A_wF_y}{1.7f_c'h_1} \right) A_wF_y \quad (3.7)$$

where

M_p plastic bending moment.

A_w web area of the encased steel shapes ($A_w = 0$ for concrete filled tubes).

Z plastic section modulus of the steel section.

c_r average distance from the face of the member to the longitudinal reinforcement.

h_1 width of the member perpendicular to the plane of bending.

2- For $\frac{P_u}{\phi P_n} < 0.2$

$$\frac{P_u}{2\phi P_n} + \left(\frac{M_{ux}}{\phi_b M_{nx}} + \frac{M_{uy}}{\phi_b M_{ny}} \right) \leq 1.0 \quad (\text{LRFD Eq. H1-1b}) \quad (3.8b)$$

where

P_u factored axial compression load.

P_n nominal compressive strength considering the member as loaded by axial compression in accordance with LRFD-E2.

M_n nominal moment strength determined in accordance with LRFD-F1.

M_u factored bending moment, including second-order effect (LRFD-E2).

x subscript relating symbol to strong axis bending.

y subscript relating symbol to weak axis bending.

ϕ strength reduction factor (resistance factor) for compression members = 0.85, (LRFD-E2).

ϕ_b strength reduction factor (resistance factor) for flexural members = 0.9, (LRFD-H1.2).

These equations and their application together with definitions of design modification factors will be discussed in the following sections. For bending about one axis only, the equations have the form shown in Figure

3.2.

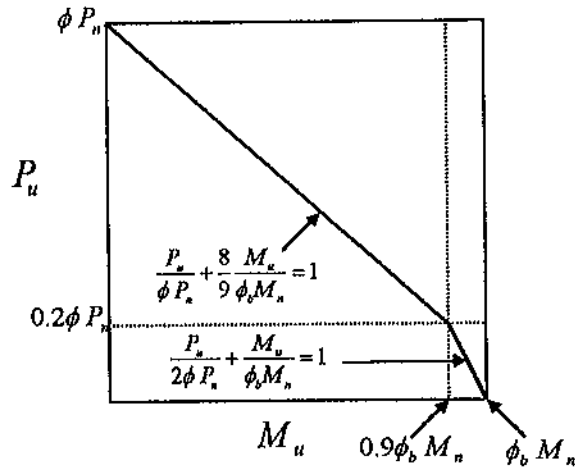


Figure 3.2 Beam-Column Interaction Equations
(LRFD Fig. C-H1.1.)

The same interaction equations are used to determine the adequacy of composite beam-columns except that some of the terms are modified. These modifications are as follows:

1. The Euler elastic buckling loads P_{ex} and P_{ey} that are used in the calculations of the bending factors B_1 and B_2 are to be determined with the following expression in which F_{my} is the modified yield stress that was defined in the previous section.

$$P_e = \frac{A_s F_{my}}{\lambda_e^2} \quad (3.9)$$

2. The resistance factor ϕ_b is to be used as it is in composite beams where it equals 0.85 if $h/t_w \leq 1680 \sqrt{F_y}$ and a plastic stress distribution is used to compute M_n ; or it is taken as 0.9 if $h/t_w > 1680 \sqrt{F_y}$ and M_n determined by superimposing the elastic stresses.

3. The column slenderness parameter, λ_c , is to be modified as it was for determining the design strengths of axially loaded composite columns in the previous section.

3.1.5.1 Calculations of flexural strength, M_u

The column shown in Fig. 3.3a is assumed to be braced against sidesway but it will bend laterally by some amount, δ , as shown and secondary moment, $P_u \delta$, will be produced.

In the LRFD specifications, the moment M_1 is assumed equal to the moment resulting from gravity loads, M_{nt} , plus the moment due to the lateral deflection $P_u \delta$. LRFD provide a factor B_1 to modify the value of M_{nt} .

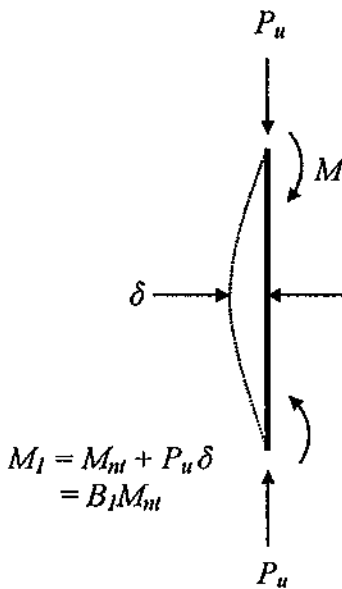


Figure 3.3a Moment Amplification of a Column that is Braced against Sidesway

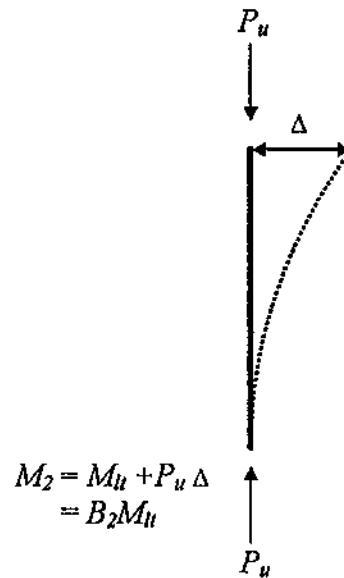


Figure 3.3b Column in an Unbraced Frame

If the frame in Fig. 3.3b is subjected to sidesway, additional secondary moments will be produced. M_2 is assumed by LRFD

specifications equal to the moment due lateral loads, M_{lt} , plus the moment due to $P_u \Delta$. For this case, LRFD provide a factor B_2 to modify the value of M_{lt} .

The total estimated first-order and second-order moment in a member subjected axial compression plus bending can then be determined from the following expression:

$$M_u = B_1 M_{nt} + B_2 M_{lt} \quad (3.10)$$

where

M_{nt} required flexural strength in member assuming no translation.

M_{lt} required flexural strength in member as a result of lateral translation of the member.

3.1.5.2 Moment magnification factors B_1 and B_2

The magnification factors B_1 and B_2 are given in the LRFD. B_1 is used to estimate the $P_u \delta$ effect for columns where the frames are braced against sidesway (McCormac, 1995), while B_2 is used to estimate the $P_u \Delta$ effect in the unbraced frames.

1. Braced Frame

For this nonsway case, LRFD section C1 gives the magnification factor, B_1 , as follows:

$$B_1 = \frac{C_m}{1 - P_u / P_e} \geq 1 \quad (3.11)$$

single curvature and positive for double curvature. Since M_E is the primary moment, then C_m is not a part of the magnification factor.

The braced frame (no translation) beam-column total factored moment is

$$M_u = M_{nt} + \delta P_u = B_1 M_{nt} \quad (3.14)$$

where

M_{nt} is the flexural strength in the member assuming no translation

2. Unbraced Frame

For this sway case, LRFD-C1 gives the magnifier as

$$B_2 = \frac{1}{1 - \sum P_u \frac{\Delta_{oh}}{\sum HL}} \quad (\text{LRFD Eq. C1-4}) \quad (3.15a)$$

or

$$B_2 = \frac{1}{1 - \frac{\sum P_u}{\sum P_{e2}}} \quad (\text{LRFD Eq. C1-5}) \quad (3.15b)$$

The sway frame (no translation) beam-column total factored moment is

$$M_u = M_{lt} + P_u \Delta = B_2 M_{lt} \quad (3.16)$$

where

M_{lt} is the flexural strength in member as a result of lateral translation of the member.

P_{e2} Euler buckling load, K in the plane of bending will be based on the unbraced frame action and will be ≥ 1.0 .

$\sum P_u$ factored axial compression load for all columns on a story subjected to sway.

Δ_{oh} translation deflection (sway deflection) of the story under consideration.

L story height, and

$\sum H$ the sum of all the story horizontal forces producing Δ_{oh} .

From practical standpoint in calculating $\sum P_u$, and $\sum P_e$, it is sufficient to calculate the values for the columns in that one frame or that single line of columns perpendicular to the wind.

3.1.6 Design procedure of composite columns

This section is devoted to the design of composite columns to resist axial loads and moments. The procedure is a trial-and-error one involving the selection of a trial section, the application of the appropriate interaction formula, probably the selection of another trial section, then the application of the formula, and so on until a satisfactory column is obtained. If the first estimate is not too good, the process can involve quite a few trials, For this reason a rough method for estimating sizes is presented below. This method usually will enable the designer to make a fairly good first size estimate and thus reduce the number of trial designs that have to be made.

For this discussion, it is assumed that a composite column is to be designed to support a certain P_u and a certain M_{ux} with M_{uy} equal to zero. It

is further assumed that Equation 3.8a applies to this composite column, this formula becomes

$$\frac{P_u}{\phi P_n} + \frac{8}{9} \frac{M_{ux}}{\phi_b M_{nx}} \leq 1.0 \quad (3.17)$$

The designer may estimate the final values of the two parts of this equation. He may very well assume the two parts are equal, i.e.:

$$\frac{P_u}{\phi P_n} = 0.5 \quad \text{and} \quad \frac{8}{9} \frac{M_{ux}}{\phi_b M_{nx}} = 0.5$$

By computing ϕP_n and $\phi_b M_{nx}$ value, the designer may go to the composite column tables and try a section that has ϕP_n and $\phi_b M_{nx}$ values somewhere in the range of these values. In other words, these values will be a good first trial.

3.1.7 LRFD Design tables

LRFD manual in part 4 presents a series of tables for determining the design axial strength of various square and rectangular encased W shapes as well as for numerous pipes and structural tubes filled with concrete. The tables were prepared for normal weight concrete and include encased W shapes with f_y values of 36 and 50 ksi and f'_c values of 3.5, 5, and 8 ksi. Pipes of steel 36 and 50 ksi filled with 3.5 and 5 ksi concrete are also included together with 46-ksi tubes filled with same concrete. In these tables, the reinforcing bars used for the encased sections are all of grade 60.

3.2 Bridge Code Method (BS 5400: Part 5: 1979)

Clause 11 in part 5 of the British Standard BS 5400 gives a design method for concrete encased steel sections and concrete filled hollow steel sections which takes account of the composite action between the various elements forming the cross section. Bending about the two principal axes of the column is considered separately for each axis. However, a method is given in section 11.3.6-BS 5400 for determining the effect of interaction when bending about both axes occurs simultaneously. Although the British Standard code of practice for the design of composite bridges BS 5400 does not permit the use of concrete other than ordinary concrete of a density less than 2300 kg/m^3 , the design loads for lightweight aggregate concrete encased columns will be estimated by the same formulas of the method.

3.2.1 Materials

3.2.1.1 Steel

In columns formed from concrete encased steel sections the structural steel section should be either:

- a) a rolled steel joist or universal section of grade 43 (275 N/mm^2) or 50 (355 N/mm^2) steel which complies with the requirements of BS 4: Part 1; or
- b) a symmetrical I-section fabricated from grade 43 or 50 steel [11.1.2.1].

The surface of the steel member in contact with concrete filling or encasement should be unpainted and free from deposits of oil, grease and loose scale or rust.

3.2.1.2 Concrete

The concrete should be of normal density (not less than 2300 kg/m^3) with a characteristic 28-day cube strength of not less than 20 N/mm^2 for concrete filled tubes nor less than 25 N/mm^2 for concrete encased sections and a nominal maximum size of aggregate not exceeding 20 mm [11.1.2.2].

3.2.1.3 Reinforcement

For concrete encased columns: stirrups to be placed throughout the length of the column with spacing not to exceed 200 mm. At least four longitudinal bars to be provided [11.3.9]. Steel reinforcement should comply with the relevant clause on strength of materials given in part 4 of BS 5400 [11.1.2.3].

3.2.2 Analysis of column cross section

3.2.2.1 General

For these calculations, the actual column should be replaced by a pinned column of a length equal to the effective length of the actual column in the plane of bending. The x-axis, also called the major axis, should be chosen so that the slenderness function, λ_x , is not greater than λ_y .

3.2.2.1.1 Squash load

The squash load, N_u , is defined as the ultimate short-term axial load for a short column, and is given by:

$$N_u = A_s \frac{f_{sk}}{\gamma_{ms}} + A_r \frac{f_{rk}}{\gamma_{mr}} + A_c \frac{f_{ck}}{\gamma_{mc}} \quad (3.18)$$

where

A_s, A_r, A_c cross sectional areas of structural steel, reinforcement, and concrete, respectively.

f_{sk}, f_{rk}, f_{ck} characteristic strengths of structural steel, reinforcement, and concrete, respectively.

$\gamma_{ms}, \gamma_{mr}, \gamma_{mc}$ material partial safety factors of structural steel, reinforcement, and concrete, taken as 1.1, 1.15, and 1.5, respectively.

The value of f_{ck} in the previous equation is given as:

$$f_{ck} = 0.67 f_{cu} \quad (3.19)$$

where

f_{cu} is the characteristic 28-day cube strength of concrete.

In applying the material partial safety factors, the squash load is given by:

$$N_u = 0.91 A_s f_y + 0.87 A_r f_r + 0.45 A_c f_{cu} \quad (3.20)$$

It should be mentioned that for the purpose of comparison between short-term test results and calculated load-carrying capacities, all material

partial safety factors was taken as unity, whence, the squash load is given by:

$$N_u = A_s f_y + A_r f_{ry} + 0.67 A_c f_{cu} \quad (3.21)$$

3.2.2.1.2 Concrete contribution factor

The method of analysis is restricted to composite cross sections where the concrete contribution factor, α_c , as given below, lies between the following limits:

$$\text{for concrete encased steel sections} \quad 0.15 < \alpha_c < 0.8$$

$$\text{for concrete filled hollow steel sections} \quad 0.10 < \alpha_c < 0.8$$

where

$$\alpha_c = \frac{A_c f_{ck}}{N_u \gamma_{mc}} \quad (3.22)$$

For comparison with the test results ($\gamma_{mc} = 1$ and $f_{ck} = 0.67 f_{cu}$), then

$$\alpha_c = \frac{0.67 A_c f_{cu}}{N_u} \quad (3.23)$$

where

A_c the area of concrete in the section.

f_{cu} the characteristic cube strength of concrete.

N_u the squash load.

3.2.2.1.3 Slenderness function

In general, the slenderness function, λ , is given by:

$$\lambda = \frac{l_e}{l_E} \quad (3.24)$$

The length of the column for which the Euler load equals the squash load, l_E , is calculated as:

$$l_E = \pi \sqrt{\frac{E_c I_c + E_s I_s + E_r I_r}{N_u}} \quad (3.25)$$

where:

l_e the effective length of the actual column in the plane of bending considered.

E_c the modulus of elasticity of concrete = $450f_{cu}$, where f_{cu} is the characteristic cube strength of concrete. However, the unfactored value of $E_c = 670 f_{cu}$, as recommended by BS 5400 (Saw and Liew, 2000), was taken for comparison with test results.

E_s, E_r modulus of elasticity for the structural steel and reinforcement, respectively.

I_c, I_s, I_r the second moments of area of the uncracked concrete cross-section, the steel section, and reinforcement, respectively.

N_u the squash load.

3.2.2.2 Axially loaded columns

In an axially loaded column, failure occurs by buckling about the minor axis due to initial imperfections in straightness of the steel member. In practice, end moments due solely to the load acting at an eccentricity may

arise from construction tolerance. The design methods given in [11.3.2.1] to [11.3.7] of BS 5400 for axially loaded columns therefore include an allowance for an eccentricity about the minor axis not exceeding 0.03 times the least lateral dimension of the composite column.

3.2.2.2.1 Short columns

Where both the ratios L_x/h and L_y/b do not exceed 12, the axial load at the ultimate limit states, N , should not exceed the axial load at failure, N_{ay} , given by:

$$N_{ay} = 0.85k_{ly} N_u \quad (3.26)$$

where

k_{ly} is a constant, which depends mainly on the slenderness ratio of the column and will be determined below using the parameters appropriate to the minor axis of bending.

N_u is the squash load, obtained from 11.1.4 or 11.3.7 of BS 5400.

h, b are the greatest and least lateral dimensions of concrete in the cross section of the composite column.

The factor 0.85 is a reduction factor to allow for the moments due to construction tolerances.

▪ Calculations of k_l

The factor, $k_l < 1$ can be determined from Tables 13.1 to 13.3-BS 5400: Part 5, depending on the value of slenderness ratio, λ . Alternatively, values

of k_l may be calculated from the following equations:

$$k_l = \frac{1}{2} \left[1 + \frac{(1+\eta)}{\lambda^2} \right] - \sqrt{\frac{1}{4} \left[1 + \frac{(1+\eta)}{\lambda^2} \right]^2 - \frac{1}{\lambda^2}} \quad (3.27)$$

where the imperfection constant η is given by:

$$\eta = \psi \lambda_E (\lambda - 0.2) \leq 0 \quad (3.28)$$

in which, λ_E , is Euler slenderness function and is given by:

$$\lambda_E = \pi \sqrt{\frac{1.1E_s}{f_y}} \quad (3.29)$$

while ψ is a factor depends on an effective breadth of the steel section.

$\psi = 0.0035$ for rolled H (UC etc.) flanges up to 40 mm

where axis of buckling is x-x according to Table 14, BS

5400 part 5.

3.2.2.2.2 Slender columns

Where either of the ratios L_x/h and L_y/b exceed 12, account should be taken of the eccentricity due to construction tolerances by considering the column in uniaxial bending about the minor axis. The load acting on the column, N , should not be greater than the design failure load, N_y , with the moment acting about minor axis, M_y , taken as the moment produced by the applied load, N , acting at eccentricity of $0.03b$ (b is the least dimension of the composite column cross section), i.e.:

$$N < N_y \quad \text{and} \quad M_y = 0.03b N \quad (3.30)$$

3.2.2.3 Columns with end moments

When the column is subjected to axial load and end moments, the squash load, as obtained previously (under axial load), has to be further reduced. The ultimate load-carrying capacity of such column is given by:

$$N = k N_u \quad (3.31)$$

where

- k reduction factor which depend on k_1 for an axially loaded column, the concrete contribution factor, the material and sectional properties, and on the shape and ratios of the bending moment distribution.

The behavior of the column with end moments can be given by an interaction curve showing the reduction in the ultimate load with increasing moment. An approximation to this curve can be obtained by ignoring the buckling effects (assuming short column; zero length) and considering fully plastic sections for different arbitrary positions of the neutral axis. The values of the moment and axial compression calculated from the stress blocks will give the points to construct the curve.

Considering the same column with a specified length and proportion of end moment, the actual column curve, shown in Figure 3.4, can be obtained by inelastic analysis Basu (1967, 1968). Basu and Sommerville (1969) studied about 100 such interaction curves and suggested the use of an approximate parabolic curve.

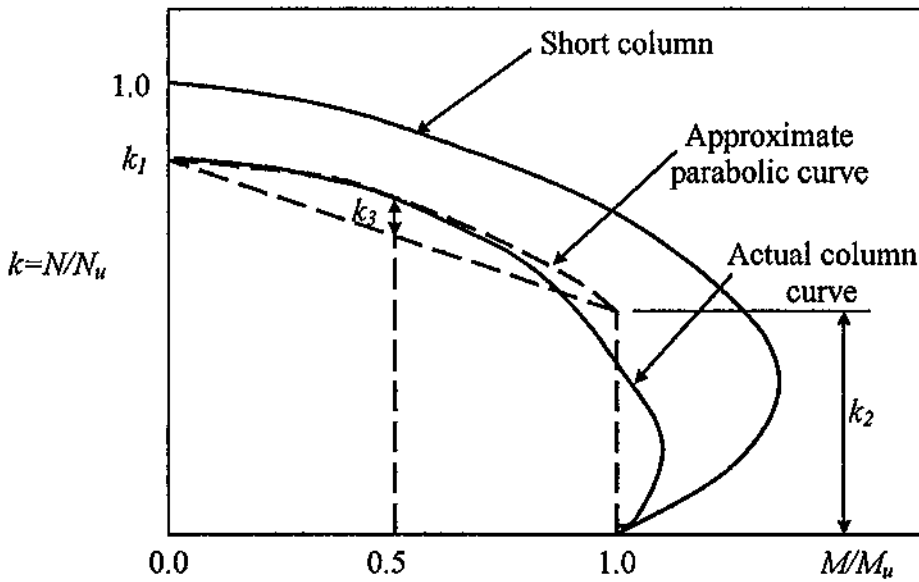


Figure 3.4 Typical Interaction Graphs for Composite Columns (Yam, 1981)

The approximation of the actual curve in Fig. 3.4 is the one used in the design by the Bridge Code Method.

3.2.2.3.1 Columns under uniaxial bending

The ultimate load-carrying capacity of a column under uniaxial bending about the appropriate axis is given by:

$$N = N_u \left[k_1 - (k_1 - k_2 - 4k_3) \frac{M}{M_u} - 4k_3 \left(\frac{M}{M_u} \right)^2 \right] \quad (3.32)$$

where

k_1 as for axially loaded columns

k_2, k_3 as determined below

M the maximum applied moment acting about the appropriate axis, and should not be taken less than $0.03bN$, where b is the

least lateral dimension of the column

M_u the ultimate moment of resistance of the column section about the appropriate axis, neglecting the buckling effects.

▪ **Calculation of k_2**

The values of the coefficient, k_2 , about the appropriate axis for concrete encased steel sections and concrete filled rectangular tubes are determined as follows:

$$k_2 = k_{20} \left[\frac{90 - 25(2\beta - 1)(1.8 - \alpha_c) - C_4 \lambda}{30(2.5 - \beta)} \right] \quad (3.33)$$

where

- β The ratio of the smaller to larger end moments acting about the appropriate axis, and being positive for single curvature bending
- λ, α_c As defined in the previous sections
- C_4 a constant taken from BS 5400 : Part 5: C.2 as:
- 100 for columns designed to curve "a" for I and H rolled sections where $h/b \geq 1.2$ and buckling about $x-x$ axis.
- 120 for columns designed to curve "b" for I and H rolled sections where $h/b \leq 1.2$ and buckling about $x-x$ axis, or $h/b \geq 1.2$ and buckling about $y-y$ axis.
- 140 for columns designed to curve "c" for I and H rolled

sections where $h/b \leq 1.2$ and buckling about y - y axis.

in which

$$k_{20} = 0.9 \alpha_c^2 + 0.2 \quad (3.34)$$

The value of k_2 should lie between the following limits:

$$0 \leq k_2 \leq k_{20}$$

and $k_{20} \leq 0.75$

and if k_2 is negative, it should be taken as zero.

▪ Calculations of k_3

The values of coefficient k_3 for concrete encased steel sections and concrete filled rectangular tubes are determined as follows:

For major axis bending:

$$k_{3x} = 0 \quad (3.35)$$

For minor axis bending:

$$k_{3y} = 0.425 - 0.075 \beta_y - 0.005 C_4 \lambda_y \quad (3.36)$$

and should be taken between the limits:

$$(0.2 - 0.25 \alpha_c) \geq k_{3y} \geq -0.83 (1 + \beta_y) \quad (3.37)$$

As the maximum applied moment, M , about the appropriate axis should not exceed the ultimate moment of resistance of the section, M_u , about the same axis, Equation 3.32 is only valid if:

$$\frac{1}{k_2} \geq \frac{N_u \cdot e}{M_u}$$

If the above condition is not satisfied, Equation (3.32) becomes

$$N = \frac{M_u}{e} \quad (3.38)$$

where

e the eccentricity of the applied load about the appropriate axis.

For columns subjected to uniaxial bending about the major axis and not restrained against failure about the minor axis, the ultimate load-carrying capacity should be taken as equal to that of a column subjected to biaxial bending with the minimum applied moment about the minor axis, i.e.:

$$M_y = 0.03 b N \quad (3.39)$$

For calculating the ultimate load, N , for an individual case, equation (3.32) (in which $M=N.e$) cannot be used as presented and should be solved for N . The solution of Equation (3.32) for the case of *minor axis bending* is given by:

$$N_y = \frac{-k_4 + \sqrt{k_4^2 + 16k_{1y}k_{3y}(N_u \cdot e_y / M_{uy})^2}}{8k_{3y}(N_u \cdot e_y / M_{uy})^2} N_u \quad (3.40)$$

in which

$$k_4 = 1 + (k_{1y} - k_{2y} - 4k_{3y})(N_u \cdot e_y / M_{uy}) \quad (3.41)$$

where

e_y is the eccentricity about the minor axis, and

N_{ux} , M_{uy} as defined previously.

and in major axis bending is given by:

$$N_x = \frac{k_{lx} N_u}{[1 + (k_{lx} - k_{2x})(N_u \cdot e_x / M_{ux})]} \quad (3.42)$$

where

e_x is the eccentricity about the major axis.

3.2.2.3.2 Columns Under Biaxial Bending

For columns failing in biaxial bending, design conditions should be satisfied by taking the ultimate load-carrying capacity as:

$$\frac{1}{N_{xy}} = \frac{1}{N_x} + \frac{1}{N_y} - \frac{1}{N_{ax}} \quad (3.43)$$

where

N_x, N_y , the ultimate load-carrying capacities of the column under uniaxial bending about the major and the minor axis, respectively, as calculated in previous sections, and

$$N_{ax} = k_{lx} N_u$$

k_{lx} the k_l coefficient with parameters appropriate to the major axis.

It should be noted that, the maximum compressive strength of concrete is taken as $0.67 f_{cu}$ (instead of $0.45 f_{cu}$) for evaluating the squash load and $0.60 f_{cu}$ (instead of $0.4 f_{cu}$) for evaluating the ultimate moment as recommended by (Saw and Liew, 2000).

3.2.2.4 Ultimate moment of resistance

The ultimate moment of resistance, M_u , in pure bending of the composite column section is determined by considering equilibrium across a fully plastic section. Calculations of the equilibrium condition are based on the standard practice of assuming rectangular stress blocks in both the steel and the concrete in which the concrete tension is ignored.

In taking account of the longitudinal reinforcement, the following assumptions can usually be made to avoid tedious trial and error procedure in finding the position of the neutral axis:

- a) The amount of reinforcement is small, and the areas in tension and in compression are equal.
- b) The design yield stress of the reinforcement in compression is assumed to be the same as in tension.
- c) The area of concrete in compression is not reduced to allow for the area occupied by steel in compression.

For major axis bending of an encased H-section, the neutral axis may be above or within the compression flange, or in the web. In practice, it is almost always in the web, as shown in Fig. 3.7.

3.2.2.4.1 Equations for calculating ultimate moment of resistance

The ultimate moment of resistance, M_u , may be calculated from the equations given in the following sections. In calculating M_u , the ratio of the

concrete strength to the steel strength, ρ , will be introduced as follows:

$$\rho = \frac{0.4 f_{cu}}{0.91 f_y} \quad (3.44)$$

where

ρ is the ratio of the average compressive stress in the concrete at failure to the design yield strength of the steel taken as $0.4 f_{cu}/0.91 f_y$.

f_{cu} is the characteristic 28-day cube strength of concrete.

f_y is the nominal yield strength of steel.

Case I. Plastic neutral axis outside the steel section

This condition (Fig. 3.5) arises when:

$$\rho b d_s \geq A_s \text{ then}$$

$$d_c = \frac{A_s}{b \rho} \text{ and} \quad (3.45)$$

$$M_{ux} = 0.91 f_y A_s \frac{(h - d_c)}{2} + 0.87 f_{ry} \frac{A_r}{2} d_r \quad (3.46)$$

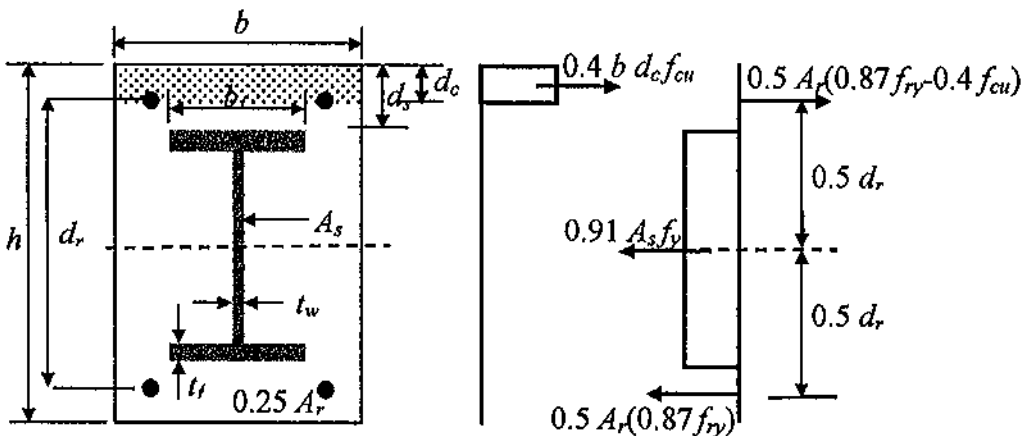


Figure 3.5 Force Diagram for Calculating M_u , Plastic Neutral Axis outside the Steel Section /Major Axis Bending

$$M_{wy} = 0.91 f_y A_s \left(\frac{b - d_c}{2} \right) + 0.87 f_y \frac{A_r}{2} d_r \quad (3.47)$$

where

- b breadth of concrete in cross section
- d_s thickness of concrete core to encased steel section
- A_s area of rolled or fabricated steel section
- d_c distance of neutral axis from the most compressed face of concrete
- M_{ux}, M_{uy} design ultimate moment of resistance about the x and y axes respectively, in the absence of axial load
- h depth of concrete cross section
- f_y characteristics yield strength of reinforcement
- A_r area of reinforcement in the cross section
- d_r distance between symmetrically placed reinforcing bars measured perpendicular to the axis of bending

Case II. Plastic neutral axis within top flange/major axis bending

This condition (Fig. 3.6) arises when:

$$\rho b d_s < A_s \text{ and}$$

$$0.91 A_s f_y \leq 0.4 f_{cu} [b d_s + t_f (b - b_f)] + 1.82 A_r f_y \quad \text{then}$$

$$d_c = \frac{A_s + 2 b_f d_s}{b \rho + 2 b_f} \quad \text{and} \quad (3.48)$$

$$M_u = 0.91 f_y \left[A_s \frac{(h - d_c)}{2} - b_f d_s (d_c - d_s) \right] + 0.87 f_{ry} \frac{A_r}{2} d_r \quad (3.49)$$

where

A_f area of the top flange of the steel section

t_f average thickness of the flange of a steel section

b_f breadth of steel flange of I-section of the external dimension of a rectangular hollow section.

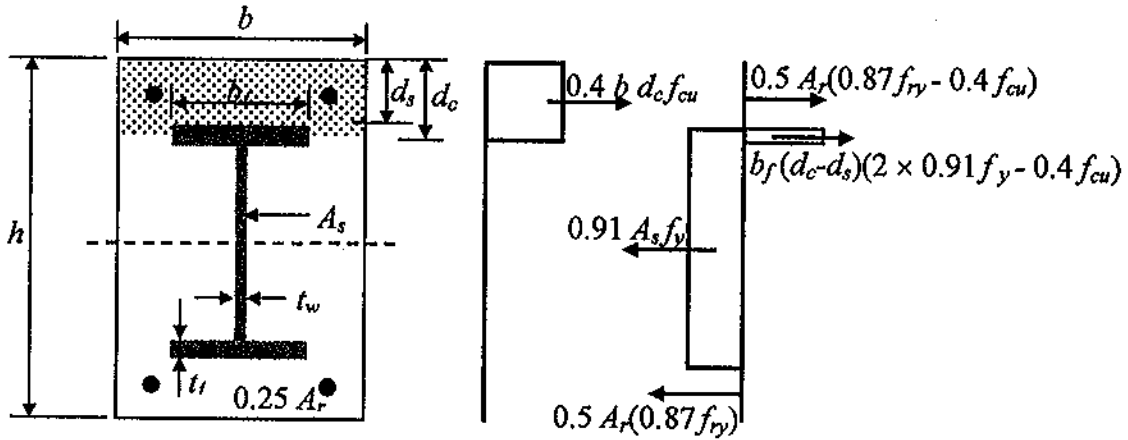


Figure 3.6 Force Diagram for Calculating M_u , Plastic Neutral Axis within Top Flange/Major Axis Bending

Case III. Plastic neutral axis in web/major axis bending

It is convenient to split up the stress block for the H-section, and here A_f is the area of one flange and $d_w t_w$ the area of web in compression (Fig. 3.7). The depth of the neutral axis, y , is most simply obtained by noting that the compressive force in the concrete is equal to the tensile force in the area $(h - 2d_c)t_w$ of web, since other longitudinal forces cancel out. Thus:

$$0.4 b d_c f_{cu} = 0.91 t_w f_y (h - 2d_c) \quad (3.50)$$

whence, the plastic neutral axis will be:

$$d_c = \frac{ht_w}{(b\rho + 2t_w)} \quad (3.51)$$

provided that: $(A_s - 2b_f t_f) > \rho [bd_s + t_f(b - b_f)]$ and $d_c \geq d_s + t_f$

Taking moments about the line of action of the force in the concrete, leads to:

$$M_u = 0.91f_y \left[A_s \frac{(h - d_c)}{2} - b_f t_f (d_s - d_w) - t_w d_w (d_c - d_w) \right] + 0.87f_{ry} \frac{A_r}{2} d_r \quad (3.52)$$

where the symbols are shown in Fig. 3.7.

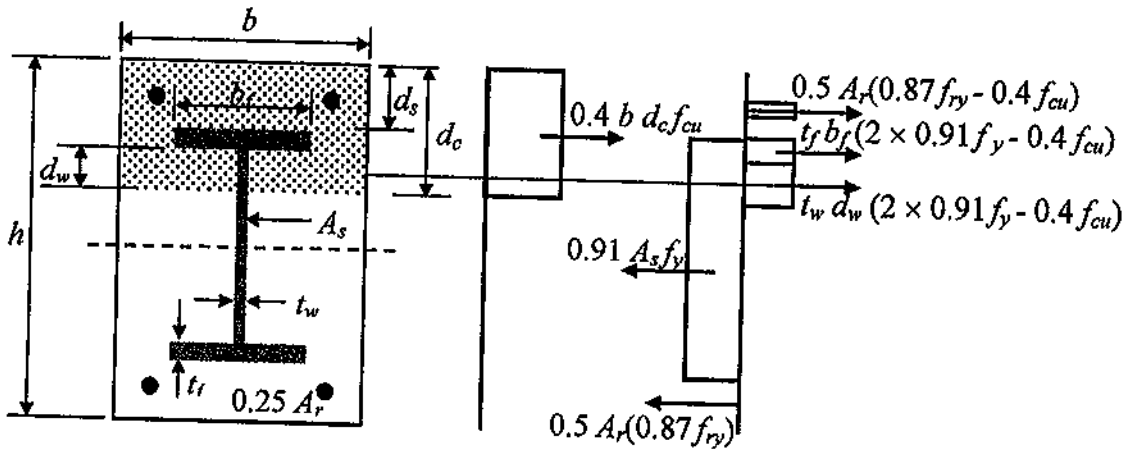


Figure 3.7 Force Diagram for Calculating M_u , Plastic Neutral Axis in Web/Major Axis Bending

Case IV. Plastic neutral axis in flange/minor axis bending

This condition (Fig. 3.8) arises when:

$$\rho b d_s < A_s \quad \text{then}$$

$$d_c = \frac{A_s + 4t_f d_s}{b\rho + 4t_f} \quad \text{and} \quad (3.53)$$

$$M_u = 0.91 f_y \left[A_s \frac{(h - d_c)}{2} - 2 t_f d_s (d_c - d_s) \right] + 0.87 f_{ry} \frac{A_r}{2} d_r \quad (3.54)$$

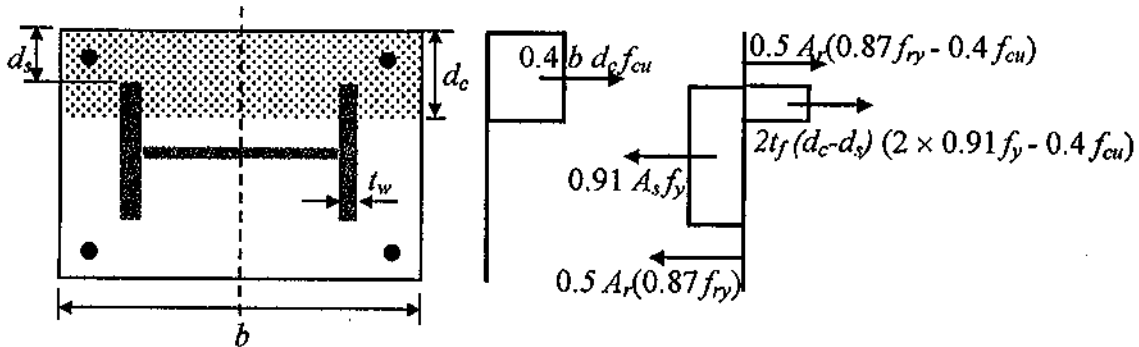


Figure 3.8 Force Diagram for Calculating M_u , Plastic Neutral Axis in Flange/Minor Axis Bending

Table 3.1 Terms and Specifications Used in the Two Codes of Practice for Composite Columns (Saw *et al*, 2000)

Item	LRFD Specifications	BS 5400 Specifications
Steel	A36 (248 N/mm ²), A50 (345 N/mm ²), A55 (379 N/mm ²) [I2.1d]	Grade 43 (275 N/mm ²) or 50 (355 N/mm ²), t ≤ 16mm [11.1.2.1]
Concrete	20.7 N/mm ² ≤ f' _c ≤ 55.1 N/mm ² for normal weight concrete f' _c ≥ 27.61 N/mm ² for lightweight concrete, where f' _c = concrete cylinder strength [I2.1c]	f _{cu} ≥ 20 N/mm ² for concrete filled tubes f _{cu} ≥ 25 N/mm ² for encased sections, where f _{cu} = concrete cubic strength. [11.1.2.2]
Steel contribution ratio	Cross-sectional area of steel section ≥ 4% of total cross-sectional area [I2.1b].	Encased steel section: 0.15 ≤ α _c ≤ 0.8 Hollow steel section: 0.1 ≤ α _c ≤ 0.8 where α _c is the ratio of the concrete contribution to total axial capacity. [11.4.1]
Limiting slenderness	KL/r ≤ 200, where KL is the effective length and r is the radius of gyration of the section.	Ratio of effective length to least lateral dimension of composite column should not exceed: 30 for concrete encased sections 55 for concrete filled circular hollow sections 65 for concrete filled rectangular hollow sections. [11.1.5]

Table 3.1 continued

Slenderness ratio, λ	<p>For concrete encased sections:</p> $\frac{l_e}{r_m \pi} \sqrt{\frac{F_y + 0.7F_{yr} \left(\frac{A_r}{A_s}\right) + 0.6f'_c \left(\frac{A_c}{A_s}\right)}{E + 0.2E_c \left(\frac{A_c}{A_s}\right)}}$ <p>For concrete filled sections:</p> $\frac{l_e}{r_m \pi} \sqrt{\frac{F_y + F_{yr} \left(\frac{A_r}{A_s}\right) + 0.85f'_c \left(\frac{A_c}{A_s}\right)}{E + 0.4E_c \left(\frac{A_c}{A_s}\right)}}$	<p>For concrete encased sections and concrete filled rectangular sections:</p> $\frac{l_e}{\pi} \sqrt{\frac{A_s f_y + A_c f_{cu} + A_r f_{ry}}{\gamma_s + \gamma_c + \gamma_r} \frac{1}{E_s I_s + E_c I_c + E_r I_r}}$ <p>For concrete filled circular sections:</p> $\frac{l_e}{\pi} \sqrt{\frac{A_s f_y + A_c f_{cc}}{\gamma_s + \gamma_c} \frac{1}{E_s I_s + E_c I_c + E_r I_r}}$
Steel reinforcement	Not less than 0.007 in ² of reinforcement per inch of bar spacing (0.178 mm ² /mm of bar spacing). [I2.1b]	For concrete encased columns: stirrups to be placed through length of column, spacing not exceed 200 mm. At least 4 longitudinal bars to be provided. [I1.3.9]
Local buckling	Minimum wall thickness, t , for hollow sections are: $t \geq b(f_y/3E)^{1/2}$ for each face of width, b , in RHS $t \geq D(f_y/8E)^{1/2}$ for CHS of outside diameter, D , [I2.1e]	Minimum wall thickness, t for hollow sections are: $t \geq b_s(f_y/3E_s)^{1/2}$ for each face of width, b_s , in RHS $t \geq D_o(f_y/8E_s)^{1/2}$ for CHS of outside diameter, D_o , [I1.1.2.1]
Modulus of elasticity of concrete	$w^{1.5} \sqrt{f'_c}$ where w is the unit weight of concrete in lb/ft ³ , or $w^{1.5} (0.043) \sqrt{f'_c}$ where w is the unit weight of concrete in kg/m ³	450 times f_{cu} [I1.3.1] 670 times f_{cu} (Recommended unfactored value)
Partial safety factors for material	Compression 1/0.85 = 1.18 Flexural: 1/0.9 = 1.11	Steel section: 1.1 Concrete: 1.5 Steel reinforcement: 1.15 Shear connector: 1.10 [4.2.1]
Partial safety factors for load	1.2 Dead Load + 1.6 Imposed Load [A4.1]	(1.05~1.2) Dead Load + (1.3~1.5) Imposed Load

CHAPTER FOUR

EXPERIMENTAL PROGRAM TEST

4.1 General

The experimental testing program was carried out on sixteen full-scale columns in order to investigate the behavior of lightweight aggregate concrete-encased H-shape steel columns subjected to uniaxial bending about the major axis in single curvature, and to compare such behavior with that of normal concrete-encased composite columns and bare steel sections.

The variables investigated in this study can be summarized as follow:

- 1- Column height of 2 and 3 meters, this was because maximum height of the testing machine is limited to approximately 3.05 m.
- 2- The eccentricity of the applied load about the major axis at the column ends were 40 mm and 70 mm in such a way to cause a single curvature bending.
- 3- Lightweight aggregate concrete strengths of 20.5, 13.7, and 9.7 MPa, and normal weight concrete with compressive strength of 28.2 MPa were used in the tests.
- 4- Structural steel ratio to gross column area, A_s/A_g , of 4% and 6% were used in this research.

Emphasis was placed on investigating the following parameters:

- 1- Failure modes.

- 2- The load carrying capacity of the specimen.
- 3- The load-deflection relationship.
- 4- Moment-curvature relationship.
- 5- Strains in steel and concrete.
- 6- Composite action between the steel section and the concrete.
- 7- Cracking development of concrete.

Details of all the tests are presented in this chapter.

4.2 Testing Machine

The tests were carried out using the universal testing machine at the structural laboratory of Jordan University of Sciences and Technology. Each column specimen was placed in a vertical position and tested under incremental monotonic loading in a 2000 kN capacity M1000/RD universal testing machine from DARTEC Limited.

The loading system consists of a pin-ended cylindrical hydraulic jack with circular end plate of 300 mm diameter and 90 mm thickness through which the load was applied, and a control panel 9500-H3, which is capable of providing data such as the load carrying capacity and vertical deformations and plotting the load against the vertical deformation. General view of the testing machine is shown in Figure 4.1.

The load was applied to the columns by means of a pair of loading plates, of 50 mm thickness, at each end of the column specimen. A

cylindrical groove of 302 mm diameter and 30 mm depth was made in the upper loading plate such that the circular end plate of the jack can be adjusted through this groove before loading.

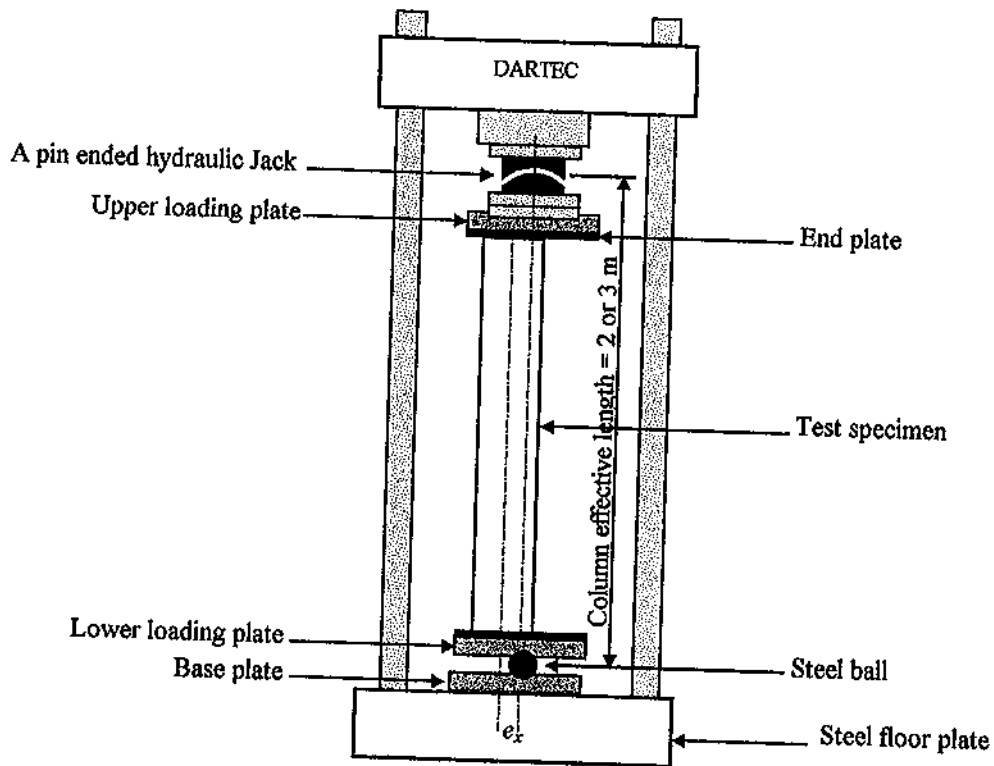


Figure 4.1 General View of the Testing Machine

The upper and lower loading plates were bolted by $4\phi 14$ mm high grade steel bolts to the column end plates of 10 mm thickness each, which were welded to the H-shape steel section with a high degree of accuracy to ensure the load application at the required eccentricities.

A 50 mm-diameter steel ball was used and positioned in an 18.5 mm-depth, 50 mm diameter spherical groove in the lower loading plate, and into the 50 mm-thick base plate having the same spherical groove as that of the lower loading plate. This arrangement was intended to give the

column a rotational freedom in all direction i.e. two pin ended column. The base plate was bolted to the lower 350 mm thick steel table of the loading system by 22 mm-diameter tie bolts.

4.3 Test Specimens

Test specimens were selected to be consistent with the objective of the research. Moreover, the specimens were chosen to reflect the effect of major parameters on the behavior of encased composite columns when subjected to eccentric loading. These parameters, as explained before, include; slenderness ratio, load eccentricity, concrete strength, and ratio of structural steel area to gross column area.



Figure 4.2 Test Specimen Placed in Testing Machine

Sixteen columns were tested under eccentric loading, bending about major axis with equal end eccentricities. Fig. 4.2 shows a test specimen placed in the testing machine.

4.3.1 Column geometry

All columns were of the same concrete cross-sectional dimensions of 230×230 mm, reinforced with $4\phi 12$ mm longitudinal steel corner bars, and Lateral ties $\phi 8 @ 140$ mm on centers. The characteristics of the column specimens are listed in Table 4.1 and their geometry is illustrated in Figure 4.3.

Test specimens were classified into four groups. Group I of the specimens (Columns 1 to 6) consists of H-section of effective length of 2000 mm ($Kl/r = 29.1$, based on gross section) and with eccentricity of the applied load of 70 mm. Three of the six columns were of HEA 100 steel sections, while the other three were of HEA 140 steel section according to German standard. Two columns were encased in class "A" lightweight aggregate concrete (see concrete mixes in Table 4.3), one was encased in class "B" lightweight aggregate concrete, and one was encased in normal concrete, while the other two specimens (HEA 140 and HEA 100) were left to be tested as a bare steel column for comparison.

Group II of the specimens (Columns 7 to 12) was the same as the first group I but with a length of 3000 mm ($Kl/r = 43.5$, based on gross section).

Group III of the specimens (Columns 13 to 15) includes HEA 100 steel section of length of 3000 mm, and a load eccentricity of 40 mm. One column of this group was encased in class "A" lightweight aggregate concrete, one was encased in class "B" lightweight aggregate concrete, while the last one was encased in normal concrete.

Group IV of the specimen (column 16, pilot test) includes HEA 100 steel section of length of 2080 mm ($Kl/r = 30.1$) and a load eccentricity of 40 mm. This column was encased in class "C" lightweight aggregate concrete.

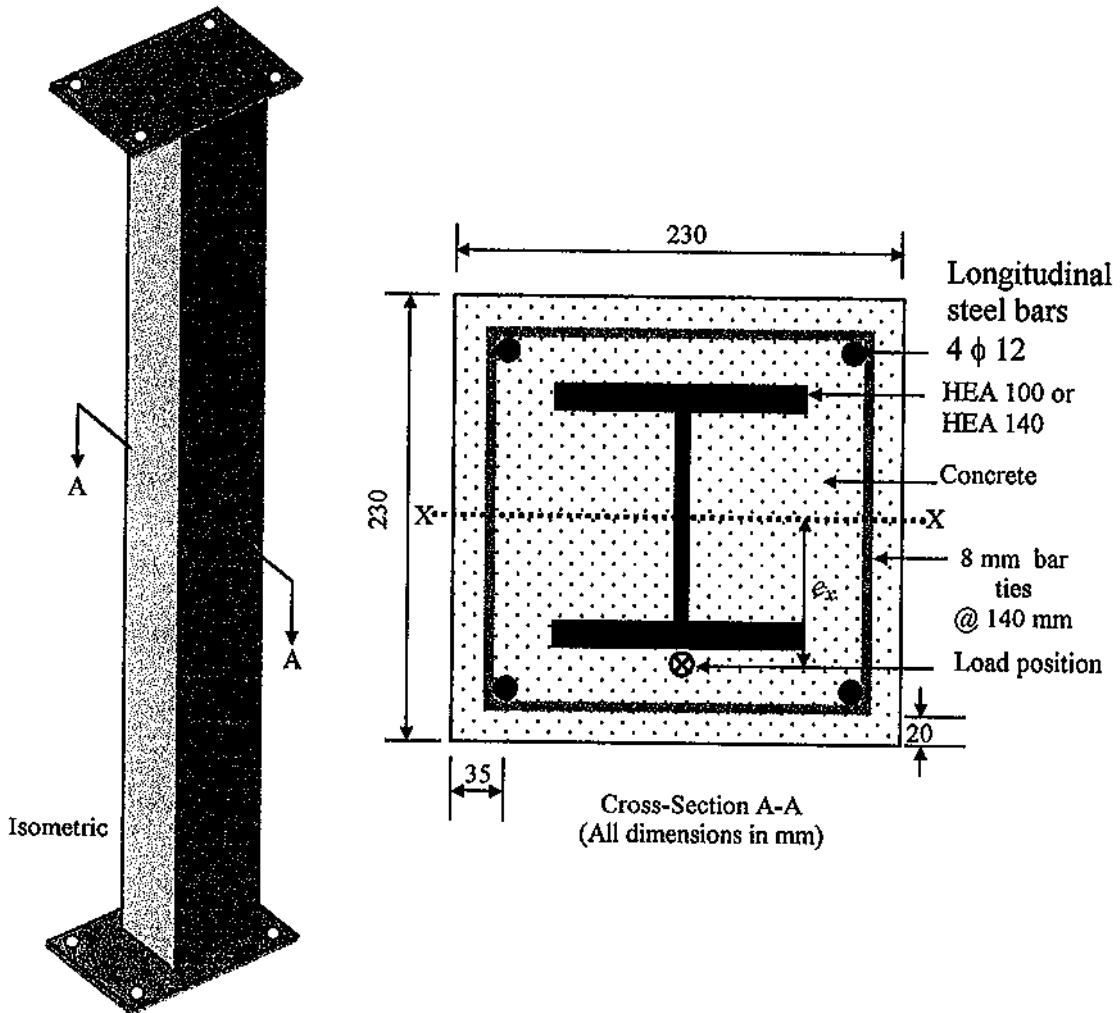


Figure 4.3 Column Geometry and Cross-sectional Properties

Table 4.1 Details and Properties of Column Specimens

Group No.	Column No.	Column designation	Concrete encasement				Steel sections			Steel bars			Load eccentricity e_x mm	Effective length KL mm
			Size mm	Type and class	Cube strength f_{cu} MPa	Density kg/m^3	Type	Area A_s mm^2	Yield strength, f_y MPa	Diameter mm	Area A_s mm^2	Yield strength, f_y MPa		
I	1	LA2e7R4	230×230	LWAC-A	20.5	1794	HEA 100	2120	337	12.16	465	459	70	2000
	2	LB2e7R4	230×230	LWAC-B	13.7	1650	HEA 100	2120	337	12.16	465	459	70	2000
	3	BS2e7H10	-	-	-	-	HEA 100	2120	337	12.16	465	459	70	2000
	4	LA2e7R6	230×230	LWAC-A	20.5	1794	HEA 140	3140	307	12.16	465	459	70	2000
	5	NC2e7R6	230×230	NC	28.2	2220	HEA 140	3140	307	12.16	465	459	70	2000
	6	BS2e7H14	-	-	-	-	HEA 140	3140	307	12.16	465	459	70	2000
II	7	LA3e7R4	230×230	LWAC-A	20.5	1794	HEA 100	2120	337	12.16	465	459	70	3000
	8	LB3e7R4	230×230	LWAC-B	13.7	1650	HEA 100	2120	337	12.16	465	459	70	3000
	9	BS3e7H10	-	-	-	-	HEA 100	2120	337	12.16	465	459	70	3000
	10	LA3e7R6	230×230	LWAC-A	20.5	1794	HEA 140	3140	307	12.16	465	459	70	3000
	11	NC3e7R6	230×230	NC	28.2	2220	HEA 140	3140	307	12.16	465	459	70	3000
	12	BS3e7H14	-	-	-	-	HEA 140	3140	307	12.16	465	459	70	3000
III	13	LA3e4R4	230×230	LWAC-A	20.5	1794	HEA 100	2120	337	12.16	465	459	40	3000
	14	LB3e4R4	230×230	LWAC-B	13.7	1650	HEA 100	2120	337	12.16	465	459	40	3000
	15	NC3e4R4	230×230	NC	28.2	2220	HEA 100	2120	337	12.16	465	459	40	3000
IV	16	LC2e4R4	230×230	LWAC-C	9.7	1494	HEA 100	2120	337	12.16	465	459	40	2080

The abbreviations used in Table 4.1 consists of the first two letters for steel or concrete type, the number followed stand for effective column height, a letter "e" and a number for eccentricity in cm , and the letter "R" and a number for a ratio of structural steel to concrete gross area.

Where

LA: Lightweight aggregate concrete class A,

LB: Lightweight aggregate concrete class B,

LC: Lightweight aggregate concrete class C,

NC: Normal weight aggregate concrete,

BS: Bare steel section,

H10: HEA 100 steel section, and

H14: HEA 140 steel section.

For example, a column designated by LA3e7R4: Lightweight aggregate concrete class A of 3 meters effective height, eccentricity of 7 cm, and a structural steel ratio to concrete gross area of 4%.

4.3.2 Fabrication of test specimens

Column specimens were fabricated at the welding workshop of the Faculty of Engineering and Technology at the University of Jordan. The structural steel sections and the deformed longitudinal reinforcing bars were cut to the desired length by using a cold sawing machine. Stirrups, made from $\phi 8 @ 140$ mm on centers smooth bars, were provided over the

column height. Two end plates of 10 mm thickness were welded to the ends of each column using 5 mm fillet welds after making four bolt-holes in each plate. These plates were extended out of the column dimensions to accommodate the applied eccentric load within their dimensions as shown in Figures 4.4 and 4.5.

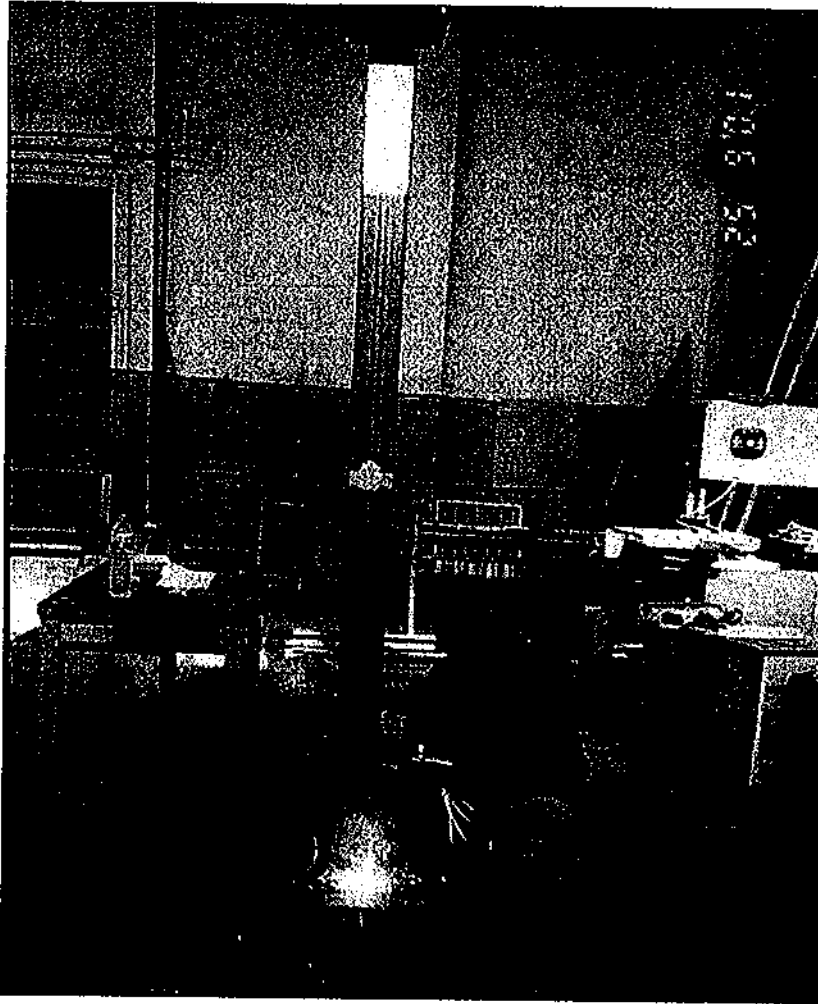


Figure 4.4 End Plates Welding to Column Specimen

Welding process was done by an experienced welder under careful supervision to ensure adequate penetration of the weld. At certain locations

along the steel sections, the surface was cleaned and prepared to install electrical strain gauges for strain measurements.

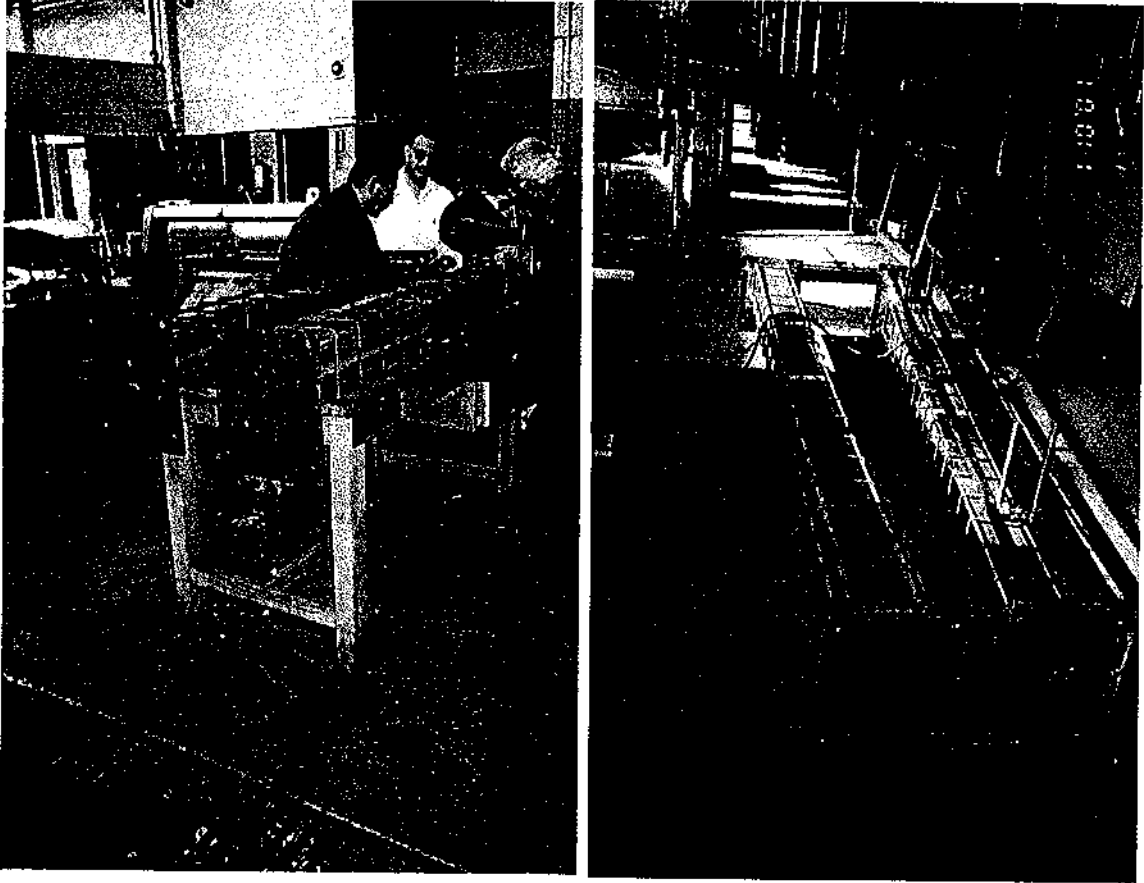


Figure 4.5 Fabrication of Test Specimens

4.3.3 Orientation of column in test machine

All columns were placed vertically in the test machine in such a way that the deflection occurred in the vertical direction (major axis bending) as illustrated in Figures 4.1 to 4.3.

4.3.4 Materials

The basic materials used to build the full-scale column specimens were lightweight aggregate concrete, normal weight concrete, longitudinal

structural steel H-shaped section, deformed longitudinal reinforcing bars, and mild steel lateral ties.

The column specimens were cast horizontally inside a formwork made out of 20 mm thick precut pieces of plywood using electrical mixer and compacted with a 25 mm vibrator rod as illustrated in Fig. 4.6.



Figure 4.6 Casting of Column Specimens

Some standard tests were performed at the material lab of University of Jordan on pumice, sand, and crushed limestone aggregate to characterize their properties, which are given in Table 4.2.

Table 4.2 Material Properties

Properties	Pumice	Sand	Crushed aggregate
Specific gravity (S. S. D.)	1.75	2.65	2.6
Water absorption %	12.7	1.6	3.5
Bulk density g/cm^3	0.752	1.58	1.35

4.3.4.1 Lightweight aggregate concrete and normal concrete

The lightweight aggregate concrete for the column specimens was obtained by mixing ordinary Portland Cement (PC 42.5) confirming to JS A30/1993, fine suweileh sand, combined fine and coarse aggregate pumice, expanded perlite, and tape water. The combined fine and coarse aggregate pumice was obtained by gradation of gravel with maximum size of 12.5mm confirming to ASTM C 330-89 Standard Specification for Lightweight Aggregate for Structural Concrete. This pumice is a brown and black volcanic material (type of Pozzolana) available in Northeast of Jordan in very large quantities. Its bulk density is 752 kg/m^3 and its water absorption is 12.7%, while the expanded perlite used in the tests is a very light white artificial material with a bulk density of 127 kg/m^3 .

Normal concrete used for the column specimens was obtained by mixing ordinary Portland Cement (PC 42.5), fine suweileh sand, normal weight aggregate, and tape water. Limestone aggregate of maximum size of 12.5 mm was also used for normal concrete encasement around and inside the steel section and bars.

Several trial mixes were attempted on the normal and the lightweight aggregate concrete before obtaining the one that would be the most appropriate with respect to the compressive strength and the density for the final specimens. The addition of 15% suweileh sand by volume to pumice aggregates, increased slump, workability, compressive strength as well as unit weight of finished concrete. The concrete mix proportion, average cubes strength, slump test results, and concrete density were given in Table 4.3.

Table 4.3 Details of Concrete Mixes

Concrete Type	28-d Cube Strength, f_{cu} Average MPa	Density Average kg/m^3	Slump Test cm	Concrete mix Proportions By volume
Lightweight aggregate concrete class A	20.5	1794	12.5	Cement: Sand: Perlite: Pumice 1: 0.5: 1.25: 2 w/c = 0.77
Lightweight aggregate concrete class B	13.7	1650	10.5	Cement: Sand: Perlite: Pumice 1: 0.5: 2: 2.5 w/c = 0.8
Lightweight aggregate concrete class C	9.7	1494	10	Cement: Sand: Perlite: Pumice 1: 0.45: 2: 2.55 w/c = 0.83
Normal weight concrete	28.2	2220	12	Cement: Sand: Aggregate 1: 1.5: 2.5 w/c = 0.6

Three standard 150 mm cube specimens were taken from each concrete mix, and tested for compression at the time of testing the column specimens in a 1200 kN capacity (M2501 Servo-hydraulic) universal testing machine as shown in Figure 4.7. The stress-strain curves of the

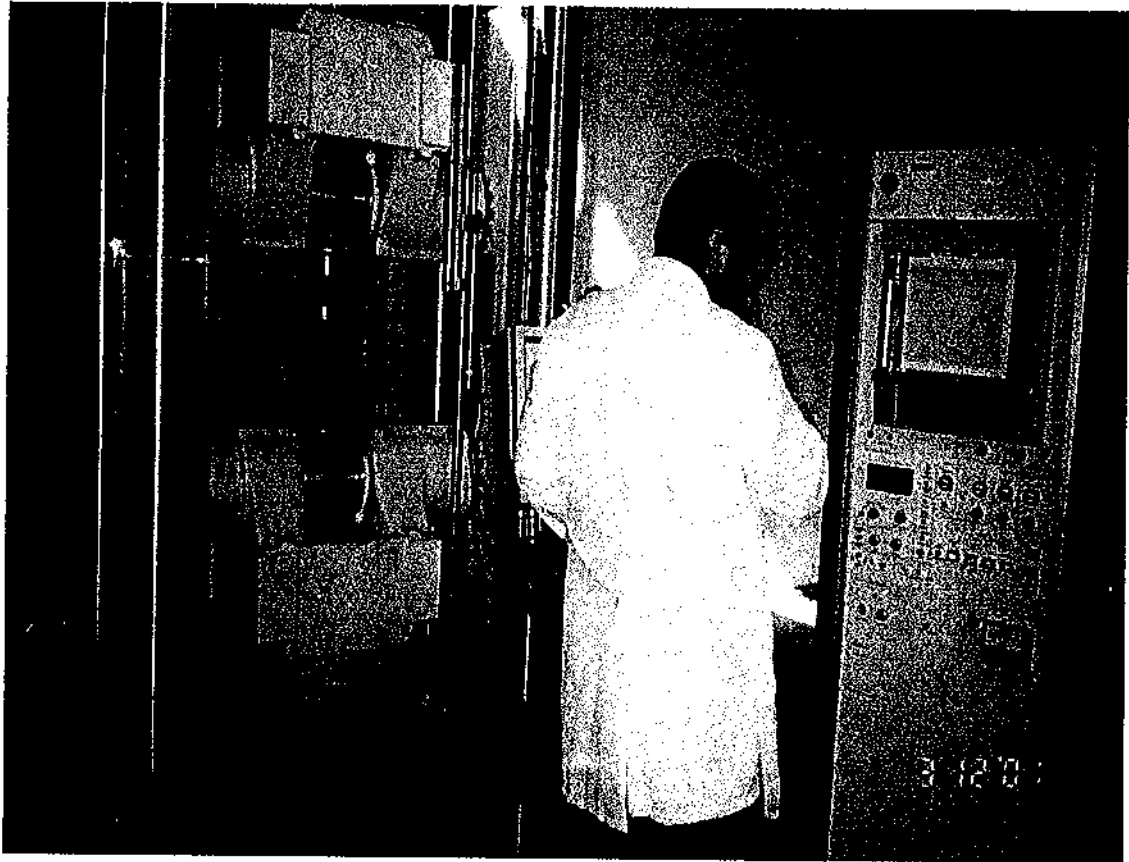


Figure 4.7 Compression and Tension Test Machine

tested cubes are illustrated in Figure 4.8.

4.3.4.2 Structural steel and reinforcing bars

Three different types of longitudinal steel reinforcement were used to build the composite column specimens. Deformed 12 mm diameter steel bars were used as secondary longitudinal reinforcement at the four corners

of the column section, whereas smooth closed square ties having a diameter of 8 mm, were placed at 140 mm on centers over the entire length of the specimens. Hot-rolled structural steel HEA100 section of 100 mm (width) \times 96 mm (depth) \times 8 mm (flange thickness) \times 5 mm web thickness and HEA140 section of 140 (width) \times 133 mm (depth) \times 8.5 mm (flange thickness) \times 5.5 mm web thickness were used as the main steel section of the composite column specimen at the centerline of the cross section.

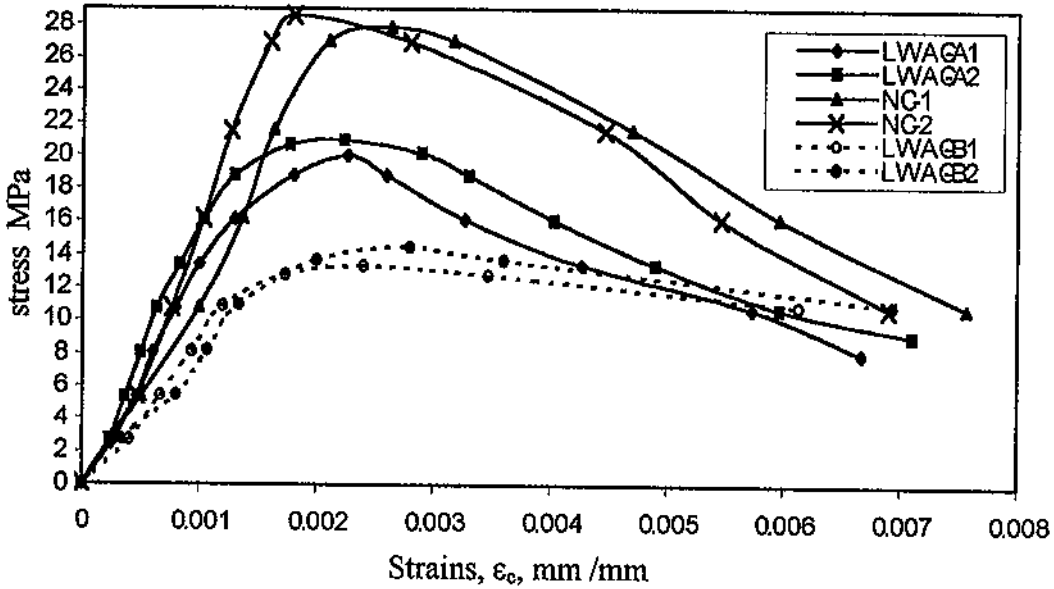


Figure 4.8 Concrete Stress-Strain Curves

Table 4.4 Details of Structural Steel and Reinforcing Bars

Type of Steel	A_s mm ²	d mm	t_w mm	b_f mm	t_f mm	Wt Kg/m	I_x mm ⁴ $\times 10^4$	r_x mm	Z_x mm ³ $\times 10^3$	I_y mm ⁴ $\times 10^4$	r_y mm	Z_y mm ³ $\times 10^3$	f_y MPa	ϵ_y %
HEA 100	2120	96	5.0	100	8	16.7	349	40.6	83	134	25.1	42.7	337	0.168
HEA 140	3140	133	5.5	140	8.5	24.7	1030	57.3	119	389	35.2	86.4	307	0.154
Reinforcing bars	Diameter = 12.16 mm, $A_r = 464.5 \text{ mm}^2$ (4 bars), $f_{ry} = 459 \text{ MPa}$, $\epsilon_{ry} = 0.229 \%$													

The steel sections were cut to the required length by using a cold sawing machine. Four holes of 16 mm diameter were done in each one of the end plates, then were welded to the column ends by fillet welds (E7018 electrode).

Several tension tests on coupons cut from the H section were carried out to determine the yield stress of the steel. Some of the coupons were taken from the web others from the flanges and were tested using the 1200 kN capacity (M2501 Servo-hydraulic) universal testing machine which was illustrated in Figure 4.7. Four stub columns cut from the H-section of height equals three times their width according to the SSRC (1998) requirements, were tested for compression using the 2000 kN capacity M1000/RD universal testing machine from DARTEC Limited as shown in Figure 4.9. The average yield strength was 337 MPa with a corresponding yield strain of 0.00168 for HEA100 section, while the strength was 307 MPa with a corresponding yield strain of 0.00154 for HEA 140 section.

Tensile tests were done on the longitudinal steel reinforcing bars using the 1200 kN capacity (M2501 Servo-hydraulic) universal testing machine shown in Figure 4.8. The average yield strength of these bars was 459 MPa with a corresponding yield strain of 0.00229. All tests on concrete cubes and steel specimens were done at the structural laboratory of the Jordan University of Sciences and Technology.

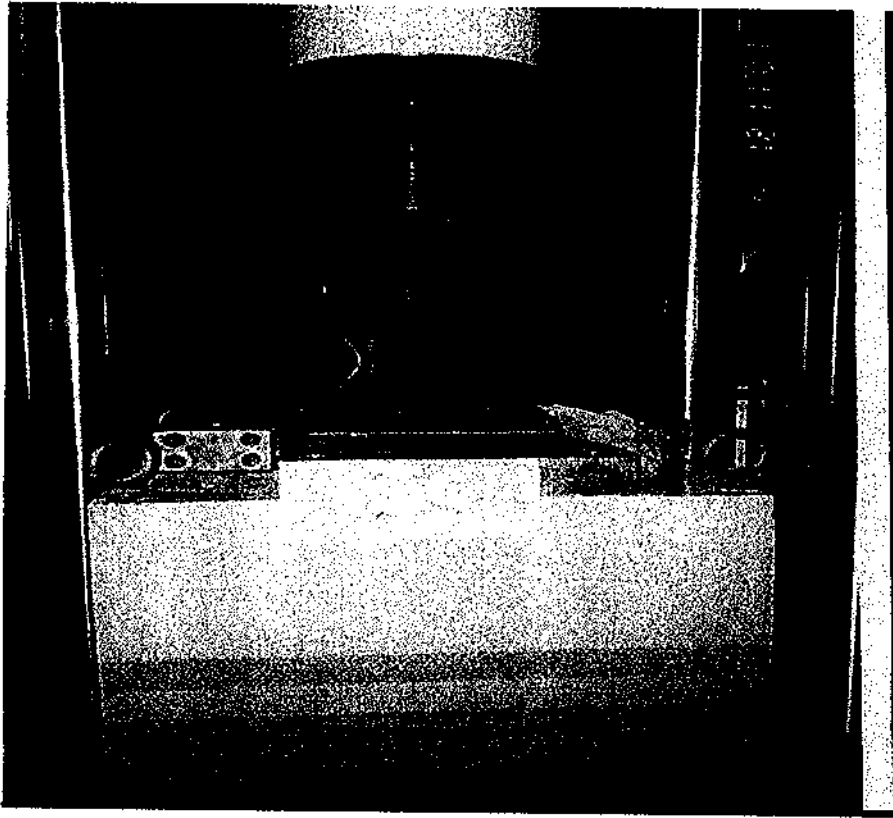


Figure 4.9 Stub Column Test

4.4 Instrumentation and Experimental Data Acquisition

The columns were instrumented to measure; loads, lateral and vertical deflections, and strains in the steel section and in the concrete face as described in the following sections. Separation between the concrete and the steel section as well as the cracks in concrete in addition to buckling modes were observed and recorded during each test.

4.4.1 Load measurements

The columns were tested under incremental monotonic loading. The applied load was recorded directly from the load indicator of the load cell

4.4.2 Deflection measurements

Deflections at the mid height in the direction of the major axis were measured by a dial gauge of 0.01 mm precision, while in the direction of the minor axis were measured by means of a Linear Variable Displacement Transducer (LVDT) as shown in Figure 4.10. Axial deformations against the applied load were recorded and plotted on the X-Y plotter of the DARTEC testing machine.

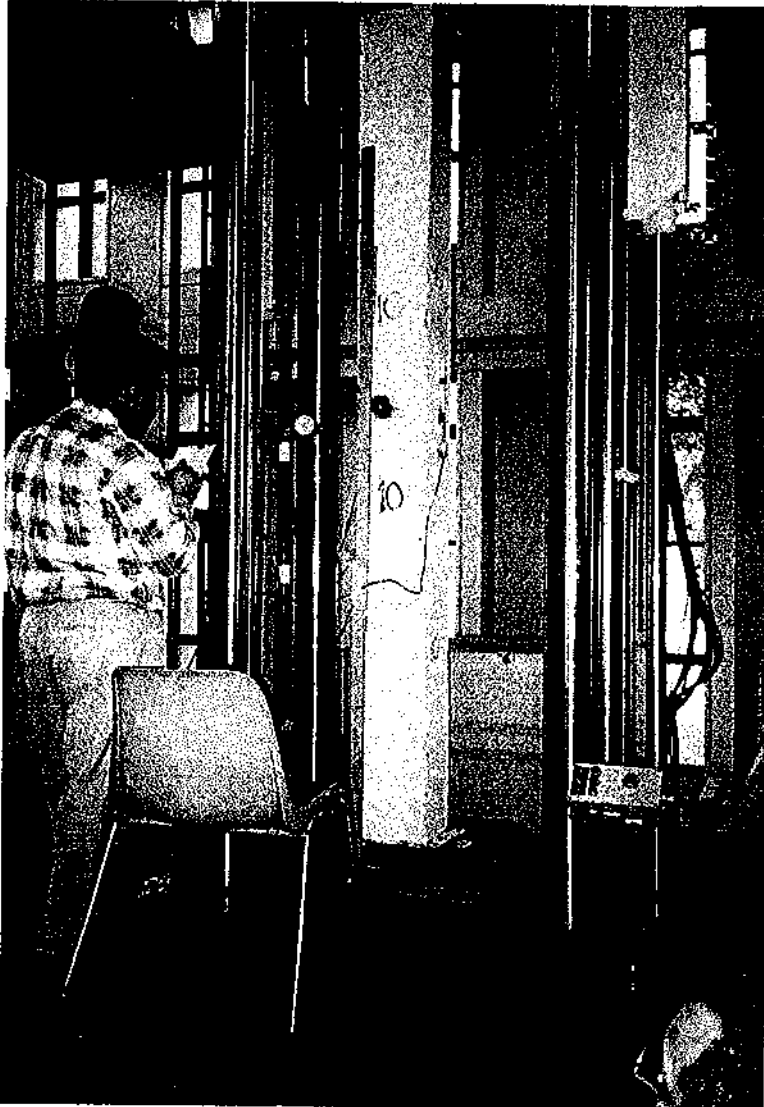


Figure 4.10 Dial Gauges and LVDTs on Column Specimen

4.4.3 Strain measurements

Four electrical strain gauges [type MM EA-06-250BG-120 of gauge resistance gauge 120 ± 0.3 % Ohms, gauge factor 2.03 ± 0.5 % at 75°F , and gauge length 10 mm] were used, one at each of the four flange tips of the H section at mid-height of column 16 (pilot test column) as shown in Figure 4.11. For the other fifteen columns, two, or one strain gauge were attached at the center of each flange of the H section also at the column mid-height as shown in Figure 4.12.

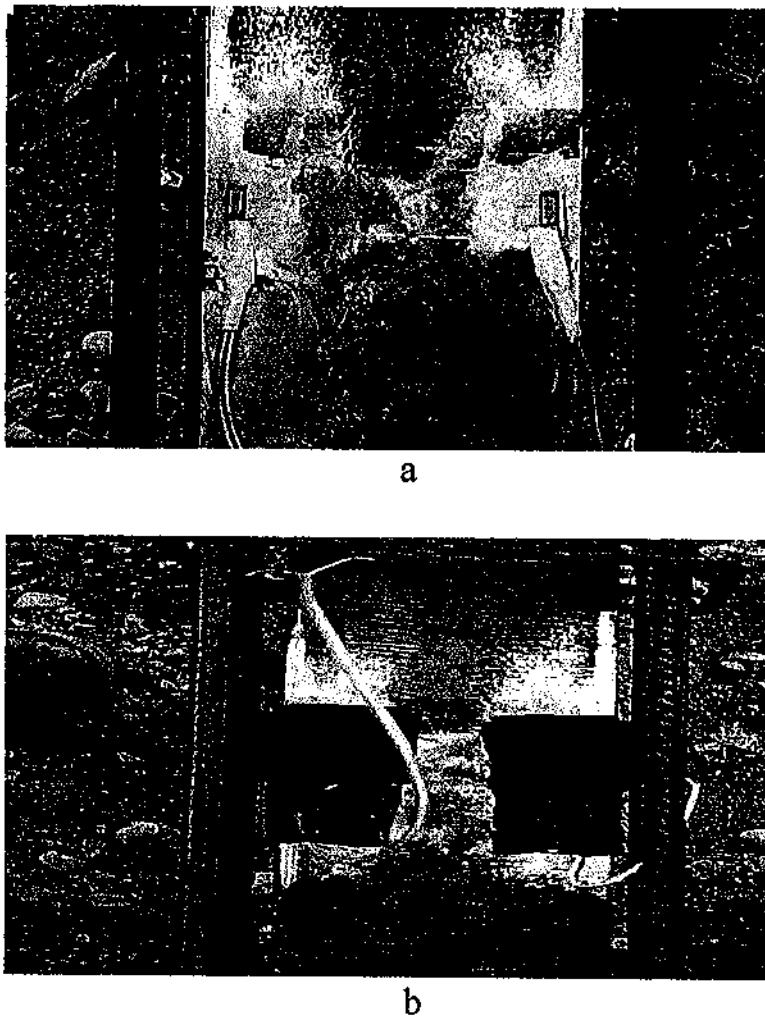


Figure 4.11 Electrical Strain Gauges Attached on The Flange Tips of The H Steel Section for Column 16 (a) Before Coating (b) After Coating

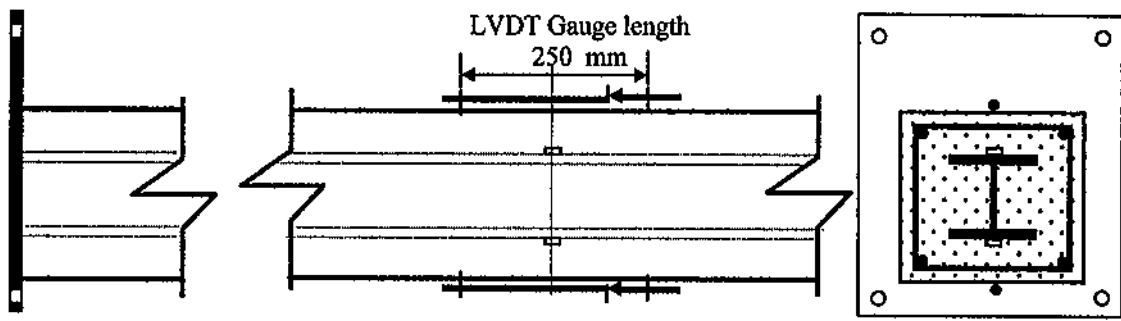


Figure 4.13 Locations of Electrical Strains Gauges and LVDTs

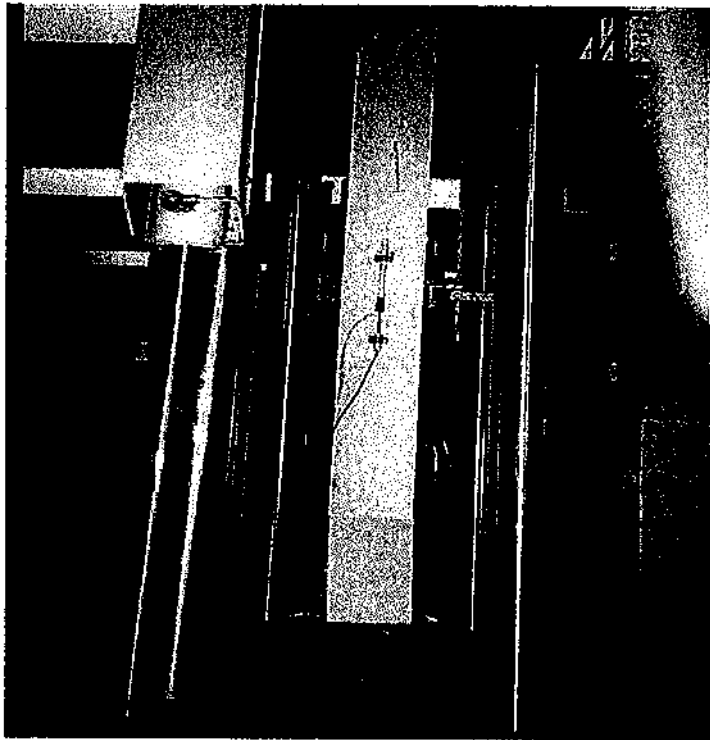


Figure 4.14 Location of the LVDT on Column Specimen

4.5 Experimental Procedure

The load was applied eccentrically to cause bending about the major axis in single curvature. The end eccentricity ratio was kept constant and equal to one in all columns. When the column specimen was placed in the testing machine, a load of 5 kN was applied and then released prior to

testing, to insure that no load loss would occur due to any movement at the column ends.

Each one of the column specimens was loaded continuously by a 2000 kN capacity M1000/RD universal testing machine from DARTEC Limited and observations were made at each load stage to detect the initiation of any visible cracks on the tensile faces of the specimen, or concrete spall-off or buckling of the reinforcing bars. The digital reading of the applied load against lateral displacements were recorder during testing, while, strains, and LVDTs readings were collected by the data acquisition system.

The rate of loading was of 0.5 to 0.7 kN/sec up to about 80 % of expected failure load, and then the mode of loading was changed to displacement control with a displacement rate of 0.01 mm/sec, in order to have reliable results to study the true behavior of the tested columns even after failure.

After the maximum load was attained, increasing lateral mid-height displacement started to take place at an increased rate of axial strains as well as decreasing of the applied load. Usually, the test was terminated when the reinforcing bars had been buckled and the spall of concrete cover had taken place whereas the load decreased to about 80-70% of its ultimate load.

CHAPTER FIVE

TEST RESULTS AND DISCUSSION

The test results and the behavior of the tested specimens are presented and discussed in this chapter based on the recorded data and observations during testing which are described in the previous chapter. A set of photographs of the column specimens after test showing failure modes is provided, together with curves showing different relationships between the recorded data.

5.1 Behavior of Column Specimens

Experimental observations of the tested specimens and recorded data are utilized in this section to explain and describe the behavior of lightweight concrete-encased columns subjected to axial load and equal end moments about the major axis.

All column specimens behaved very well under load, and as expected the failure loads of all columns were always well in excess of design values predicted by the LRFD, 93 and Bridge Code, BS 5400 recommendations.

Minor hairline cracks on the tension side of the concrete were observed early at a load level of about 50% of the failure load, especially in long columns of 3 m height encased in lightweight aggregate concrete and

large eccentricity of 70 mm (columns 7, 8, and 10). Furthermore, the cracks were observed at load ratio of 60% of failure load in columns encased in lightweight aggregate concrete of 2 m height and large eccentricity of 70 mm, as in columns 1 and 2. These cracks were very little, and increased very slowly as the load was increased. For columns encased in lightweight aggregate concrete of 3 m height and low eccentricity of 40 mm, the cracks were first observed at load ratio of 70% of failure load as in columns 13 and 14. However, in no case did the cracks seem to affect the load carrying capacity of the columns, as in most cases the crack widths remained stable when the load was further increased.

Separation between the end plates and concrete was very small in most tests at loads very close to failure loads. This confirms the composite action between steel and concrete for both NC and LWAC.

The ductility of bare steel columns was very high and decreased by the concrete encasement. Furthermore, the ductility of LWAC columns decreases by the decrease in concrete strength and density as shown in moment-thrust- curvature curves. The tension flanges of all columns did not reach the yield strain; this is due to the low moment applied compared to the axial load as shown in the strain results. A little twist at the mid-height of the bare steel column specimens was observed, while no twist was observed in the lightweight or normal concrete encased columns, this indicates that concrete encasement of steel columns prevents lateral or

torsional buckling.

5.2 Failure Modes of Column Specimens

A convenient definition of a failure state has been considered to be the load stage at which any concrete fiber reaches a critical limit strain value, commonly set as 0.003, although any value from 0.0025 to 0.004 could produce reasonable result. At a strain near 0.002 concrete begins to crush and spall before higher strains are reached. Steel would yield also after concrete fails (Furlong, 1988).

The type of failure mode observed for all composite column specimens during testing was typically that of crushing of concrete on the compression face of the column with some noticeable cracking on the tensile face. Photographs of the composite column specimens after testing were shown in Figs. 5.1 to 5.4. From the load-strain curves of column specimens No. 1, 2, 4, 5, 7, 8, 10, and 14, it is noted that none of the column specimens had any steel elements yielding throughout the complete loading stages. Instead, concrete failed at load levels close to the maximum axial load. At that point, some of the unconfined concrete elements at the extreme side of the most compressed area of the cross section had failed under compression. Columns No. 11, 13, 15, and 16 followed an almost similar course. The first stage always corresponds to yielding in the compression flange of the H section. The strain in the steel flange at the tensile zone was

next to reach yield. A continuous deterioration in column stiffness was observed. Final collapse was accompanied by spalling of concrete in the compression zone. This immediately resulted in buckling between ties of the longitudinal reinforcement bars at the compression corners, reducing the column to a mechanism. Steel columns No. 3, 6, 9, and 12 fail due to yielding in the compression flange of the H section. The strain in the steel flange at the tension zone was next to reach yield.

The first sign of damage to concrete (crushing cracks or some

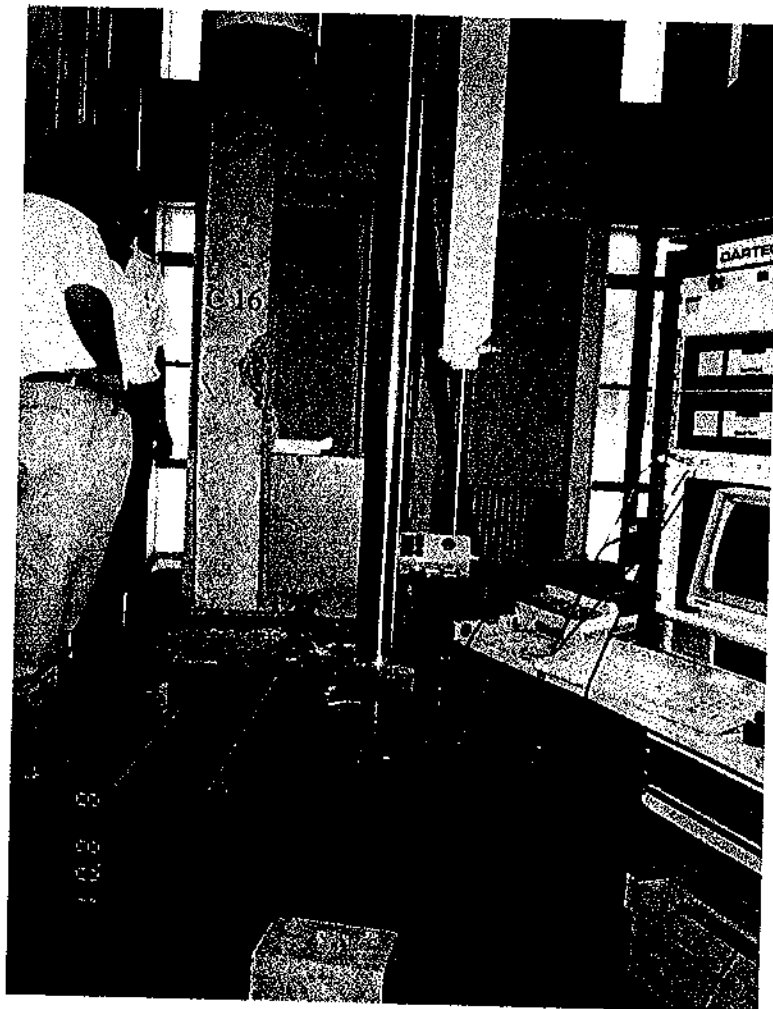


Figure 5.1 Failure Mode of Column No. 16

spalling of concrete in the compression region) occurred at loads not less than 95% of the failure load in all the tests. Serious spalling and crushing of concrete lumps always occurred at, or beyond, failure load.

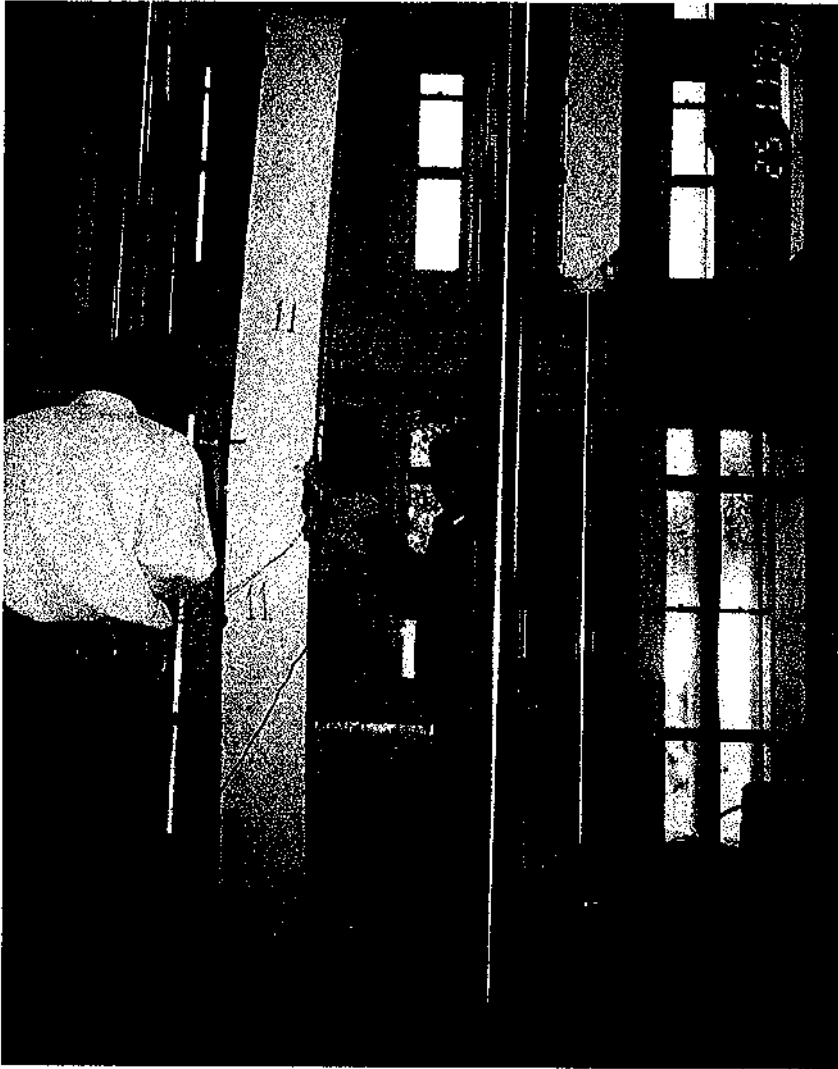


Figure 5.2 Failure Mode of Column No. 11

557056

It was expected that severe damage due to failure will occur at mid-height in all columns because all columns were tested in single curvature and equal end moments, i.e. equal eccentricities. Some specimens showed different behavior, that is; failure took place near the bottom end plate of



Figure 5.3 Failure Mode of Column No. 12

the column as shown in Figure 5.4. Hence the strains at mid-height did not reach the steel yield strain. This premature crushing of the concrete near the bottom end plate is possibly due to a misalignment of the top and bottom eccentricities that could have created an unsymmetrical pinned-ended condition. Although, it was thought that voids in the concrete encasement of those columns caused such behavior, inspection of the concrete at the end regions of columns suggested other reasons. Lack of homogeneity of

the concrete mix, excessive stresses, and curvature at the end plates caused by welding, might have caused such behavior. In addition, the low strength and density of LWAC are not the reason for that behavior because the column of lower concrete strength and density (column 16 of 9.7 MPa) failed in a typical failure mode; i.e. at mid-height as shown in Figure 5.1.

There is, therefore, no reason to assume that the localized compression force due to the loading system caused the end panel of some



Figure 5.4 Failure Mode of Column No. 4

columns to suffer the reported failure. Furthermore, whatever the reason for this type of failure it had no adverse effect on the load-carrying capacity of these columns, but the ductility of those columns reduced.

5.3 Load Carrying Capacity

The experimental failure loads of the tested columns are given in Table 5.1 and are compared with the predicted loads, as calculated by the AISC-LRFD, and the Bridge Code BS 5400. Although no material safety factors were taken into account in the calculations, the experimental failure loads were always well in excess of the estimated values. In other words, the two codes yield conservative predictions of the failure loads for LWAC concrete-encased composite columns. The maximum compressive strength of concrete was taken as $0.67 f_{cu}$ (instead of $0.45 f_{cu}$) for evaluating the squash load and $0.60 f_{cu}$ (instead of $0.4 f_{cu}$) for evaluating the ultimate moment by the Bridge Code method BS 5400. Failure loads are also shown graphically against displacements in the next sections.

A careful examination of Table 5.1 shows the following:

1. The design provisions of the present code procedure LRFD as well as BS 5400 are found to be adequate to predict the strength of lightweight aggregate concrete-encased composite columns.
2. The predicted column strengths using the two methods are on the conservative side and are in reasonable agreement with the test results.

Table 5.1 Test Results of Columns

Group No.	Column No. and designation	Load eccentricity about major axis e_x mm	Average concrete cube strength and unit weight $f_{cu} \cdot \gamma_c$ MPa-kg/m ³	Experimental			AISC-LRFD				Bridge Code BS 5400				
				Failure load N_e kN	Mid-height deflection at failure about major axis u mm	Mid-height moment at failure M_{ex} kN.m	Ultimate load P_{LRFD} kN	Nominal load P_{ex} kN	Ultimate moment of resistance M_{rx} kN.m	$\frac{P_{LRFD}}{N_e}$	Ultimate load N_{BS} kN	Squash load N_{sq} kN	Concrete contribution factor α_c	Ultimate moment of resistance M_{rx} kN.m	$\frac{N_{BS}}{N_e}$
I	1LA2e7R4	70	20.5-1794	654	8.13	51.1	487.5	1358.8	53.9	0.75	512.9	1618.7	0.427	55.7	0.78
	2LB2e7R4	70	13.7-1650	558	7.04	43.0	453.5	1194.6	51.8	0.81	470.9	1389.5	0.332	57.8	0.84
	3BS2e7H10	70	-	248	18.2	21.9	188.3	714.4	27.8	0.76	182.0	714.4	-	28.0	0.73
	4LA2e7R6	70	20.5-1794	962	8.15	75.2	670.8	1598.3	82.4	0.70	675.9	1854.3	0.365	81.5	0.70
	5NC2e7R6	70	28.2-2220	949	8.85	74.8	715.0	178.5	84.6	0.75	789.3	2108.6	0.442	91.9	0.83
	6BS2e7H14	70	-	417	10.02	33.4	366.5	964	53.11	0.88	336.7	964.0	-	53.1	0.81
II	7LA3e7R4	70	20.5-1794	641	11.96	52.6	443.0	1358.8	53.9	0.69	448.6	1618.7	0.427	55.7	0.70
	8LB3e7R4	70	13.7-1650	554	14.2	46.7	412.8	1194.6	51.8	0.75	421.2	1389.5	0.332	57.8	0.76
	9BS3e7H10	70	-	240	35.35	25.3	127.9	714.4	27.8	0.53	134.4	714.4	-	28.0	0.56
	10LA3e7R6	70	20.5-1794	895	17.0	77.9	612.0	1598.3	82.4	0.68	588.8	1854.3	0.365	81.5	0.66
	11NC3e7R6	70	28.2-2220	900	19.95	81.0	653.0	178.5	84.6	0.73	671.5	2108.6	0.442	91.9	0.75
	12BS3e7H4	70	-	404	31.0	40.8	290.5	964	53.11	0.72	278.0	964.0	-	53.1	0.69
III	13LA3e4R4	40	20.5-1794	813	15.8	45.4	581.5	1358.8	53.9	0.72	591.1	1618.7	0.427	55.7	0.73
	14LB3e4R4	40	13.7-1650	704	9.51	34.9	537.0	1194.6	51.8	0.76	538.7	1389.5	0.332	57.8	0.77
	15NC3e4R4	40	28.2-2220	1115	17.3	63.9	631.5	1544.8	54.98	0.57	664.2	1878.3	0.506	58.6	0.60
IV	16LC2e4R4	40	9.7-1494	680	5.4	30.9	556.5	1098	49.3	0.82	538.0	1254.7	0.261	52.8	0.79

$$M_{xe} = N_e(e_x + u)$$

3. The average ratio of the ultimate load capacity obtained by AISC-LRFD Code to the experimental load carrying capacity ($P_{LRFD}/N_e = 0.726$) is nearly the same or slightly lower than that obtained by Bridge Code BS 5400 ($N_{BS}/N_e = 0.731$).
4. The concrete encasement enhanced the load carrying capacity of the bare steel columns by about 264% for LWAC class A and 225% for LWAC class B (columns 1, 2, and 3). Furthermore, Comparing columns 7, 8, and 9 which have similar properties as columns 1, 2, and 3, but the height of 3 meters indicted that the increase in the failure load of bare steel was about 267% for LWAC class A and 231% for LWAC class B. Comparing columns 4, 5, and 6 which have similar steel ratio of 0.6%, eccentricity of 70 mm, and height of 2 meters indicted that the increase in failure load of bare steel columns was about 231% for LWAC class A and 228% for normal concrete. Moreover, columns 10, 11, and 12 which have the same properties of columns 4, 5, and 6 except the height was 3 m, showed that the increase in the failure load of bare steel columns was about 222% for LWAC class A and 223% for normal concrete. Thus, it would be sufficiently accurate to state that the LWAC significantly enhance the load carrying capacity of the steel sections.
5. The load carrying capacity is inversely proportional to the eccentricity of the applied load as indicated by comparing columns 13, 14, and 15

of 40 mm eccentricity with columns 7 and 8 of 70 mm eccentricity. The load carrying capacity of columns 13 and 14 was 127% on average of that of columns 7 and 8.

6. The effect of column height on the load carrying capacity was very small as indicated by comparing columns 7 and 8 of 3 m height to columns 1 and 2 of 2 m height. The load carrying capacity of columns 1 and 2 was about 101.4% on average of that of columns 7 and 8. Thus, the strength of the columns with lightweight casings is closer to those of columns with casings of normal concrete. This results have been confirmed by study conducted by smith (1980).
7. The effect of steel ratio on the load carrying capacity of the composite column was significant, where 2% increase in steel ratio causes an increase in the load carrying capacity by about 47% as indicated by comparing columns 1 and 4, and was about 40% for columns 7 and 10.
8. Comparing columns 13 to 15 in Table 5.1, which have the same height and eccentricity and contains LWAC and Normal concrete, showed that, the failure load increases as the strength and density increase. Thus, the load carrying capacity of encased composite columns depends on the strength and density of concrete.
9. The effect of type of concrete on the load carrying capacity of the composite columns may be demonstrated by comparing specimens 4, 5, 10, and 11, which have large eccentricity of 70 mm. The comparison

reveals that sections with normal concrete were stronger than columns with lightweight concrete, but with negligible amount. However, for columns 13, 14, and 15, which have low eccentricity of 40 mm, the trend is different, i.e. the load carrying capacity of the column encased in normal concrete was higher than those encased in lightweight concrete. Thus, the type of concrete considerably affects concrete contribution to the ultimate strength. In addition, the strength of the column encased in lightweight aggregate class "A" reaches 73% and class "B" reaches 63% of strength of columns encased in normal concrete as in the case of columns 13, 14, and 15.

It can be concluded that using LWAC for encasing the steel sections instead of normal concrete is useful in reducing the weight of the columns by about 20% of normal concrete while the load carrying capacity (compared to normal concrete) is almost the same for columns with large eccentricity (Columns 10 and 11). On the other hand, for columns with low eccentricity (Columns 13, 14, and 15) the reduction in the weight of columns is about 20%, while the load carrying capacity is reduced by about 27% for LWAC class A. For class B of LWAC the reduction in weight is about 26%, but the reduction in failure load is about 37%. This leads to the conclusion that using LWAC class A (20.5 MPa, 1794 kg/m³) is more appropriate than using Class B (13.7 MPa, 1650 kg/m³).

5.4 Strains

The load-strain response was recorded during tests for all column specimens in steel and concrete at column mid-height. Load-strain curves are illustrated in Figures 5.5 to 5.20. As mentioned before, four electrical strain gauges were attached, one at each of the four flange tips of the H section at mid-height of column 16 (pilot test column). For the other fifteen columns, one or two strain gages were attached at the center of each flange of the H section at the column mid-height (Figures 4.10 and 4.11).

Concrete strains were evaluated by means of two linear variable displacement transducers (LVDTs) centered vertically at mid-height of the compression and the tension faces of each specimen with a gauge length of 250 mm as shown in Figure 4.12.

The steel yield strains which were obtained from the coupon tensile tests (Table 4.1) varied between 0.154 % and 0.17% and the concrete ultimate strains were between 0.25% and 0.4%. None of the tested columns that failed at the mid-height reached the yield strain at loads less than 95% of the failure load. It can be seen from load-strain results for columns 3, 6, 9, 11, 12, 13, 14, 15, and 16, which failed at the mid-height, that the strains reached the yield strain and the ultimate concrete strain at compression side, while the strains in the steel flange at the tension zone was next to reach yield. In contrast, it can be seen from similar results for columns 1, 2,

4, 5, 7, 8, and 10, which failed at the column end that the compression steel flange did not reach the yield strain because strain gages were attached at mid-height. However, the ultimate concrete strain reached in these columns. In addition, for all columns, none of the tension steel flanges reached the yield strain at failure, this is possibly due to low moment compared to axial load.

It was noticed that the strains in columns encased in LWAC (columns No. 13 and 15) were lower than that encased in normal concrete (columns No. 15), this indicate that LWAC columns are less ductile than those of normal concrete. The experimental observations, as well as the strain curves show that columns encased in LWAC or normal concrete have more resistance to the deformation than bare steel columns.

The effect of steel ratio on strain values is insignificant as indicated when comparing columns 1, 2, and 3 of steel ratio of 4% and height of 2 m, to columns 4, 5, and 6 of 6% steel ratio and the same height. This can be noticed also from comparing columns 7, 8, and 9 of steel ratio of 4% and height of 3 m, to columns 10, 11, and 12 of 6% steel ratio and the same height.

The ACI recommendation of 0.003 as the maximum usable concrete strain appear to be an acceptable lower bound for lightweight aggregate concrete columns.

4, 5, 7, 8, and 10, which failed at the column end that the compression steel flange did not reach the yield strain because strain gages were attached at mid-height. However, the ultimate concrete strain reached in these columns. In addition, for all columns, none of the tension steel flanges reached the yield strain at failure, this is possibly due to low moment compared to axial load.

It was noticed that the strains in columns encased in LWAC (columns No. 13 and 14) were lower than that encased in normal concrete (columns No. 15), this indicate that LWAC columns are less ductile than those of normal concrete. The experimental observations, as well as the strain curves show that columns encased in LWAC or normal concrete have more resistance to the deformation than bare steel columns.

The effect of steel ratio on strain values is insignificant as indicated when comparing columns 1, 2, and 3 of steel ratio of 4% and height of 2 m, to columns 4, 5, and 6 of 6% steel ratio and the same height. This can be noticed also from comparing columns 7, 8, and 9 of steel ratio of 4% and height of 3 m, to columns 10, 11, and 12 of 6% steel ratio and the same height.

The ACI recommendation of 0.003 as the maximum usable concrete strain appear to be an acceptable lower bound for lightweight aggregate concrete columns.

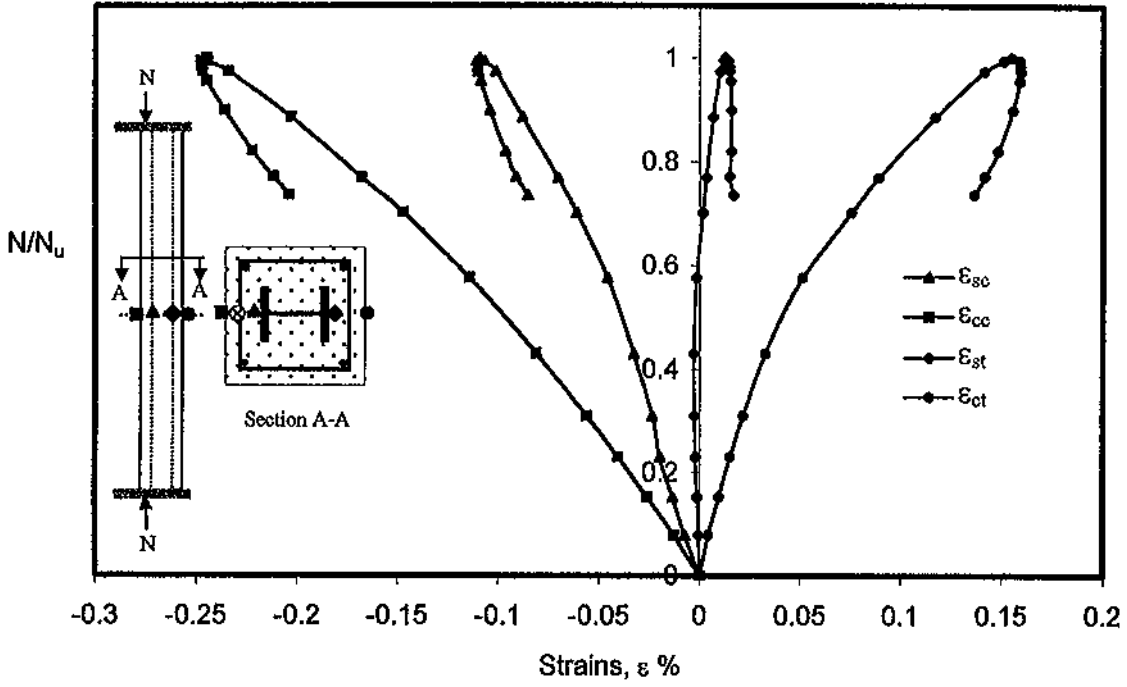


Figure 5.5 Strains in Steel and Concrete at Mid-height of Column No.1

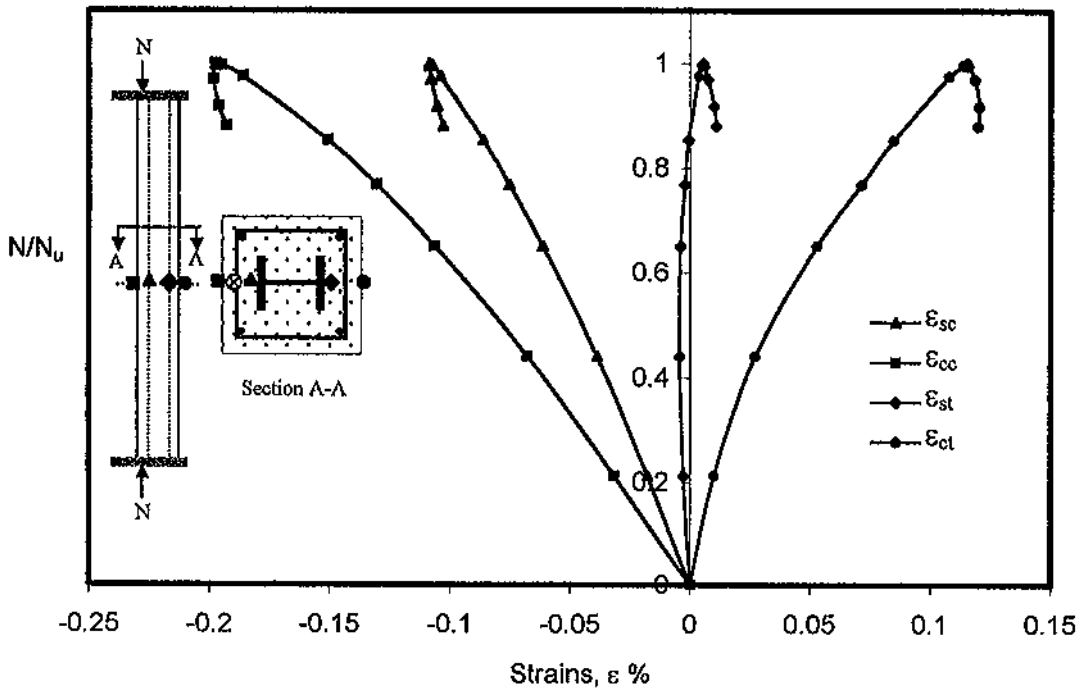


Figure 5.6 Strains in Steel and Concrete at Mid-height of Column No.2

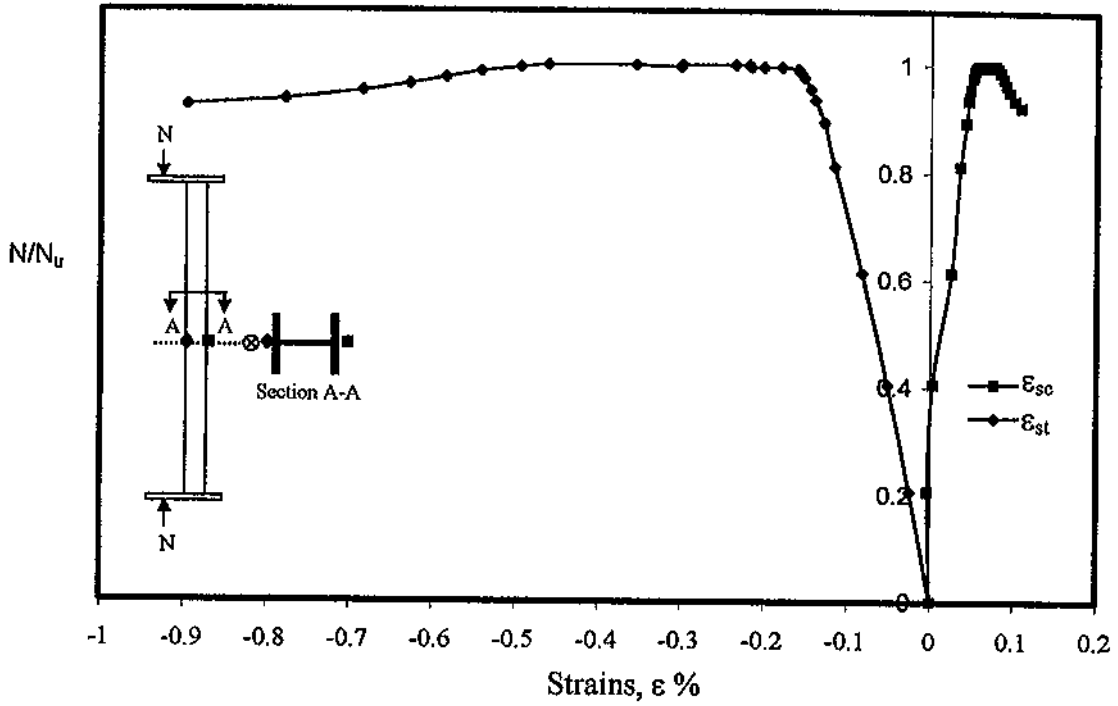


Figure 5.7 Strains in Steel at Mid-height of Column No. 3

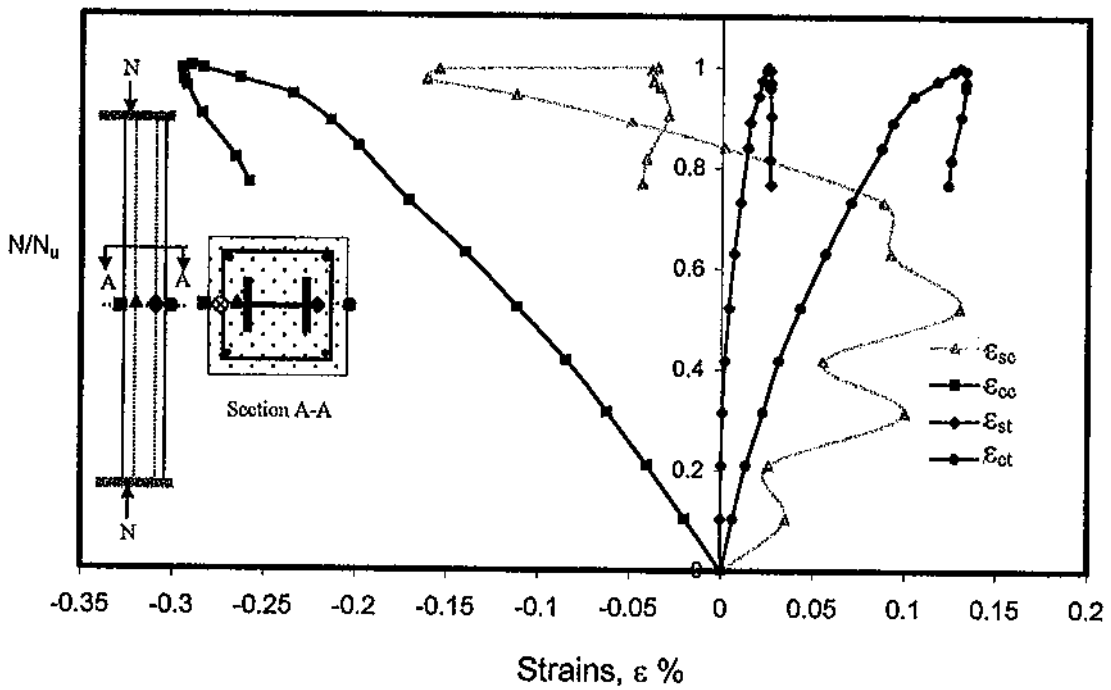


Figure 5.8 Strains in Steel and Concrete at Mid-height of Column No. 4

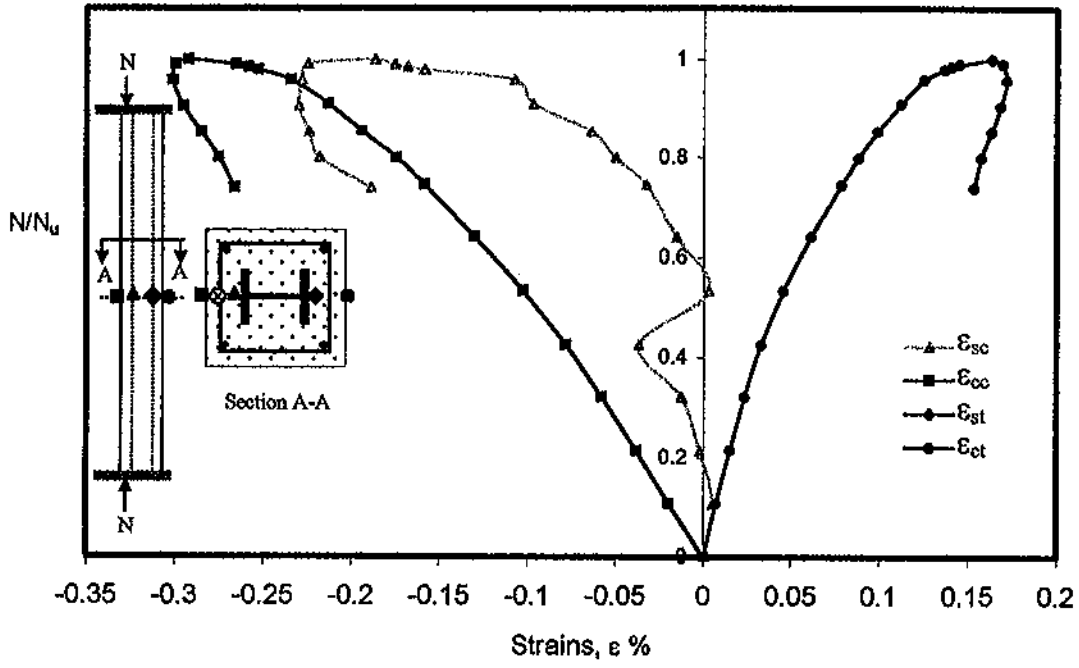


Figure 5.9 Strains in Steel and Concrete at Mid-height of Column No.5

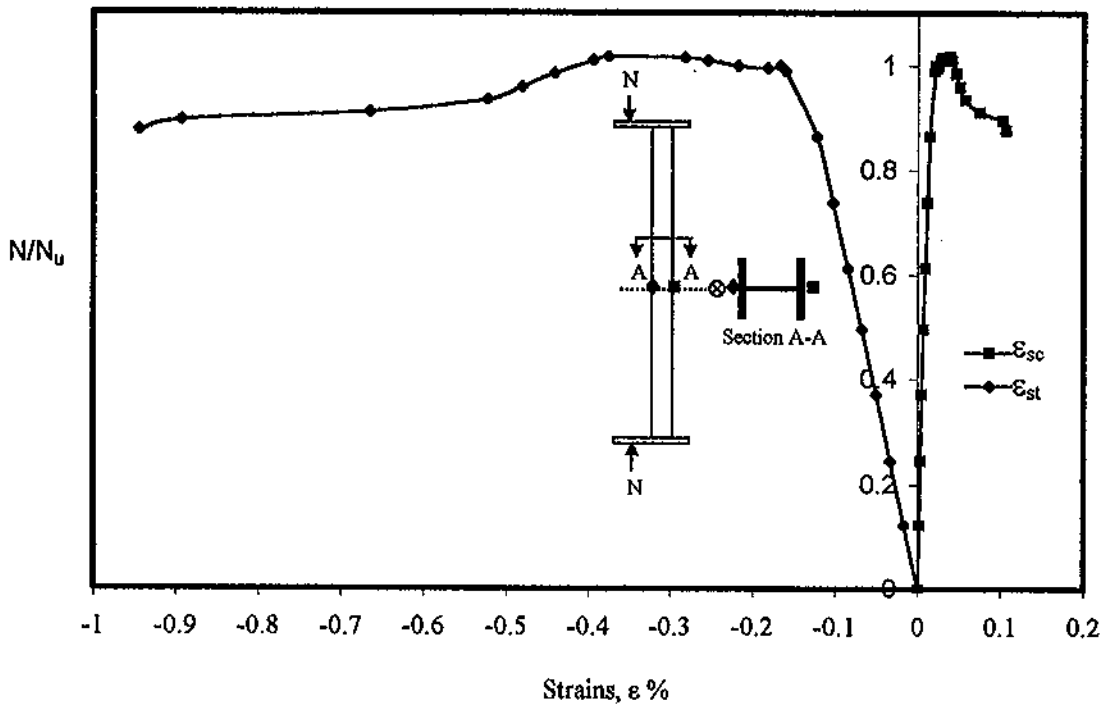


Figure 5.10 Strains in Steel at Mid-height of Column No. 6

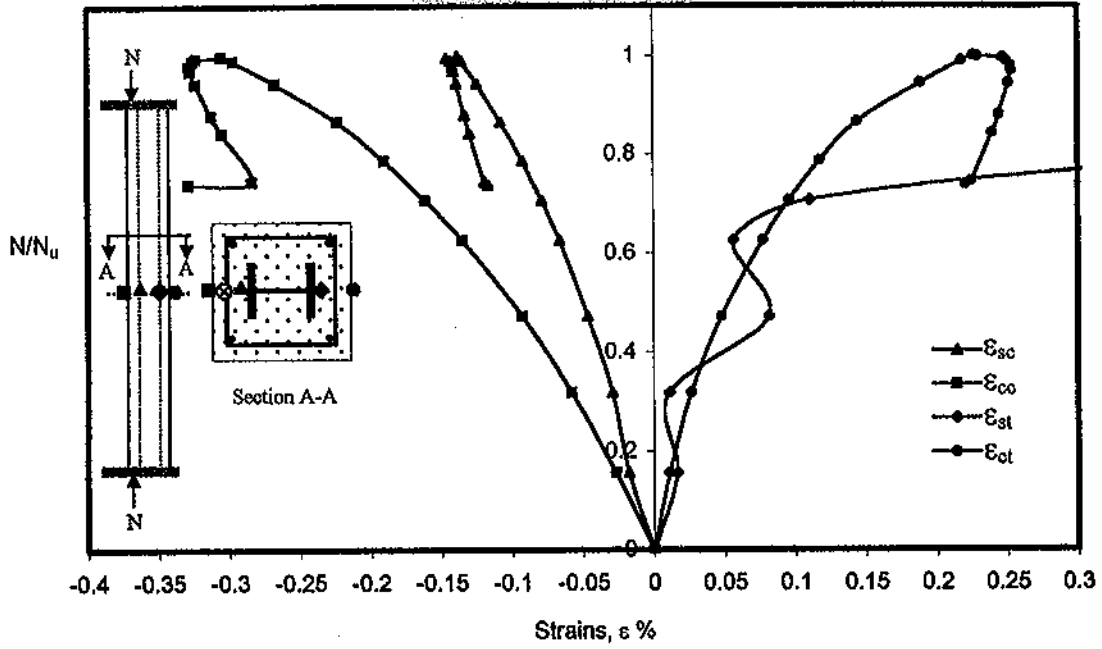


Figure 5.11 Strains in Steel and Concrete at Mid-height of Column No.7

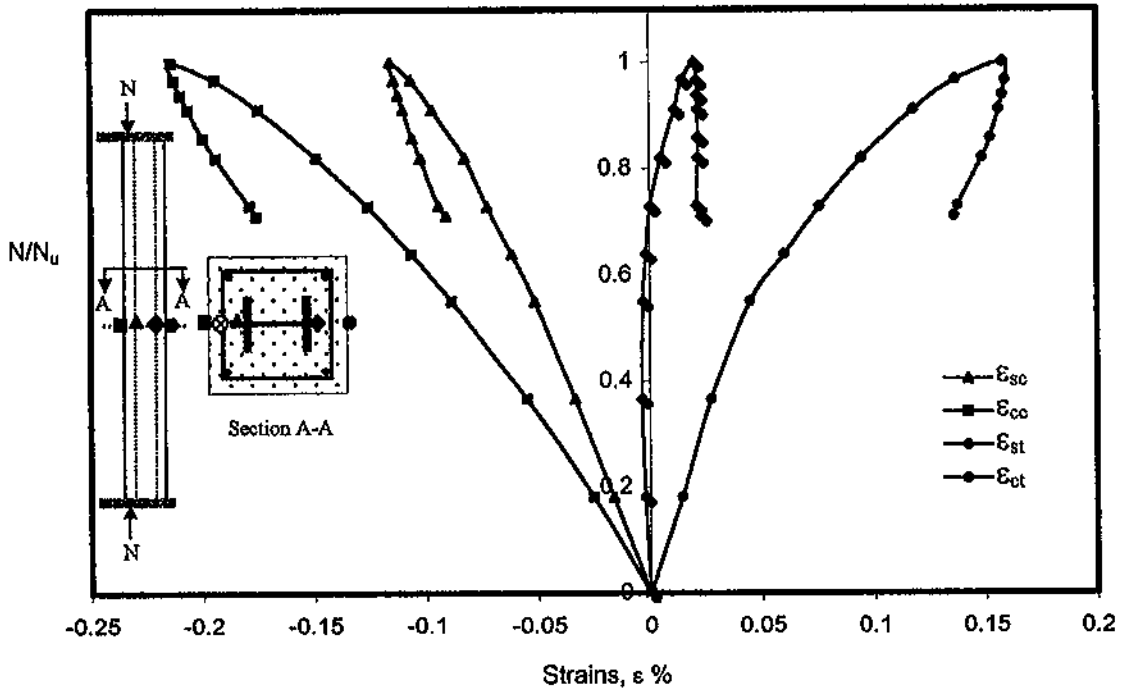


Figure 5.12 Strains in Steel and Concrete at Mid-height of Column No.8

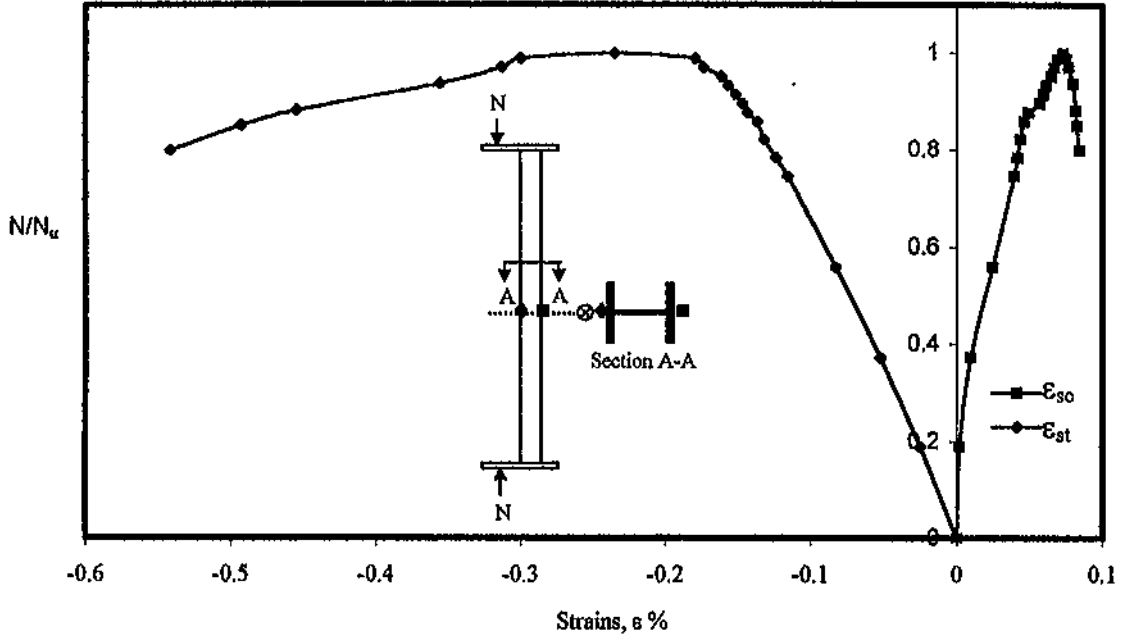


Figure 5.13 Strains in Steel at Mid-height of Column No. 9

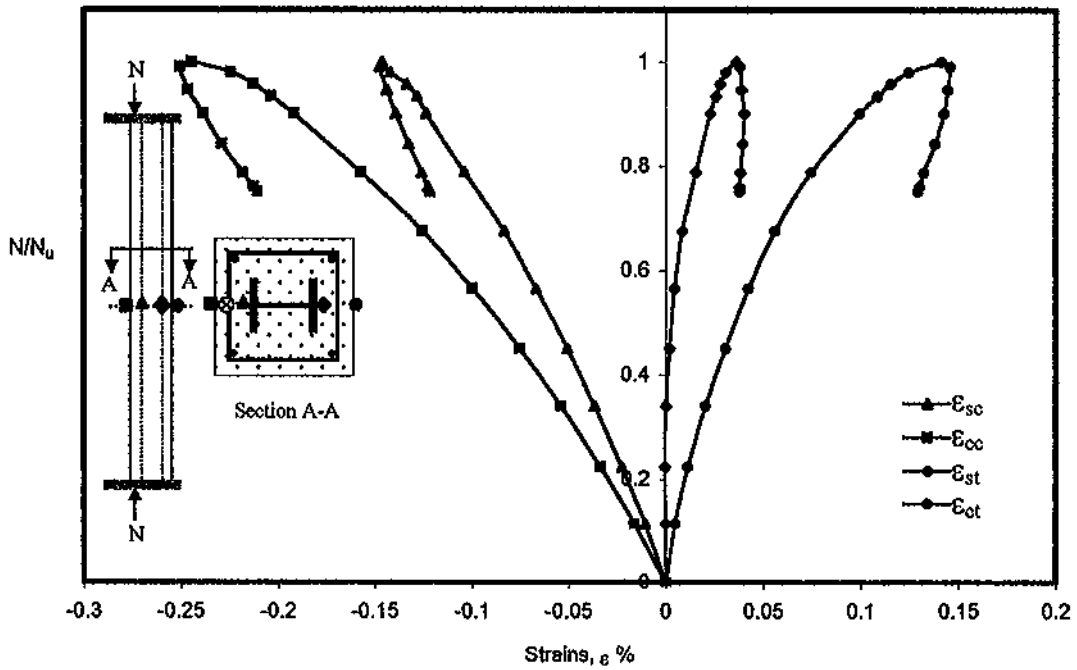


Figure 5.14 Strains in Steel and Concrete at Mid-height of Column No.10

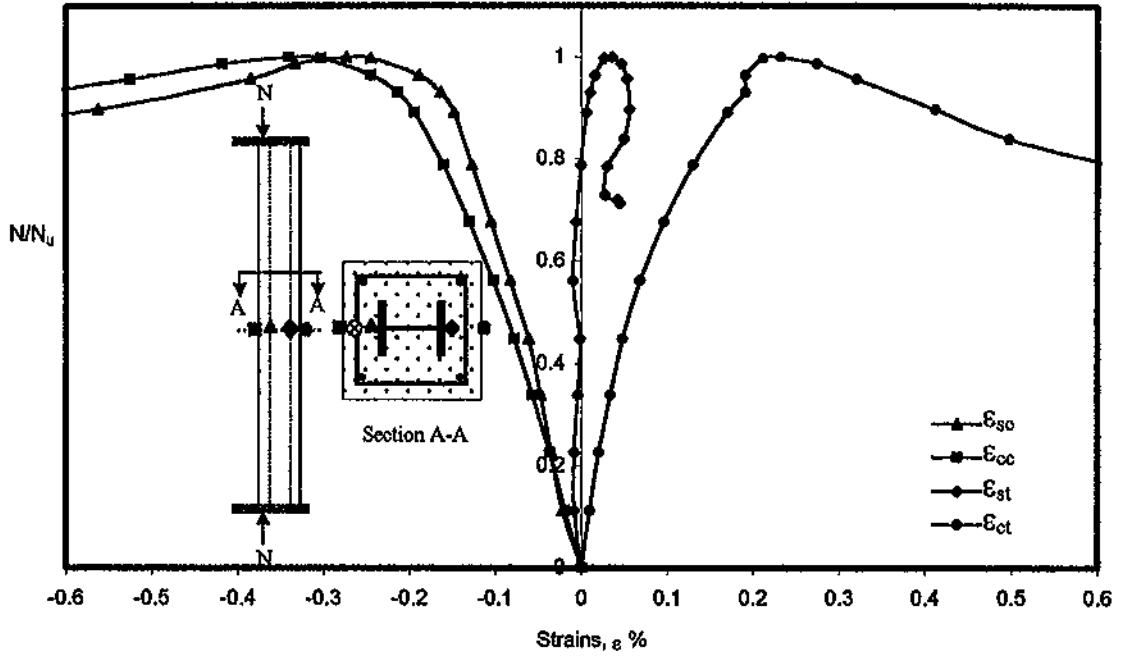


Figure 5.15 Strain in Steel and Concrete at Mid-height of Column No. 11

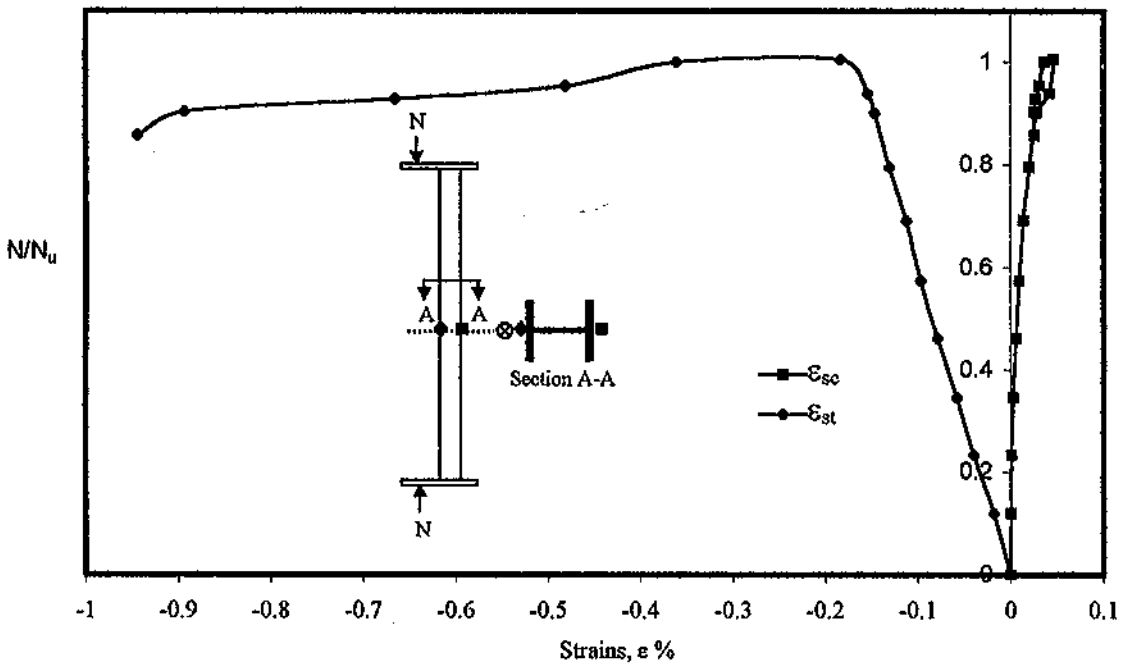


Figure 5.16 Strains in Steel at Mid-height of Column No. 12

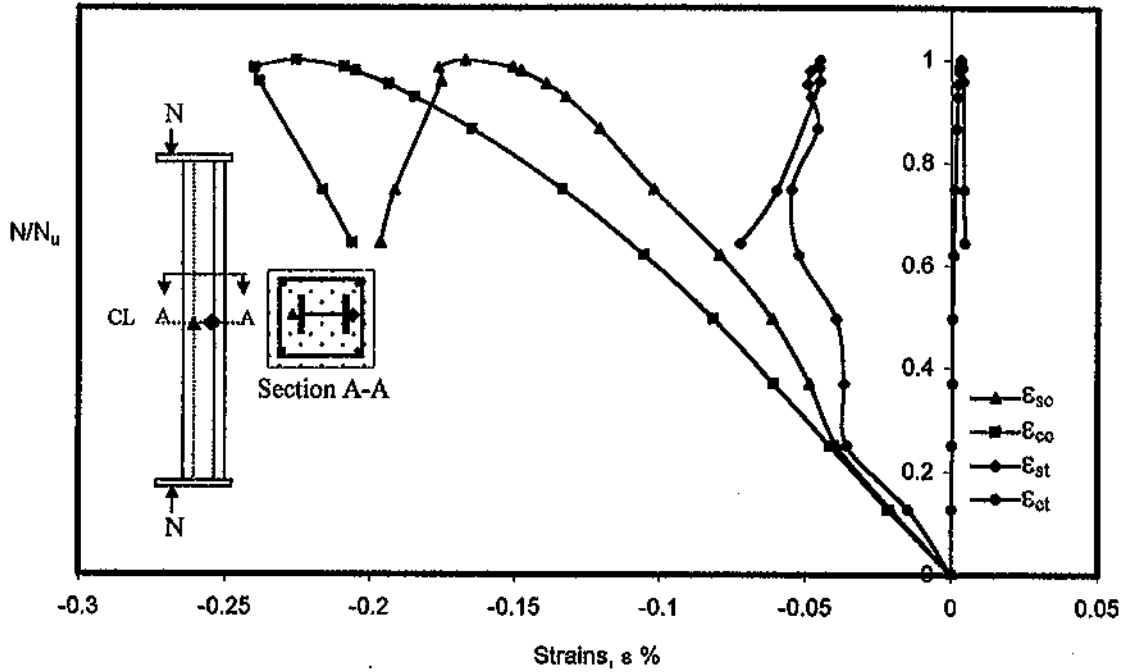


Figure 5.17 Strains in Steel and Concrete at Mid-height of Column No.13

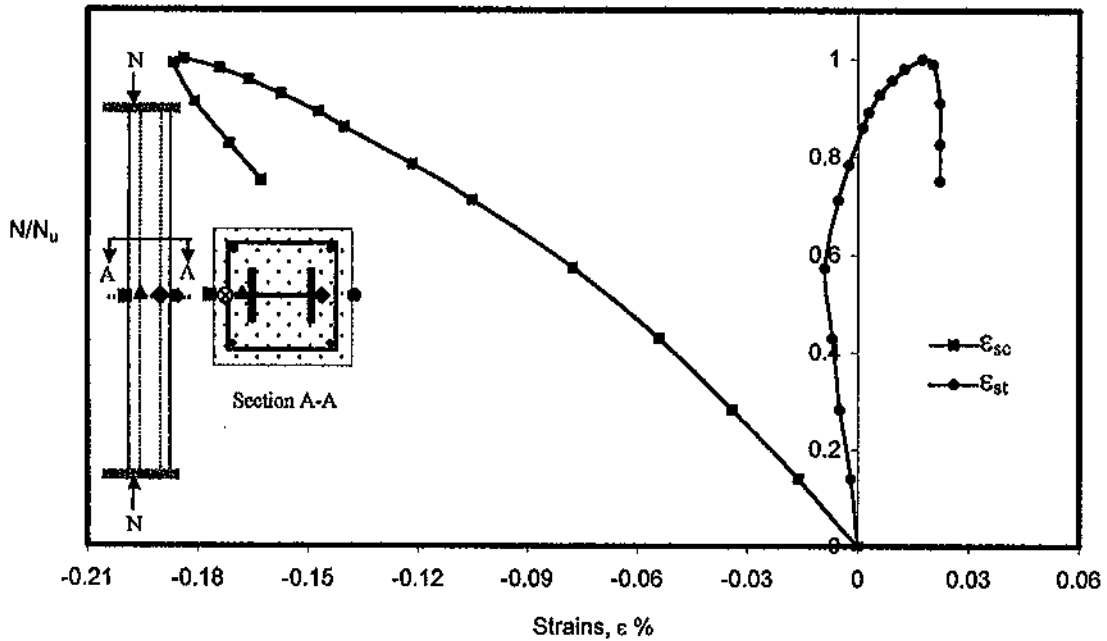


Figure 5.18 Strains in Steel and Concrete at Mid-height of Column No. 14

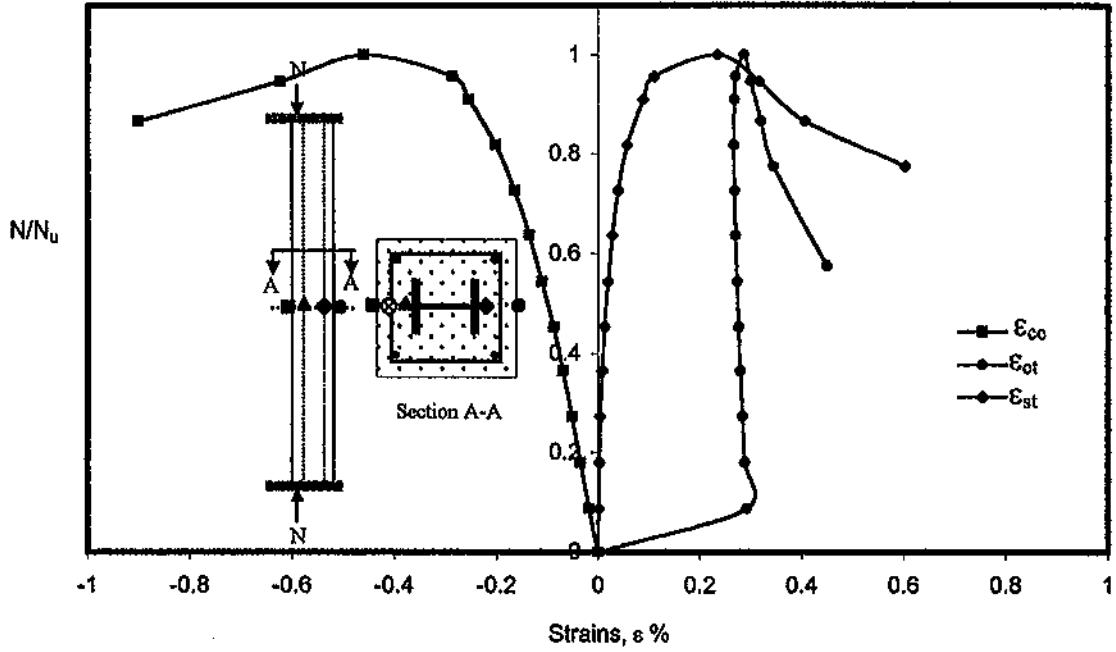


Figure 5.19 Strains in Steel and Concrete at Mid-height of Column No. 15

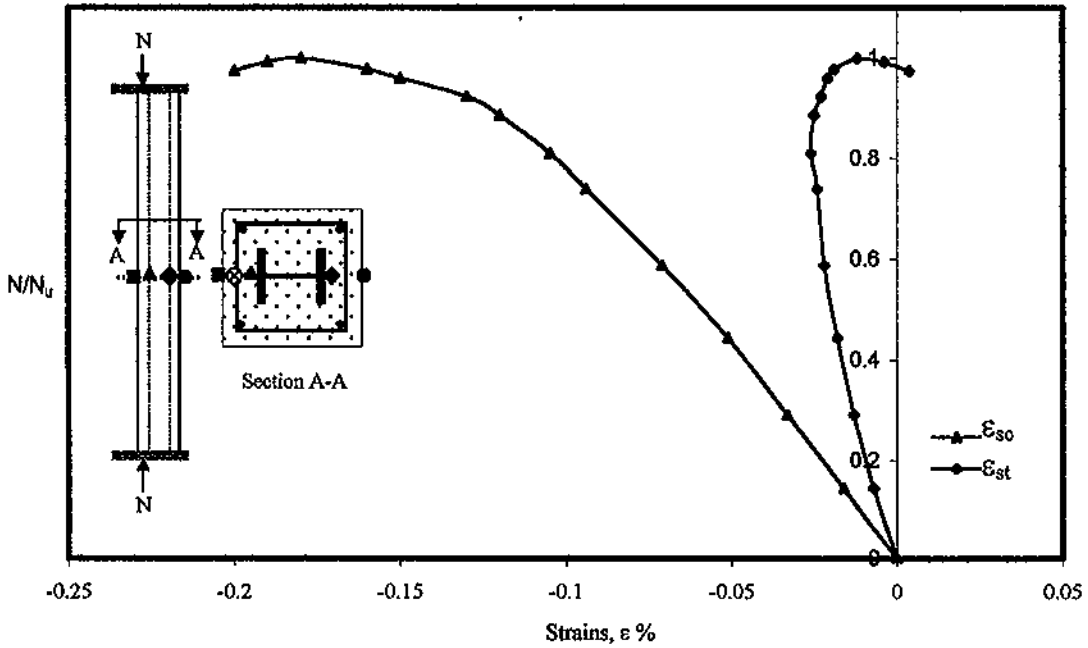


Figure 5.20 Strains in steel at Mid-height of column No. 16

The composite action was also confirmed by plotting the strains measured in steel and concrete across the column section at mid-height. Strain distribution in the mid-height section of columns 1, 6, and 11, at several load levels, are shown in Figure 5.21. As seen from the figure, the

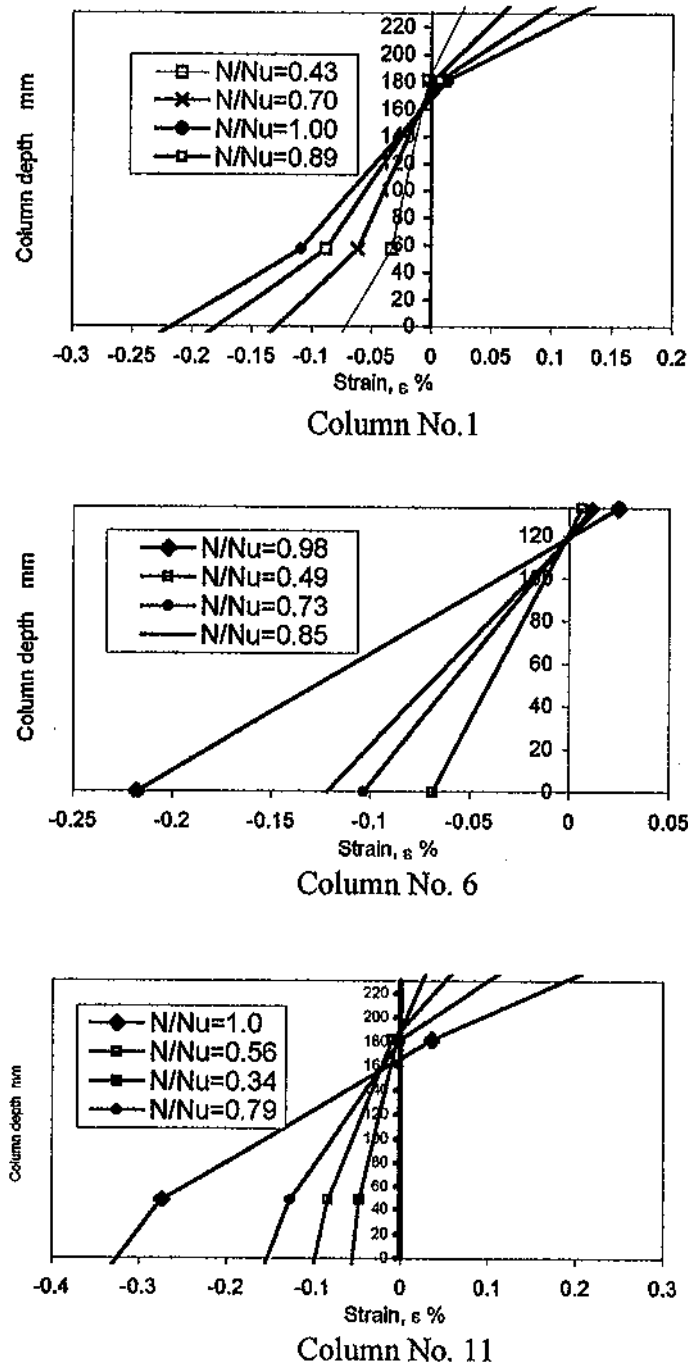


Figure 5.21 Mid-Height Strain Distribution Across the Section at Different N/N_u Ratios for Columns 1, 6, and 11

applied load and moment were resisted by the action of composite section. This is seen from approximately linear variation of strain distribution across the section as recorded in the structural steel section and the concrete encasement. This linear strain distribution across the section was maintained up to over 90% of the failure load, above which the strain in steel and concrete did not exhibit similar linear relationships. It should be mentioned that the strain distribution for the rest of the columns are similar to those presented in Figure 5.21.

5.5 Deflections

Deflections including lateral displacement in the major and the minor axes directions and axial shortening will be discussed in the following two sections.

5.5.1 Lateral Deflections

Lateral deflections in the directions of the major and the minor axes at mid-height of all columns were plotted against the applied load as shown in Figures 5.22 to 5.26. Furthermore, these curves show the effect of concrete type, steel ratio, column height, and eccentricity value on the deflections and on the behavior of the columns.

All columns were tested under major axis bending and showed very small deflections in the minor axis direction especially for concrete-

encased columns. These deflections were very small and started to increase at loads more than 90% of the failure load for bare steel columns, while for concrete encased columns, started to increase beyond failure load.

The load-deflection curves confirm the visual observations that the type of failure the column exhibited indicated that some columns, such as bare steel sections, failed due to overall buckling. Some of the columns encased in lightweight aggregate concrete exhibit overall buckling, while some of them exhibit local buckling at 70% of the failure load, and when the column reached failure load an overall buckling took place. Nevertheless, such negative effect (local buckling) did not significantly reduce the load bearing capacity of the column. However, two columns with normal concrete exhibit overall buckling with no signs of local buckling prior to failure, while the third one exhibit local buckling, and at failure load an overall buckling took place.

For lightweight aggregate concrete-encased columns, the deflections about the major axis were very small at low loads and started to increase at loads between 20-30% of the failure load as shown in Figures 5.24 and 5.26.

It can be seen from the figures, that columns encased in lightweight aggregate concrete exhibited less lateral deflection than those incased in normal concrete and the bare steel columns.

The steel ratio has insignificant effect on the lateral deflections as shown in figure 5.22 for columns of steel ratio of 4% and Figure 5.23 for columns of steel ratio of 6%.

The effect of column height was significant, longer columns exhibited more deformations; this is shown by comparing Figures 5.22 and 5.23, which have a height of 2m, to Figures 5.24 to 5.23 which have a height of 3m.

Referring to Figures 5.24 and 5.26 where the columns have eccentricities of 70 mm and 40 mm, respectively, it can be seen that the increase in eccentricity cause considerable increase in lateral deflection.

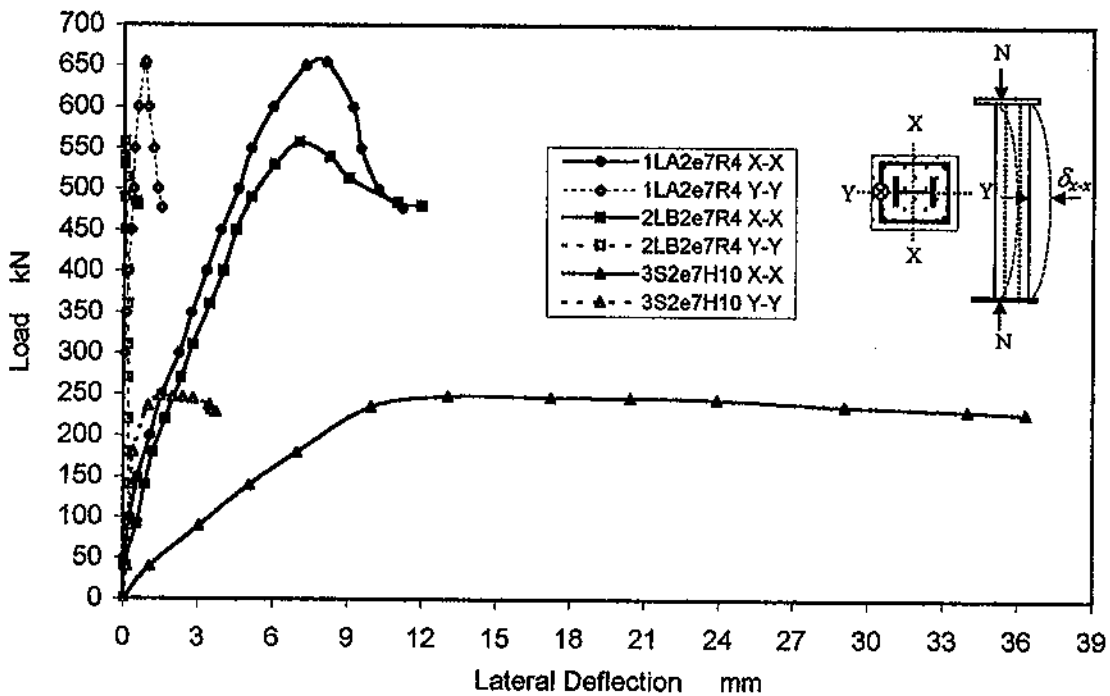


Figure 5.22 Load-Lateral Deflection Curves about Major and Minor Axes at Mid-height of Columns 1, 2, and 3

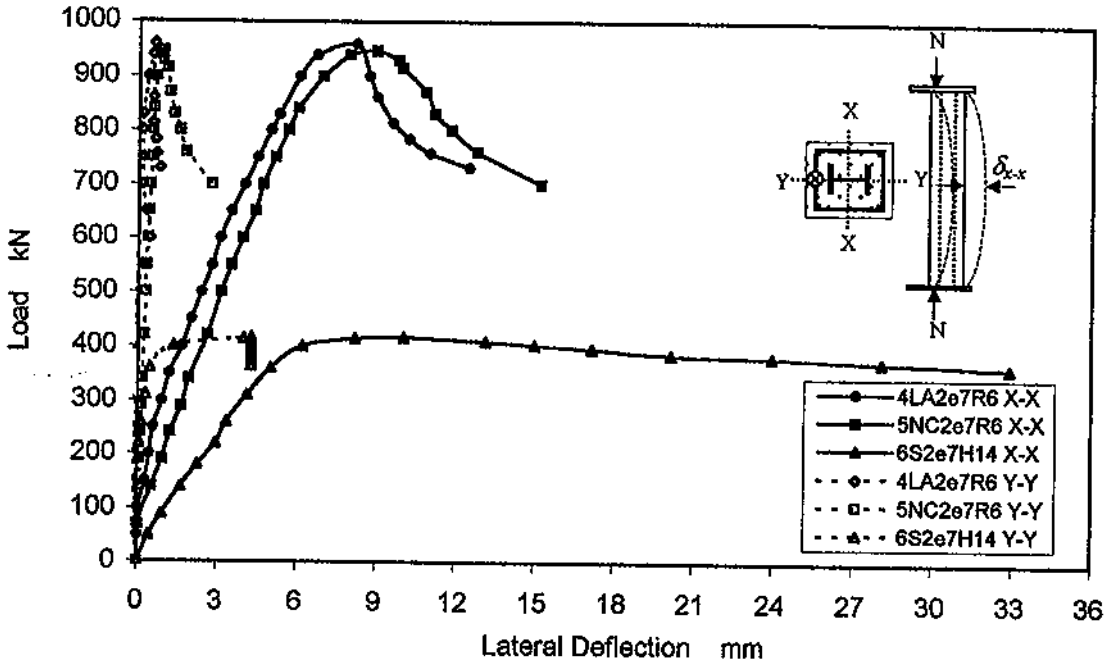


Figure 5.23 Load-Lateral Deflection Curves about Major and Minor Axes at Mid-height of Columns 4, 5, and 6

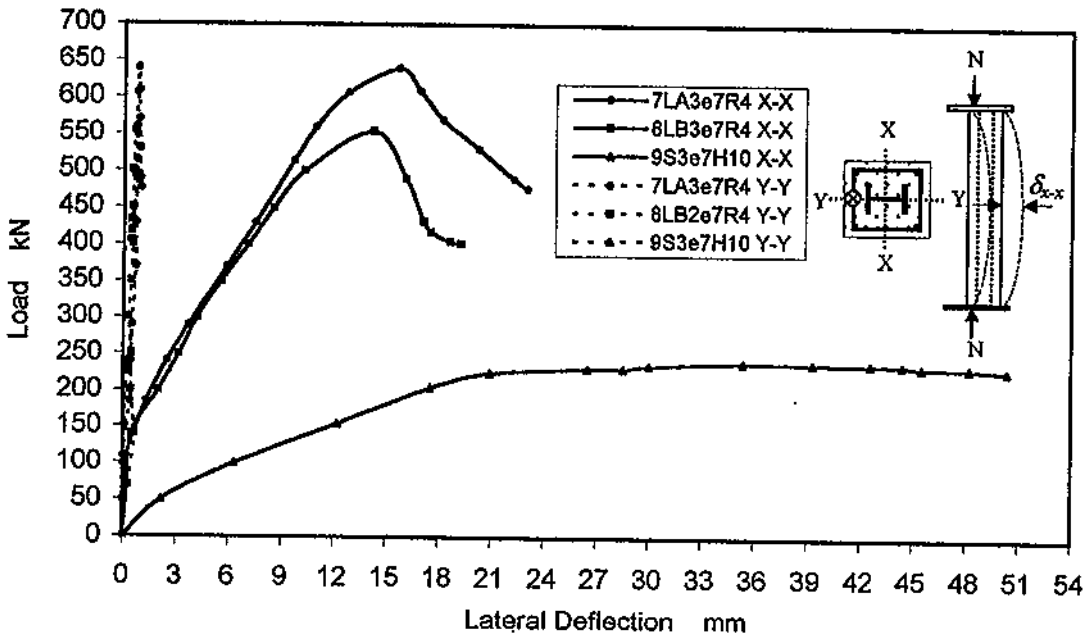


Figure 5.24 Load-Lateral Deflection Curves about Major and Minor Axes at Mid-height of Columns 7, 8, and 9

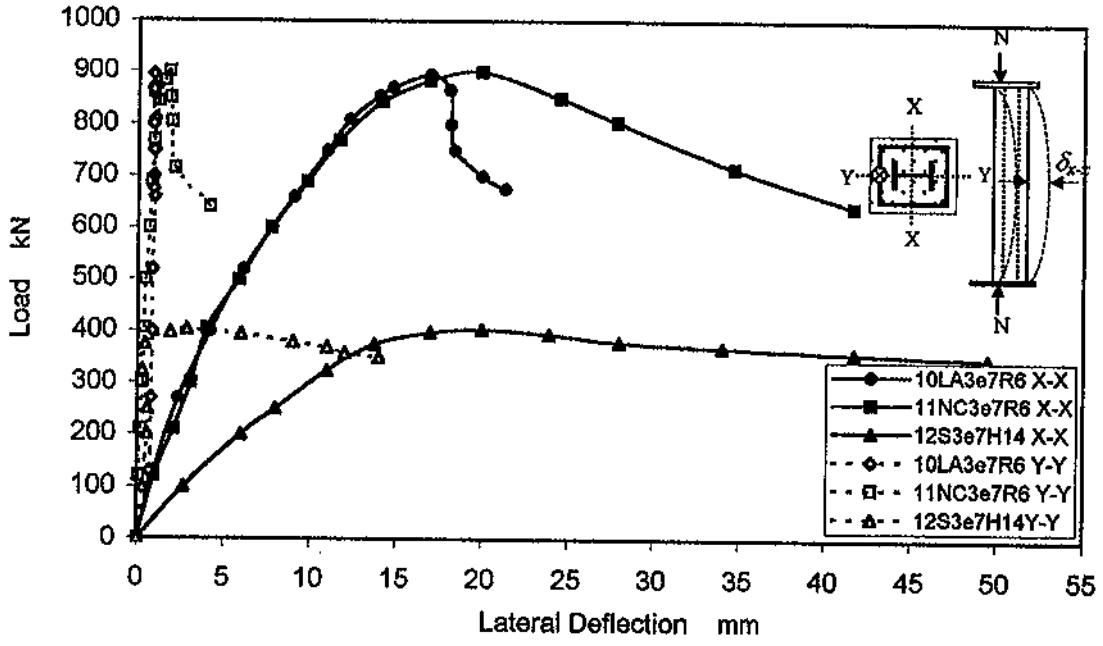


Figure 5.25 Load-Lateral Deflection Curves about Major and Minor Axes at Mid-height of Columns 10, 11, and 12

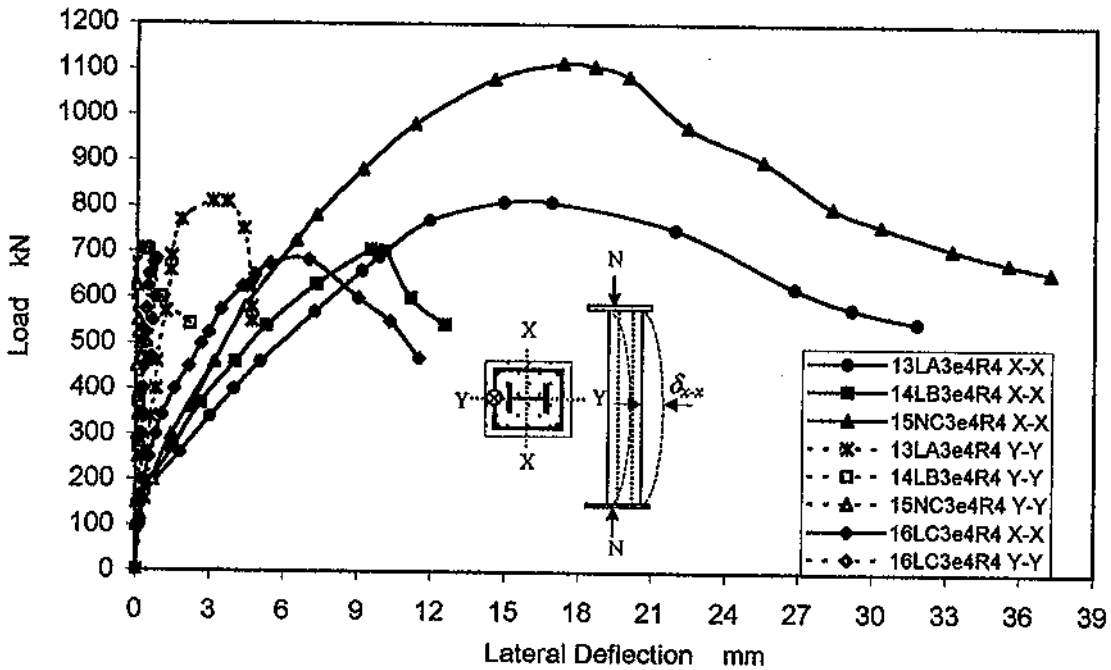


Figure 5.26 Load-Lateral Deflection Curves about Major and Minor Axes at Mid-height of Columns 13, 14, 15, and 16

5.5.2 Axial Shortening

The load-axial shortening results were recorded for all column specimens, and these are illustrated for both LWAC and normal concrete encased columns in addition to the bare steel columns in Figures 5.27 to 5.31. The load-axial shortening curves were used in ascertaining the onset of yielding of each test, together with the determination of the ultimate load of each individual member. It can be seen from the Figures that the axial shortening increase slowly with the increase in the load up to failure then it increase faster with the load decrease especially for bare steel columns.

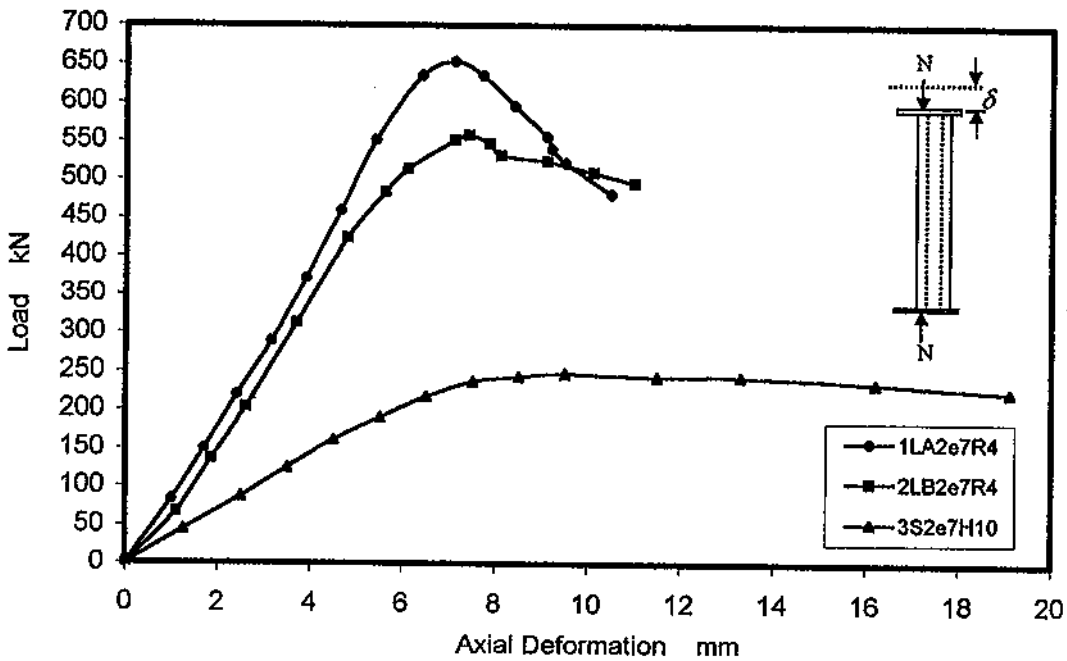


Figure 5.27 Load Versus Axial Shortening of Columns 1, 2, and 3

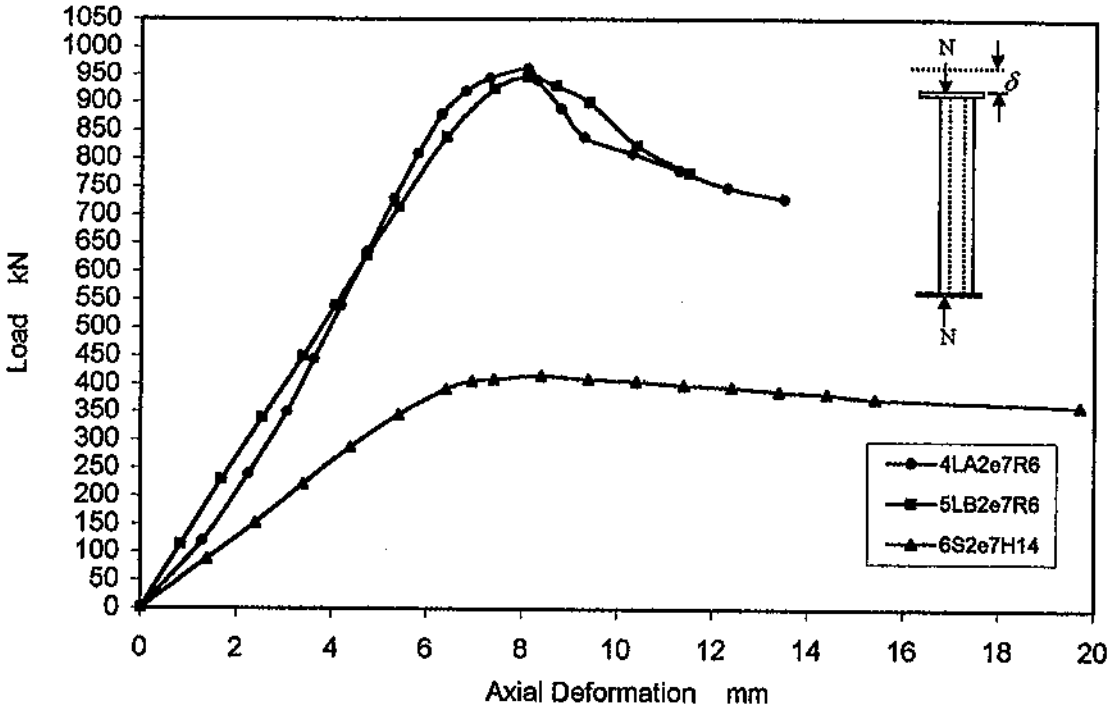


Figure 5.28 Load Versus Axial Shortening of Columns 4, 5, and 6

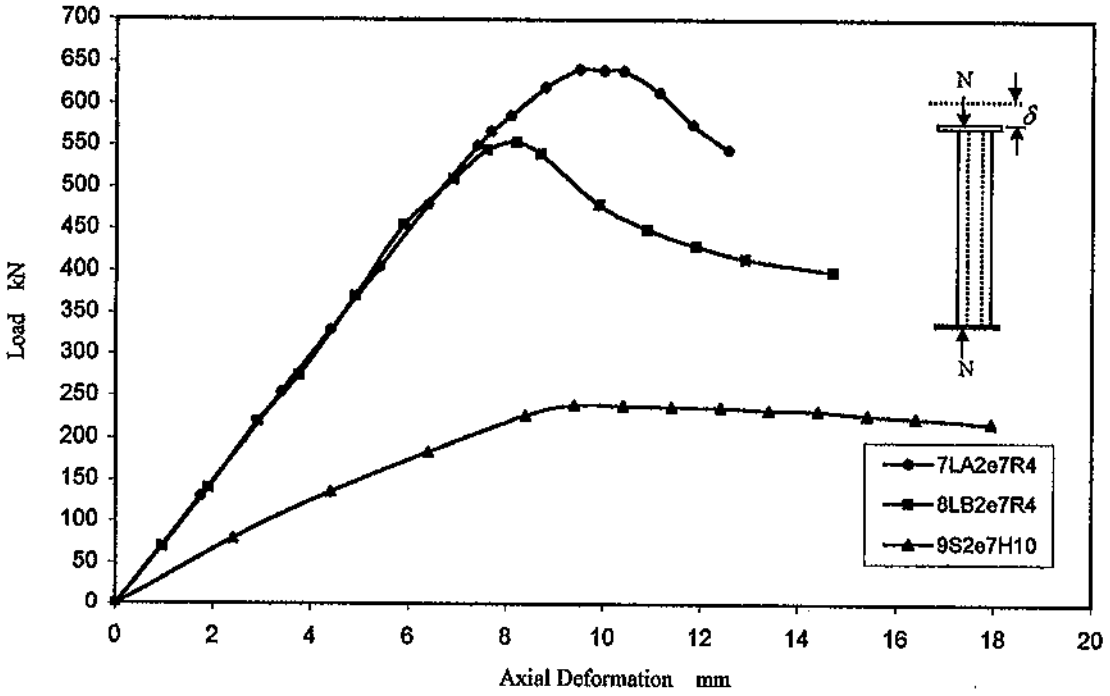


Figure 5.29 Load Versus Axial Shortening of Columns 7, 8, and 9

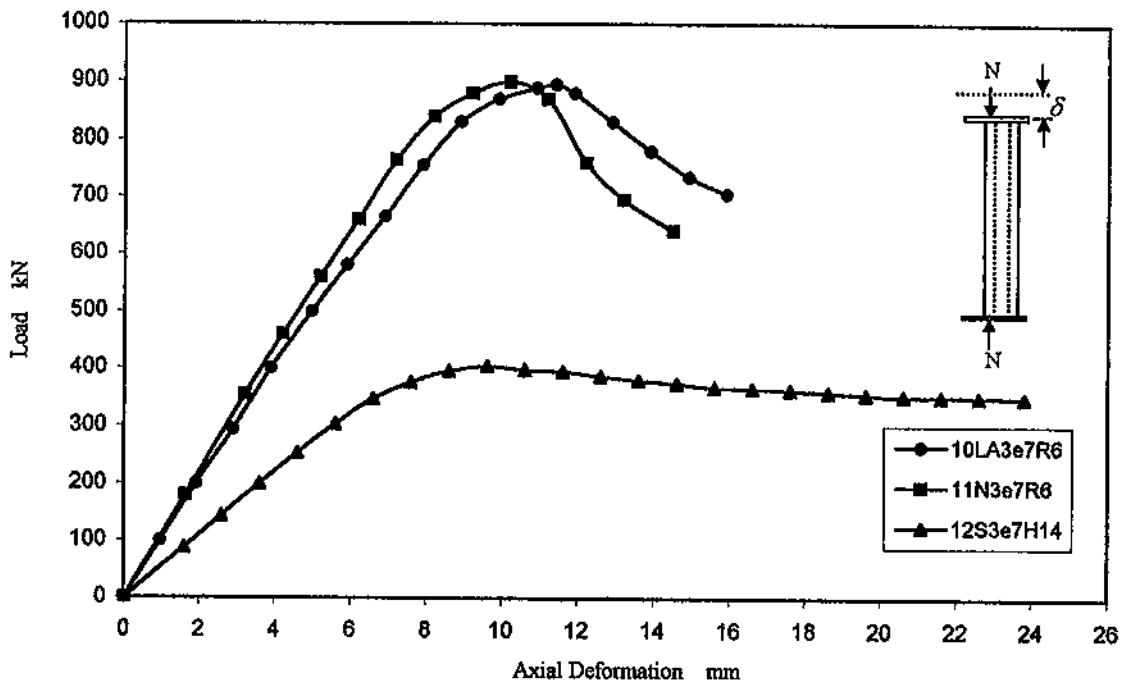


Figure 5.30 Load Versus Axial Deformation of Columns 10, 11, and 12

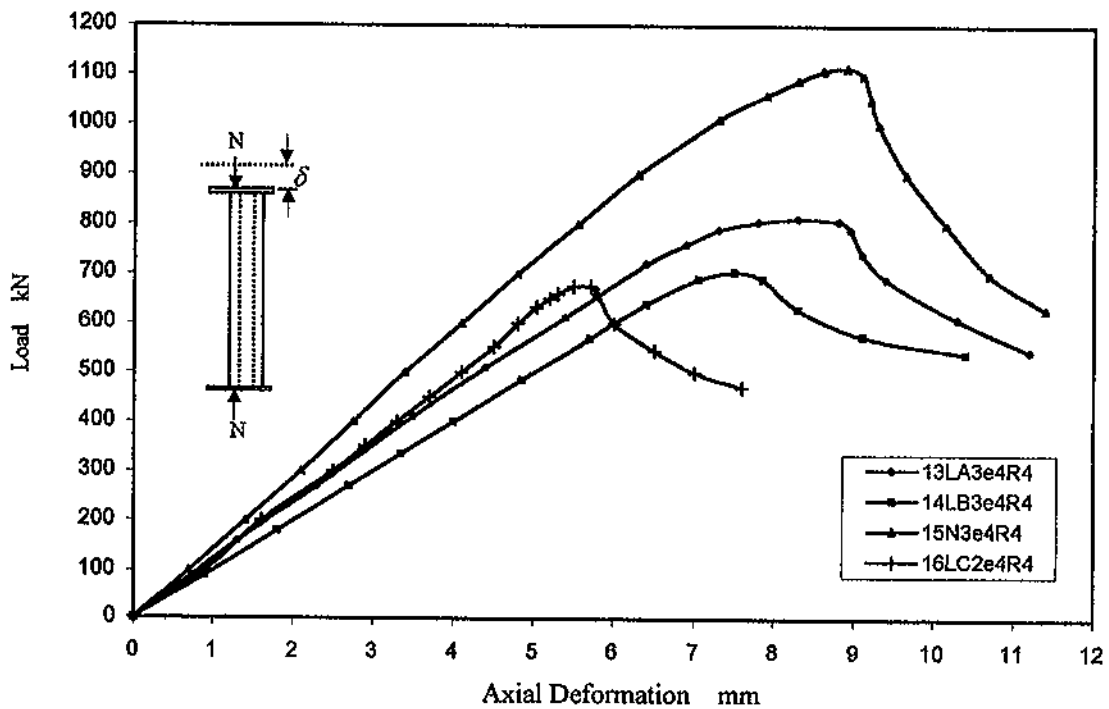


Figure 5.31 Load Versus Axial Shortening of Columns 13, 14, 15, and 16

5.6 Moment-Thrust-Curvature Relationship

The moment-thrust-curvature relationships were determined from the strain distribution across the column section at mid-height. Plots of the moment-thrust-curvature for all column specimens are presented in Figures 5.32 to 5.36.

The curvature value at each load level was determined by taking the average of the two strain values on each steel flange and concrete strains at the compression and tension faces, as follow:

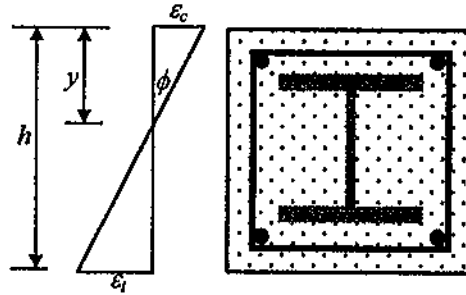
$$\phi = \frac{\epsilon_c}{y}$$

and

$$y = h \frac{\epsilon_c}{\epsilon_c + \epsilon_t}$$

hence

$$\phi = \frac{\epsilon_c + \epsilon_t}{h}$$



where

- ϕ the curvature in radian/mm.
- y the distance from extreme fiber to the neutral axis.
- ϵ_c strain in most compressed fiber in concrete.
- ϵ_t strain in extreme concrete fiber in tension
- h column overall depth.

The experimental moment, M , is given by:

$$M_x = P_e(e_x + u)$$

where

- P_e applied load.
- e eccentricity of the applied load about the major axis.
- u deflection due to the applied load.

It can be seen from the curves that the stiffening effect of the lightweight concrete encasement is higher for low eccentricities and as the eccentricity increases the curvature decreases. This is because as the eccentricity increase a large area of concrete will be subjected to tension and hence cracked, thus causing a reduction in the stiffening effect of the concrete.

The increase in steel ratio cause a slight increase in curvature as shown in Figure 5.32 for columns having a steel ratio of 4% and in Figure 5.33 for columns having a steel ratio of 6%. For the same steel ratio, as the column height increase the curvature increase as shown when comparing columns of 2 m height in Fig. 5.32 to those having 3 m height in Fig. 5.34.

Composite columns exhibit less ductility than the bare steel columns. Furthermore, lightweight concrete encased columns have lower curvature than normal concrete encased columns as indicated in Figures 5.32 to 5.36.

The ductility of the column specimens may be assessed also by examining the difference in strains at $0.95 P_u$ before and after the peak load.

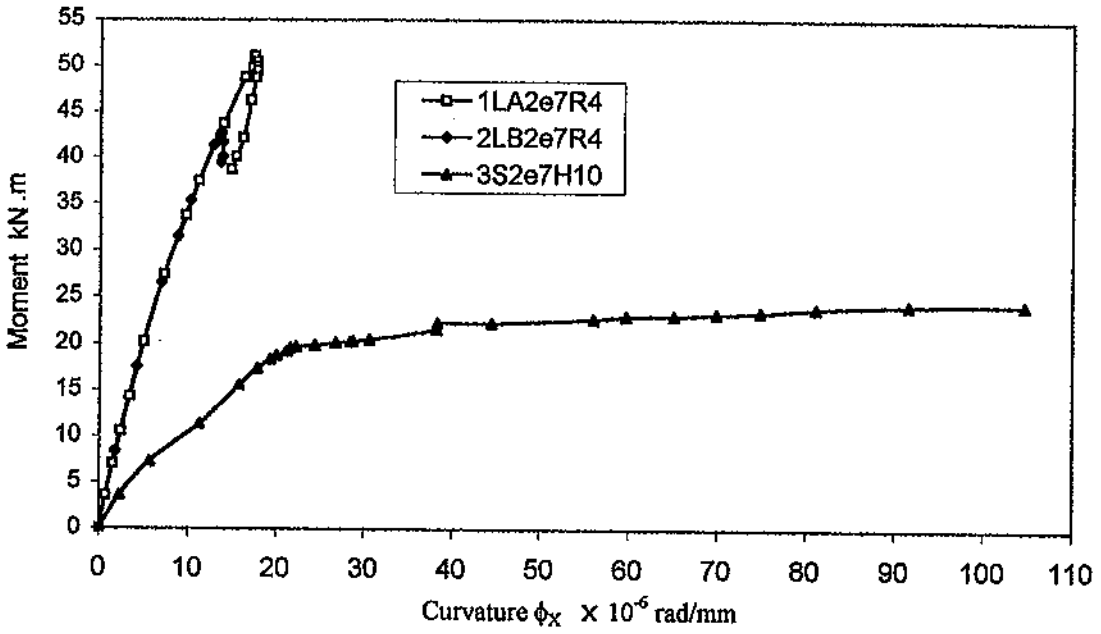


Figure 5.32 Moment-Thrust-Curvature Relationship about Major Axis at Mid-height for Columns 1, 2, and 3

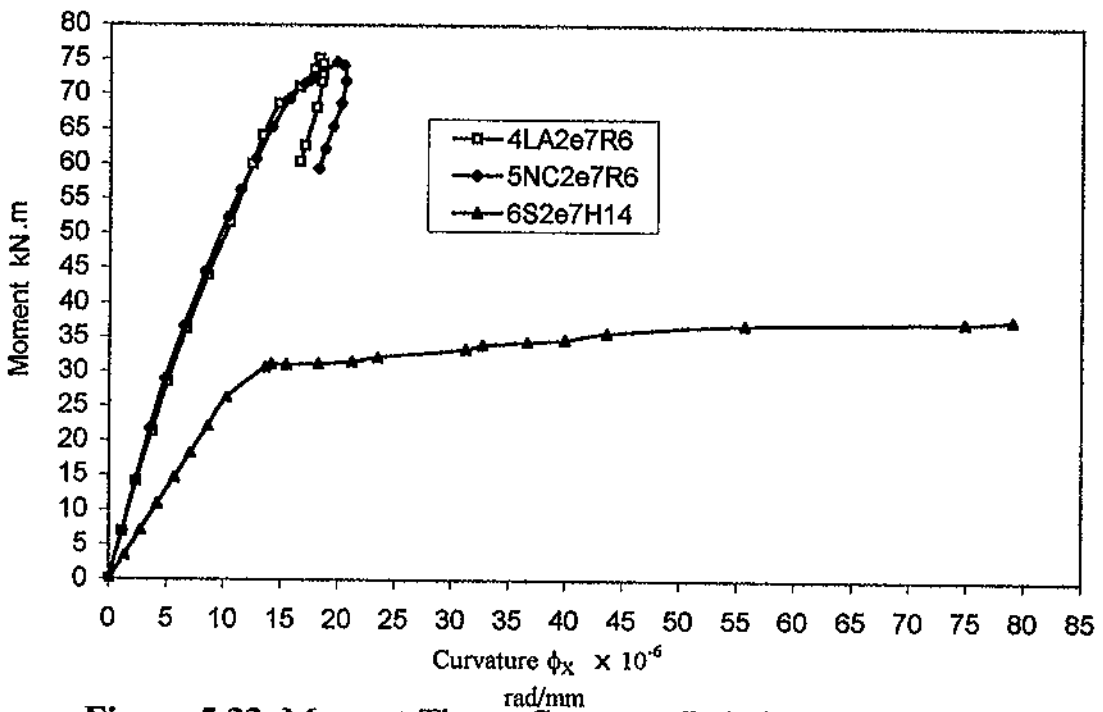


Figure 5.33 Moment-Thrust-Curvature Relationship about Major Axis at Mid-height for Columns 4, 5, and 6

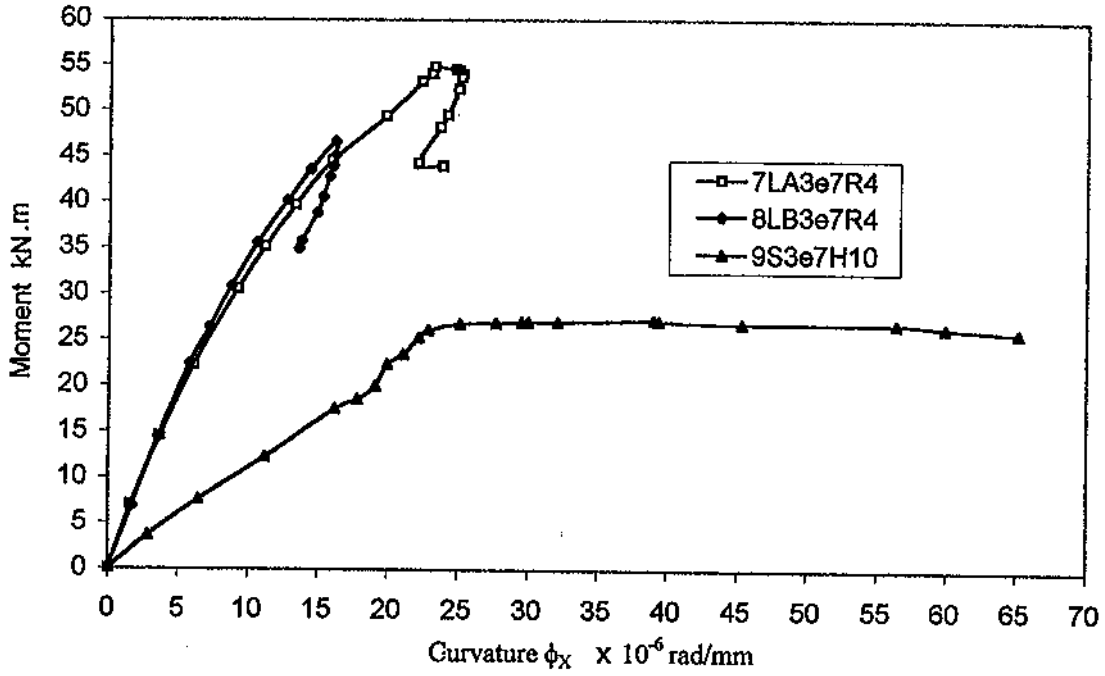


Figure 5.34 Moment-Thrust-Curvature Relationship about Major Axis at Mid-height for Columns 7, 8, and 9

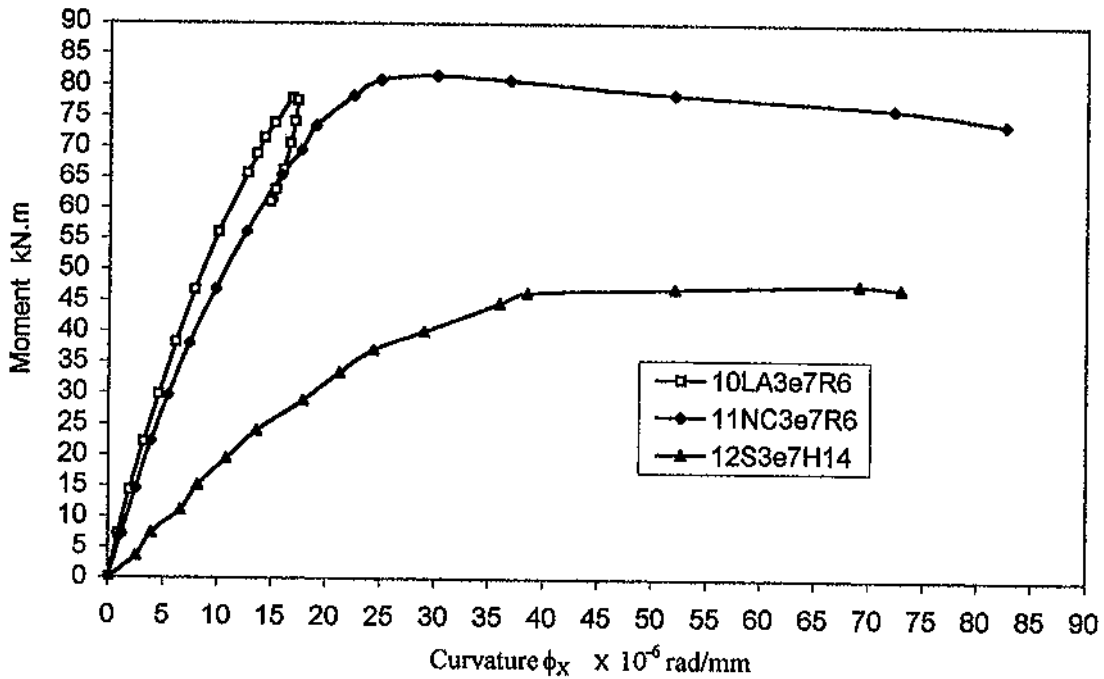


Figure 5.35 Moment-Thrust-Curvature Relationship about Major Axis at Mid-height for Columns 10, 11, and 12

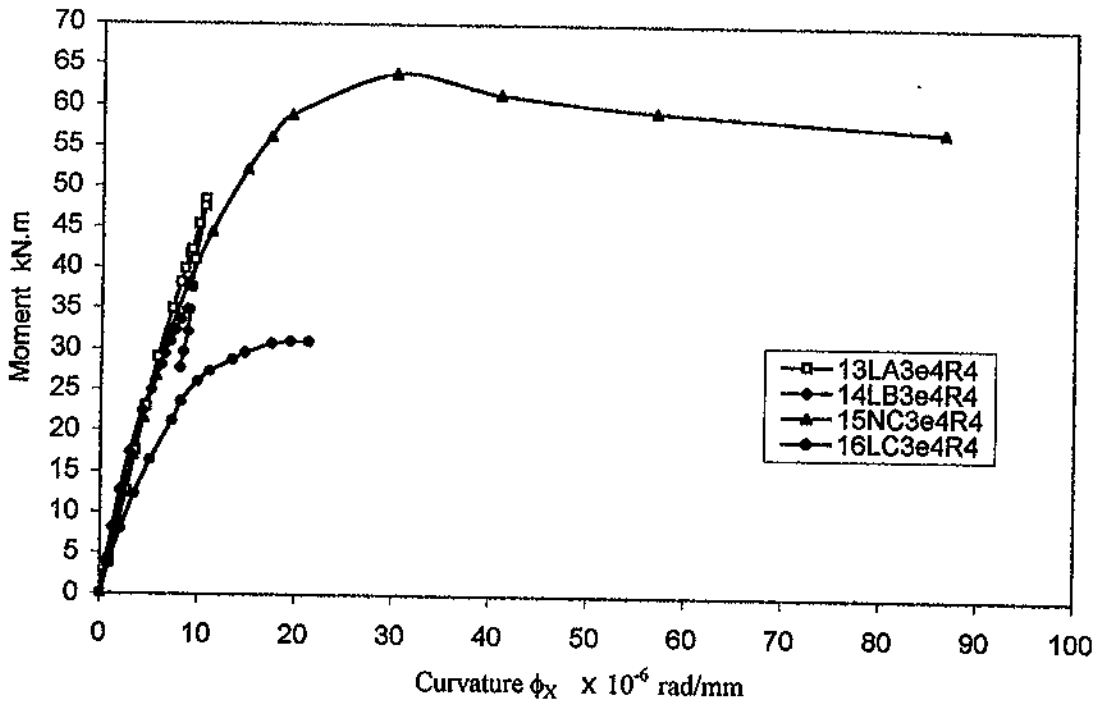


Figure 5.36 Moment-Thrust-Curvature Relationship about Major Axis at Mid-height for Columns 13, 14, 15, and 16

5.7 Separation and Bond

Separation between the concrete and the column end plates was observed in some specimens throughout the test especially at high load levels (usually more than 90% of the failure load). The separation occurred at the tension side and was very small (0-1 mm) in columns with 40 mm eccentricity and between 1 to 3 mm in columns with 70 mm eccentricity. The test results showed that the type of concrete has no distinct effect on separation. It seems that the relatively large separation in the lower end in some columns was due to localized effects as a result of the loading arrangements, which caused a rather high-localized compression force to

one face and tension in the other face of the column section. However, under design conditions (factored design load) the test results clearly show that the separation measured so far is very small and negligible.

The concrete encasement at the mid-height of column No. 16 was removed for inspection as shown in Figure 5.37. It is indicated that the

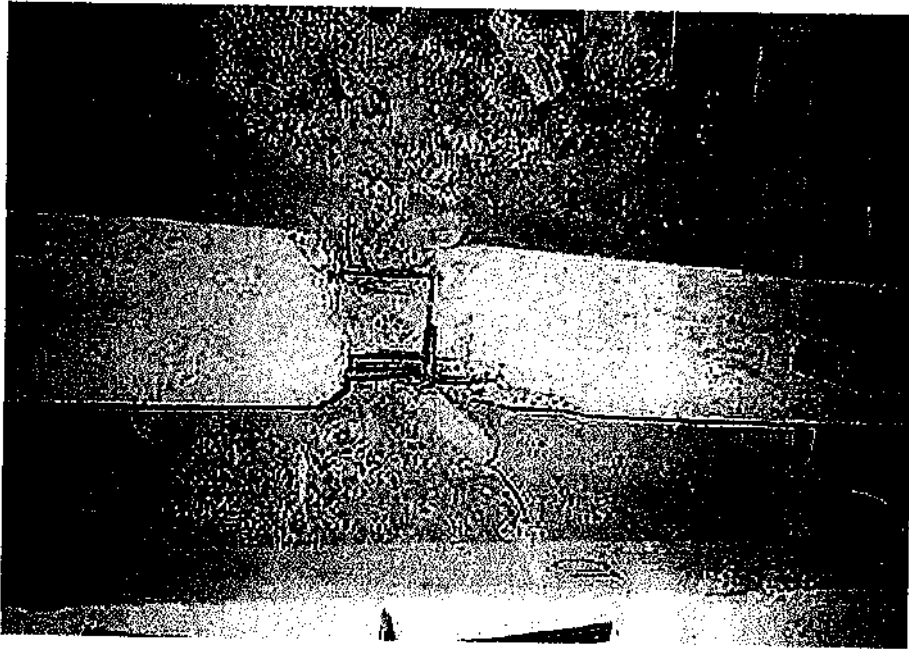


Figure 5.37 Mid-height Region of Column 16, with Part of Concrete Encasement Removed

bond, which existed between the H section and the concrete was strong and reliable. Furthermore, there is no sign for any local buckling in the compression steel flange at the crushed concrete position, thus the concrete encasement prevent steel local buckling.

5.8 Cracks

It was noticed that cracks developed quite early in the long columns

encased by LWAC and subjected to large eccentricities. However, in no case did the cracks seem to affect the load carrying capacity of the columns.

Columns of 2 m height and large eccentricity of 70 mm (columns 1, 2, 4, and 5) showed minor hairline cracks at a load ratio of about 60-70% of failure load on the tension sides of the specimens. Beyond the maximum load level, major cracks started to appear on the tension sides of the specimens at locations near the middle of the columns. As the axial load started to drop and the lateral displacement increased, concrete on the compression sides of the column started to spall off. Furthermore, columns of 3 m height and large eccentricity of 70 mm (columns 7, 8, 10, and 11) showed minor hairline cracks at a load ratio of about 50-60% of failure load on the tension sides of the specimens. Signs of concrete crushing started to appear on the compression sides of the specimens at a load level near the maximum load.

In addition, for columns encased in lightweight aggregate concrete with 3 m height and low eccentricity of 40 mm, the cracks were observed at load ratio of 70-75% of failure load as in columns 13, 14, 15, and 16. These cracks were very little, and increased very slowly as the load increased.

5.9 Tensile Cracking of Concrete (BS 5400)

It has been recommended by the Bridge Code BS 5400: 5 [11.3.8]

that, no check for crack control need to be made in the following cases:

- a) concrete-filled hollow steel sections, or
- b) concrete-encased steel sections provided that the design axial load at the ultimate limit state is greater than $0.2 f_{cu} A_c$

where

f_{cu} the characteristic 28-day cube strength.

A_c the area of the concrete section.

Where the design axial load in concrete encased steel sections is less than the value given in (b) and tensile stresses due to bending can occur in one or more faces of the composite section, the column should be considered as a beam for the purpose of crack control.

5.10 Remarks on the Test Results

5.10.1 Casting of columns

As previously mentioned, the columns were cast horizontally and may some air pockets formed beneath the top flanges of the H steel section. However, there is no indication of any ill-effect resulting from such voids, and it seems reasonable to ignore such a fault, as it would not occur in practice where the columns are cast vertically.

5.10.2 Local spalling of concrete at the column ends

It has been indicated before that the local spalling of the concrete at the column lower end had no effect on the bearing capacity of the columns.

However, the spalling mentioned above always occurred at high load levels, and would not occur under serviceability conditions.

CHAPTER SIX
SUMMARY, CONCLUSIONS, AND
RECOMMENDATIONS

6.1 Summary

In this research, an experimental study was undertaken to investigate the behavior of lightweight aggregate concrete-encased H-shaped steel columns. The study was carried out on sixteen Full-scale pin-ended columns subjected to uniaxial bending about the major axis in single curvature, i.e. equal end eccentricities. Emphasis have been placed on investigating the following parameters:

- 1- Failure mode.
- 2- The load carrying capacity of the specimens
- 3- Strains in concrete and steel.
- 4- The load-deflection relationship.
- 5- The moment-thrust-curvature relationship.
- 6- Bond characteristics and slippage criterion.
- 7- Cracks.

The composite column specimens, had square cross sections of (230×230 mm), 4 ϕ 12 mm longitudinal reinforcing bars, one at each corner, and lateral ties ϕ 8 @ 140 mm on centers.

The main variables considered in this experimental investigation were concrete compressive strength, slenderness ratio, structural steel ratio

lightweight composite column, where 2% increase in steel ratio causes an increase in the load carrying capacity between 40-47% as in columns 1, 4, 7, and 10.

3. Lightweight concrete columns of low load eccentricity reached between 63% and 73% of the load carrying capacity of columns encased in normal concrete, while the load carrying capacity (compared to normal concrete) is almost the same for columns with large eccentricity.
4. Concrete type is of little influence on the ultimate capacity of concrete-encased composite columns of high eccentricity load. Non appreciable reduction in the carrying capacity of the composite sections was observed when lightweight aggregate concrete is used as an alternative to normal weight concrete, keeping in mind that normal weight concrete was with a higher strength than lightweight concrete. Hence, Lightweight aggregate concrete may be considered as a good choice for steel encasement that provides both economy and strength.
5. Experimental results indicated that, as the eccentricity value increases the failure loads decrease, while the lateral deflections increase.
6. Composite action between steel and lightweight aggregate concrete was confirmed in this investigation. Lightweight aggregate concrete can provide perfect bond to sections up to failure.
7. Lightweight aggregate concrete-encased composite columns exhibited limited post-peak deformation, i.e. lower displacement and lower

ductility than normal concrete or bare steel section even when the steel ratio was 4%.

8. The Ductility of concrete-encased composite columns can be improved by using Spirals instead of ties.
10. The experimental results of the composite columns indicated that the factors that most affect the strength and curvature of a particular composite column specimen are the ultimate compressive strength of concrete and its corresponding maximum compressive strain. The shape of the concrete stress distribution had minor effects on the ultimate strength and behavior of the tested columns.
11. The predicted column strengths using the two methods (AISC-LRFD and BS 5400) are on the conservative side and are in reasonable agreement with the test results.
12. The average ratio of the ultimate load capacity obtained by AISC-LRFD Code to the experimental load carrying capacity ($P_{LRFD}/N_e = 0.726$) is nearly the same or slightly lower than that obtained by Bridge Code BS 5400 ($N_{BS}/N_e = 0.731$).
13. The ACI recommendation of 0.003 as the maximum usable concrete strain appears to be an acceptable lower bound for lightweight aggregate concrete columns (Fig. 4.8).
14. The design provisions of the present code procedures; LRFD as well as BS 5400 were found to be adequate to predict the strength of

lightweight aggregate concrete-encased composite columns of brittle behavior.

15. The results obtained from the experimental tests of the lightweight aggregate concrete-encased composite column specimens provide valuable information to help in understanding the behavior of short and slender columns with different steel ratios and different eccentricities.
16. Although, the quality control of lightweight aggregate concrete is somewhat difficult, it is still valuable to replace ordinary concrete by lightweight aggregate concrete in certain cases due to its good performance and distinct advantages. Using lightweight concrete is one way of reducing the self-weight of a structure. In addition to reducing stresses through the lifetime of the structure, due to using smaller elements, the total weight of materials to be handled during construction is also reduced, which consequently increases productivity. Furthermore, lightweight concrete offers better thermal insulation and better fire protection than ordinary concrete.

6.3 Recommendations

The research on lightweight aggregate concrete-encased composite columns, which has been carried out cannot be considered as complete, therefore, it is necessary to conduct further tests in order to establish a

better understanding of the behavior of this type of structural members. For such tests the following suggestions are recommended:

1. All the tested columns were subjected to uniaxial single curvature bending with equal end eccentricities. It seems desirable to carry out more tests on column subjected to biaxial bending and unequal end eccentricities as well as columns subjected to double curvature bending.
2. Tests on columns with higher slenderness ratio, higher steel ratio, and large eccentricities still need to be carried out.
3. Further research may be carried out to include the effect of high-strength lightweight concrete on the composite column behavior, and to verify the adequacy of the existing code design provisions to determine if modifications are needed for high-strength lightweight concrete.
4. Tests on frames, with normal and high-strength lightweight concrete, where the loading of the columns will be through the actual beam to column connection could be another topic of research. Such tests will allow for the investigation of the joint as well as the beam itself.

REFERENCES

- Abo-Hamd, M. 1988. Slender Composite Beam-Columns. *Journal of Structural Engineering, ASCE*, 114 (10): 2254-2267.
- ACI 213-87, Guide for Structural Lightweight Aggregate Concrete. ACI Manual of Concrete Practice, Part 1: Materials and General Properties of Concrete, 27 PP. Detroit, Michigan, 1994.
- Al-Ryalat S. S. 1990. Load Carrying capacity of Battened Columns under Major Axis Bending. M.Sc. thesis, University of Jordan, Amman, Jordan.
- American Concrete Institute (ACI). Building Code Requirements for Structural Concrete (ACI 318M-99) and Commentary (ACI 318 RM-99). Detroit, Michigan, 1999.
- American Institute of Steel Construction. Load and Resistance Factor Design Specification for Structural Steel Buildings (AISC-LRFD). Chicago, Illinois. 1993.
- Armin, Z. Hongqiang, Y. and Fengyang, C. 1991. Study and Design of Eccentric Loaded Encased Steel Strut. Proc. 3rd. Int. Conf. *On Steel-Concrete Composite Structures*, 293-298, Fukuoka.
- Barbero, E. J. 2000. Prediction of Buckling-Mode Interaction in Composite Columns. *Journal of Mechanics of composite materials and structures*, 7: 269-284.
- Basu, A. K. 1967. Computation of Failure Loads of Composite Columns. *Proceedings, Institution of Civil Engineers*, 36: 557-578.
- Basu, A. K. and Hill, W. F. 1968. A More Exact Computation of Failure Loads of Composite Columns. *Proceedings, Institution of Civil Engineers*, 40: 37-60.

- Basu, A.K. and Sommerville, W. 1969. Derivation of Formula for the Design of Rectangular Composite Columns. *Proceedings, Institution of Civil Engineers*, Suppl. Vol. 233-280.
- Bazlamit J. 1993. *Composite Columns of Semi-Encased Sections*. M.Sc. thesis, University of Jordan, Amman, Jordan.
- Bondale, D. S. 1966. Column Theory with Special Reference to Composite Columns. *Consulting Engineer*, London, 30 (8): 43, 68-72.
- Brian, U. 2001. Local and Postlocal Buckling of Fabricated Steel and Composite Cross Section. *Journal of Structural Engineering, ASCE*, Vol. 127(6): 666-677.
- Bridge, R. Q. 1979. Composite Columns under Sustained Loads. *Journal of the Structural Division, ASCE*, 105(ST3): 563-576.
- Bridge, R. Q. 1988. The Long-term Behavior of Composite Columns. In: Buckner, D. and Viest, I. M. (editors), *Composite Construction in Steel and Concrete*, ASCE, New York.
- Bridge, R. Q. and Roderick, J. W. 1978. Behavior of Built-Up Composite Columns. *Journal of the Structural Division, ASCE*, 104 (ST7): 1141-1155.
- British Standards Instit. (BSI), Steel Concrete and Composite Bridges: Part 5: BS 5400 Code of Practice for Design of Composite Bridges. London, England, 1979.
- Burr, W. H. 1912. Composite Columns of Concrete and Steel. *Proceedings, The Institution of Civil Engineers*, Vol. 188, pp. 114-126.
- Campoine, C. Miraglia, N. and Papia, M. 2001. Mechanical Properties of Steel Fiber Reinforced Lightweight Concrete with Pumice Stone or Expanded Clay Aggregates. *Material and Structures*, Vol. 34, May,

pp 201-210.

- Cook, J. P. 1976. *Composite Construction Methods*. John Wiley & Sons, New York.
- El-Tawil S. and Deierlein G. 1999. Strength and Ductility of Concrete Encased Composite Columns. *Journal of Structural Engineering, ASCE*, 125 (9): 1009-1019.
- European Committee for Standardization. (Eurocode 4). Design of Composite Steel and Concrete Structures-Part 1: General Rules and Rules for Building, Brussels, Belgium, 1992.
- Furlong R.W. 1967. Strength of Steel-Encased Concrete Beam Columns. *Journal of Structural Division, ASCE*, 93 (ST5): 113-125.
- Furlong R.W. 1968. Design of Steel-Encased Concrete Beam-Columns. *Journal of Structural Division, ASCE*, 94 (ST1): 267-281.
- Furlong R.W. 1974. Concrete Encased Steel Columns: Design Tables. *Journal of Structural Division, ASCE*, 100 (ST9): 1865-1882.
- Furlong R.W. 1976. AISC Column Design Logic Makes Sense for Composite Columns, Too. *AISC Engineering Journal*, 13 (1st. Quarter).
- Furlong R.W. 1978. A Recommendation: Composite Columns Design Rules Consistent with Specification of the American Institute of Steel Construction. paper presented to the Structure Stability Research Council, Boston.
- Furlong R.W. 1988. Steel-Concrete Composite Columns II. In: Narayanan R. (editor), *Steel-Concrete Composite Structures: Stability and Strength*, Elsevier Applied Science Publishers LTD, London.
- Furlong, R.W. 1983. Columns Rules of ACI, SSLC, and LRFD Compared.

- Journal of Structural Engineering, ASCE*, 109 (ST10): 113-124.
- Ghannam, S. 2001. *Behavior of Lightweight Concrete-Filled Steel Tubular Columns*. Ph. D. Thesis, University of Jordan, Amman, Jordan.
- Griffis, L. G. 1986. Some Design Considerations for Composite-Frame Structures, *AISC Engineering Journal*, 2nd Quarter: 59-65.
- Hamdan M. and Hunaiti, Y. M. 1991. Factors Affecting Bond Strength in Composite Columns. Proc. 3rd Int. Conf. *On Steel-Concrete Composite Structures*, Fukuoka, 213-218.
- Hatanaka, S. Morino, S. and Kawaguchi, J. 1991. Fundamental Study on Compressive Ductility of SRS Short Columns. Proc. 3rd. Int. Conf. *On Steel-Concrete Composite Structures*, Fukuoka, 287-292.
- Hunaiti, Y. M. 1991. Bond Strength in Battened Composite Columns. *Journal of Structural Engineering, ASCE*, 117 (3): 699-714.
- Hunaiti, Y. M. 1993. Composite Columns of Semi-Encased Sections. Dirasat, J. Pure and Applied Sciences, University of Jordan, 20 B (1): 138-150.
- Hunaiti, Y. M. 1994. Aging Effect on Bond Strength in Composite Sections. *Journal of Materials in Civil Engineering, ASCE*, 6(4): 496-473.
- Hunaiti, Y. M. 1996. Composite Actions of Foamed and Lightweight Aggregate Concrete. *Journal of Materials in Civil Engineering, ASCE*, 8(3): 111-113.
- Hunaiti, Y. M. 1997. Strength of Composite Sections with Foamed and Lightweight Concrete. *Journal of Materials in Civil Engineering, ASCE*, 9(2): 58-61.
- Hunaiti, Y. M. and Abdel Fattah B. 1994. Design Considerations of

- Partially Encased Composite Columns. *Proc. Instn Civ. Engrs Structs & Bldgs*, 106, 75-82.
- Irshidat H. S., 1990. Effect of Residual Stresses on the Capacity of Battened Columns under Minor Axis Bending. MSc. thesis, University of Jordan, Amman, Jordan.
- Johnson, R. P. 1975. *Composite Structures of Steel and Concrete: Volume I Beams, Columns, Frames and Applications in Building*, Granada Publishing, London.
- Johnson, R. P. 1997. Statistical Calibrations of Safety Factors for Encased Concrete Columns. In: Buckner, D. and Shahrooz B. (editors), *Composite Construction in Steel and Concrete III*, ASCE, New York.
- Johnson, R. P. and Smith, D. G. 1980. A Simple Design Method for Composite Columns. *The Structural Engineer*, 58A(3): 85-93.
- Jones R. and Rizk A. 1963. An Investigation on the Behavior of Encased Steel Columns under Load. *The Structural Engineer*, 41(1): 21-33.
- Lachance, L. 1982. Ultimate Strength of Biaxially Loaded Composite Sections. *Journal of the Structural Division, ASCE*, 108(ST10): 2313-2329.
- MacGinley, T. J. and Ang T. C. 1995. *Structural Steelwork: Design to Limit State Theory, 2nd. edition*. Butterworth-Heinemann Ltd. London.
- McCormac J. C. 1995. *Structural Steel Design LRFD Method. 2nd. edition*. Harper Collins Publisher Inc., New York.
- Mirza A. Hyttinen V. and Hyttinen E. 1996. Physical Tests and Analysis of Composite Steel-Concrete Beam-Columns. *Journal of Structural Engineering, ASCE*, 122(11): 1317-1326.

- Mirza, S. A. and Skrabek, B. W. 1991. Reliability of Short Composite Beam-Column Strength Interaction. *Journal of Structural Engineering, ASCE*, 117(8): 2320-2339.
- Mirza, S. A. and Skrabek, B. W. 1992. Statistical Analysis of Slender Composite Beam-Column Strength. *Journal of Structural Engineering, ASCE*, 118(5): 1312-1332.
- Munoz, P. R. and Hsu C. H. 1997a. Behavior of Biaxially Loaded Concrete-Encased Composite Columns. *Journal of Structural Engineering, ASCE*, 123(9): 1163-1171.
- Munoz, P. R. and Hsu C. H. 1997b. Biaxially Loaded Concrete-Encased Composite Columns: Design Equation. *Journal of Structural Engineering, ASCE*, 123(12): 1576-1585.
- Neville, A. M. 2000. *Properties of Concrete. 4th. edition*, Prentice Hall, London.
- Odeh H. M. 1993. *Behavior Study of Lightweight Concrete Structure with Pumice and Perlite*. M.Sc. Thesis, University of Jordan, Amman, Jordan.
- Park, R. and Paulay, T. 1975, *Reinforced Concrete Structures*, John Wiley & Sons, Inc. New York.
- Pinkham, C. W. 1988. 1986 AISC LRFD Design for Composite Buildings. In: Buckner, D. and Viest, I. M. (editors), *Composite Construction in Steel and Concrete*, ASCE, New York.
- Portland Cement Associations (PCA), *Special Concretes and Concrete Products*, John Wiley & Sons, Inc. New York, 1975.
- Proctor, A. N. 1967. Full Size Test Facilitate Derivation of Reliable Design Methods. *Consulting Engineer*, London, 31(8): 54-55, 57-58, 60.

- Robert, E. H. and Yam, L. P. 1983. Some Recent Methods for the Design of Steel, Reinforced Concrete, and Composite Steel-Concrete Columns in the U.K. *ACI Journal*, 80 (15): 139-149.
- Roderick, J. W. 1972. Further Studies of Composite Steel and Concrete Structures. Preliminary Report, International Association for Bridge and Structural Engineering, *Ninth Congress*, Amsterdam, 165-172.
- Roderick, J. W. and Rogers, D. F. 1969. Load Carrying Capacity of Simple Composite Columns. *Journal of the Structural Division, ASCE*, 95(ST2): 209-228.
- Roik, K. and Bergmann, R. 1989. Report in Eurocode 4: Clause 4.8 and 4.9 Composite Columns. EC4/6/89, Minister für Raumordnung, Bauwesen, und Stadtegbau der Bundesrepublik Deutschland, Bonn, Germany.
- Roik, K. and Bergmann, R. 1992. Composite Column. In: Dowling P. et al. (editors), *Constructional Steel Design*, Elsevier Applied Science Publishers LTD, London.
- Sabalieish, A. 1988. The Feasibility of Producing and Developing Lightweight Concrete from Local Jordanian Raw Materials. Rep. (in Arabic), Royal Scientific Society (RSS), Amman, Jordan.
- Salmon, C. G. and Johnson, J. E. 1996. *Steel Structures: Design and Behavior, Emphasizing LRFD. 4th. edition*. Harper Collins College Publishers, New York.
- Saw, H. S. and Liew, J. R. 2000. Assessment of Current Methods for the Design of Composite Columns in Buildings. *Journal of Constructional Steel Research*, 53:121-147.
- Shakir-Khalil, H. 1988. Composite in Multi-Story Structure. In: Buckner, D. and Viest, I. M. (editors), *Composite Construction in Steel and*

- Concrete*, ASCE, New York.
- Shakir-Khalil, H. 1988. Steel-Concrete Composite Columns I. In: Narayanan R. (editor), *Steel-Concrete Composite Structures: Stability and Strength*, Elsevier Applied Science Publishers LTD, London.
- Sharif, R. L. 1988. The Use of Pozzolans for Lightweight Concrete in Jordan. *Dirasat, J. Pure and Appl. Sciences*, University of Jordan, XV (6): 94-111.
- Short, A. 1978. *Lightweight Concrete. 3rd. edition*, Applied Science Publishers, London.
- Smith, D. G. E. 1980. Composite Columns with Lightweight Concrete Casing. *The Structural Engineer*, 58A(8): 246-248.
- Spratt B. H. 1974. *The Structural Use of Lightweight Aggregate Concrete. 1st. edition*, Cement and Concrete Association, London.
- SSRC 1998. Composite Columns and Structural Systems. In: Galambos, T. V. (editor), *Guide to Stability Design Criteria for Metal Structures. 5th edition*. John Wiley & Sons, Inc. New York.
- SSRC Task Group 20, 1979. A Specification for the Design of Steel-Concrete Composite Columns. *AISC Engineering Journal*, 16, 4th. Quarter: 101-115.
- Stark, J. B. 1988. Eurocode 4: A European Code for Composite Construction, In: Buckner, D. and Viest, I. M. (editors), *Composite Construction in Steel and Concrete*, ASCE, New York.
- Stevens, R. S. 1965. Encased Stanchions. *The Structural Engineer*, 43 (2): 59-66.
- Videla, C. and López, M. 2000. Mixture Proportioning Methodology for Structural Sand Lightweight Concrete. *ACI Materials Journal*, Vol.

- 97, No. 3 May-June: 281-289.
- Viest, I. M., 1974. Composite Steel-Concrete Construction. *Journal of the Structural Division, ASCE*, 100(ST5): 1085-1139.
- Virdi, K. S. And Dowling, P. J. 1973. The Ultimate Strength of Composite Columns in Biaxial Bending. *Proc. Instn. Civil Engineers*, Part 2, 55, Mar. 251-272.
- Virdi, K. S. And Dowling, P. J. 1976. The Ultimate Strength of Biaxially Restrained Columns. *Proc. Instn. Civil Engineers*, Part 2, 61, Mar. 41-58.
- Wakabayashi, M. 1980. Standards for the Design of Concrete Encased-Steel and Concrete-Filled Tubular structures in Japan. *Proc. U.S.-Japan Sem. Compos. Struct. Mixed Struct. Sys.*, Gihodo Shuppan, Tokyo, pp. 69-84.
- Walter, P. M. 1988. An Overview of Composite Construction in the United States. In: Buckner, D. and Viest, I. M. (editors), *Composite Construction in Steel and Concrete*, ASCE, New York.
- Wang, C. K. and Salmon, C. G. 1998. *Reinforced Concrete Design*. 6th. edition, Harper & Row, Publisher, New York.
- Yam, L. C. 1981. *Design of Composite Steel-Concrete Structures*, 1st. edition. Surrey University Press, London.

APPENDIX A

Illustrative Example

A.1 Introduction

The purpose of this section is to illustrate, by means of numerical example, the application of the design methods of composite columns given in chapter three. The design calculations comply with the Load and Resistance Factor Design method (AISC-LRFD, 1993) and Bridge Code method (BS 5400: part 5: 1979). It should be noted that the symbols used in this example are identical to these in the codes.

A.2 Design Data and Column Properties

The pin-ended composite column shown in Fig. A.1 is subjected to uniaxial bending about the major axis, with an eccentricity of 40 mm at both ends; calculate the load carrying capacity of the column using the AISC-LRFD and the Bridge Code BS 5400 methods.

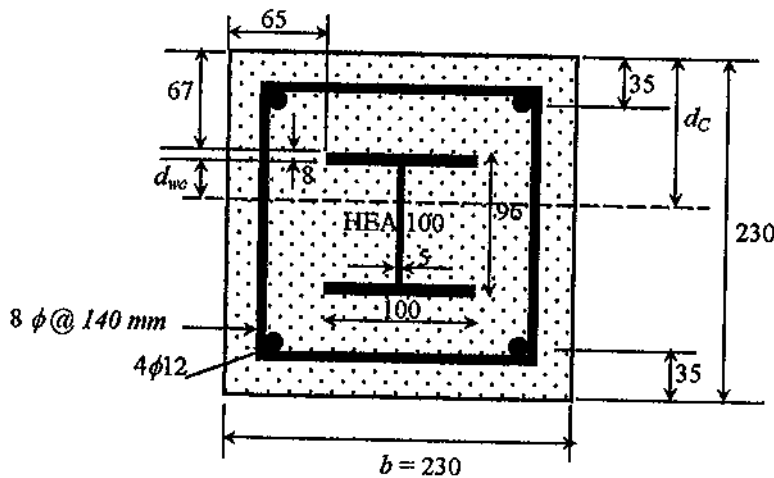


Figure A.1 Column Cross-Section of the Example (Column No. 16)

Effective length	$l =$	2080	mm
Composite column dimension	$h, b =$	230×230	mm
Structural steel: HEA 100	$f_y =$	337	MPa
	$E_s =$	200000	MPa
	$A_s =$	2120	mm ²
	$I_{sx} =$	3.49 × 10 ⁶	mm ⁴
	$I_{sy} =$	1.34 × 10 ⁶	mm ⁴
	$d =$	96	mm
	$b_f =$	100	mm
	$t_f =$	8.0	mm
	$t_w =$	5.0	mm
	Reinforcement: 4φ12 high-yield bars	$f_{ry} =$	459
$E_r =$		200000	MPa
Concrete: 28-day characteristic cube strength cylinder strength $f'_c = 0.8 \times f_{cu}$	$f_{cu} =$	9.7	MPa
	$f'_c =$	6.76	MPa
	$w =$	1494	kg/m ³

A.3 Preliminary calculations

$A_r = 4(\pi D^2/4) = \pi(12.16)^2$	$A_r =$	464.53	mm ²
$I_{rx} = A_r(h/2 - c_r)^2 = 464.5(230/2 - 35)^2$	$I_{rx} =$	2.973 × 10 ⁶	mm ⁴
$I_{ry} = I_{rx}$	$I_{ry} =$	2.973 × 10 ⁶	mm ⁴
$A_c = A_{cg} - A_s - A_r = 230 \times 230 - 2120 - 464.5$	$A_c =$	50315.5	mm ²
$I_{cx} = I_{cgx} - I_{sx} - I_{rx}$ $= 230 \times 230^3/12 - 3.49 \times 10^6 - 2.973 \times 10^6$	$I_{cx} =$	2.2674 × 10 ⁸	mm ⁴
$I_{cy} = I_{cgy} - I_{sy} - I_{ry}$ $= 230 \times 230^3/12 - 1.34 \times 10^6 - 2.973 \times 10^6$	$I_{cy} =$	2.289 × 10 ⁸	mm ⁴

A.4 Design of Columns According to AISC-LRFD Method

- Modulus of elasticity of concrete, $E_c = (0.043) w_c^{1.5} \sqrt{f'_c}$

$$= (0.043) 1494^{1.5} \sqrt{9.7 \times 0.8} = 6917.12 \text{ MPa}$$

- Check structural steel ratio to gross column area

$$A_s/A_g = [2120/(230 \times 230)] \times 100 = 4\% \quad \text{OK (Composite)}$$

- Area of lateral ties and longitudinal reinforcement each must be at least $0.178 \text{ mm}^2/\text{mm}$ ($0.007 \text{ in}^2/\text{in}$) of bar spacing.

- Minimum required Area of lateral ties $= \pi D^2/4 = 0.178 \times 140 = 24.92 \text{ mm}^2$, hence, minimum required tie diameter =

$$\sqrt{4 \times 24.92 / \pi} = 5.6 \text{ mm} \quad \text{OK (the used tie diameter} = 8 \text{ mm)}$$

- Minimum required area of long. reinf. $= \pi D^2/4 = 0.178 \times 160 = 28.48 \text{ mm}^2$, hence, minimum required long. reinf. dia. =

$$\sqrt{4 \times 28.48 / \pi} = 6.02 \text{ mm} \quad \text{OK (the used long. reinf. dia.} = 12 \text{ mm)}$$

A.4.1 Nominal axial capacity of the column, P_n

A.4.1.1 Modified yield stress, F_{my}

$$F_{my} = F_y + c_1 F_{yr} \frac{A_r}{A_s} + c_2 f'_c \frac{A_c}{A_s}$$

$$F_{my} = 337 + 0.7 \times 459 \frac{464.53}{2120} + 0.6 \times 7.76 \frac{50315.5}{2120} = 517.91 \text{ MPa}$$

A.4.1.2 Modified radius of gyration, r_m

$$r_m = \max. (r, 0.3h_t)$$

$$r(\text{steel}) = \sqrt{\frac{I_{sy}}{A_s}} = \sqrt{\frac{1340000}{2120}} = 25.14 \text{ mm}$$

$$0.3h_f = 0.3 \times 230 = 69 \text{ mm}$$

hence, $r_m = 69 \text{ mm}$

A.4.1.3 Modified modulus, E_m

$$E_m = E + c_3 E_c \frac{A_c}{A_s}$$

$$E_m = 200 \times 10^3 + 0.2 \times 6917.12 \frac{50315.5}{2120}$$

$$E_m = 232.834 \times 10^3 \text{ MPa}$$

A.4.1.4 Slender parameter, λ_c

$$\lambda_c = \sqrt{\frac{F_y}{F_e}} = \frac{kl}{r_m \pi} \sqrt{\frac{F_{my}}{E_m}} = \frac{1 \times 2080}{69 \times \pi} \sqrt{\frac{517.91}{232.834 \times 10^3}} = 0.452552$$

$\lambda_c < 1.5$, hence, Plastic buckling

The design axial compressive strength of steel columns is given as:

$$P_u = \phi_c P_n$$

where $\phi_c = 0.85$, and $P_n = A_s F_{cr}$.

If $\lambda_c \leq 1.5$, $F_{cr} = (0.658^{\lambda_c^2}) F_{my}$

$$P_n = A_s (0.658^{\lambda_c^2}) F_{my}$$

$$P_n = 2120 (0.658^{0.452552^2}) 517.91 = 1008 \text{ kN}$$

A.4.2 Nominal flexural strength, M_n

$$M_{nx} = ZF_y + \frac{1}{3}(h_2 - 2c_r)A_r F_{yr} + \left(\frac{h_2}{2} - \frac{A_w F_y}{1.7 f'_c h_1} \right) A_w F_y \quad (\text{LRFD C-I4-1})$$

$$\begin{aligned} M_{nx} &= 83000 \times 337 + \frac{1}{3}(230 - 2 \times 35)464.53 \times 459 + \left(\frac{230}{2} - \frac{96 \times 5 \times 337}{1.7 \times 7.76 \times 230} \right) 96 \times 5 \times 337 \\ &= 49.3 \text{ kN.m} \end{aligned}$$

A.4.3 Equation of axial load and bending about major axis

$$\text{For } \frac{P_u}{\phi P_n} \geq 0.2$$

$$\frac{P_u}{\phi P_n} + \frac{8}{9} \left(\frac{M_{ux}}{\phi_b M_{nx}} \right) \leq 1.0 \quad (\text{LRFD Eq. H2-1a})$$

For comparison purpose with the experimental failure load, the reduction factors, ϕ and ϕ_b , are taken as unity.

$$M_{ux} = \beta_1 M_{nx} = \beta_1 \cdot P_u \cdot e_x$$

$$\beta_1 = C_m / (1 - P_u / P_e) \geq 1$$

$$C_m = 0.6 - 0.4 M_1 / M_2$$

In this example $M_1 / M_2 = -1$ (equal end moments and single curvature)

$$\text{hence, } C_m = 0.6 - 0.4(-1) = 1$$

$$P_e = A_s F_{my} / \lambda_c^2$$

$$P_e = 2120 \times 517.91 / 0.452552^2 = 5361.09 \text{ kN}$$

Try $P_u = 556.5 \text{ kN}$ and substitute in interaction equation to see if both sides are equal, if not decrease or increase P_u , till both sides be equal.

$$\beta_1 = 1/(1-556.5/5361.09) = 1.116 \geq 1 \quad \text{OK}$$

$$\frac{P_u}{\phi P_n} = \frac{556.5}{1 \times 1007.77} = 0.5522 \geq 0.2 \quad \text{hence, use LRFD Eq. H2-1a}$$

$$\frac{P_u}{\phi P_n} + \frac{8}{9} \left(\frac{M_{ux}}{\phi_b M_{nx}} \right) \leq 1.0$$

$$\frac{556.5}{1 \times 1007.77} + \frac{8}{9} \left(\frac{1.116 \times 556.5 \times 0.04}{1 \times 49.32} \right) \leq 1.0$$

$$0.99994 = 1 \quad (\text{both sides are equal}) \quad \text{OK}$$

Hence, the ultimate load of the column, $P_u = 556.5 \text{ kN}$

The experimental failure load of the column, $N_e = 680 \text{ kN}$

The ratio of the calculated ultimate load to the experimental load

$$(P_u)_{\text{LRFD}} / N_e = 556.5/680 = 0.82.$$

A.5 Design of Columns According to BS 5400: part 5: 1979

Modulus of elasticity of concrete, $E_c = 670 f_{cu} = 670 \times 9.7 = 6499 \text{ MPa}$

A.5.1 Calculation of the squash load, N_u

$$N_u = A_s f_y + A_r f_{ry} + 0.67 A_c f_{cu}$$

$$N_u = [2120 \times 337 + 464.53 \times 459 + 0.67 \times 50315.5 \times 9.7] \times 10^{-3} = 1254.66 \text{ kN}$$

Note that all material partial safety factors was taken as unity for comparison purpose with experimental results.

- Concrete contribution factor

$$\alpha_c = \frac{A_c f_{ck}}{N_u \gamma_{mc}} = \frac{0.67 A_c f_{cu}}{N_u} \quad (\gamma_{mc} = 1 \text{ and } f_{ck} = 0.67 f_{cu})$$

$$\alpha_c = \frac{0.67 A_c f_{cu}}{N_u} = \frac{0.67 \times 50315.5 \times 9.7}{1254.66 \times 10^3} = 0.26063, 0.15 < \alpha_c < 0.8 \quad \text{OK}$$

$$l/b = 2080/230 = 9.04 < 12 \quad (\text{If no bending then } N_{ax} = 0.85N_u)$$

A.5.2 Ultimate moment of resistance, M_u

$$\rho = 0.6f_{cu}/f_y = 0.6 \times 9.7/337 = 0.01727$$

A.5.2.1 Plastic neutral axis in web/major axis bending (Fig. 3.7)

Provided that $(A_s - 2b_f t_f) > \rho [bd_s + t_f(b - b_f)]$

$$= 2120 - 2 \times 100 \times 8 > 0.0173 [230 \times 67 + 8(230 - 100)]$$

$$520 > 284.6 \quad \text{OK}$$

hence,
$$d_c = \frac{ht_w}{(b\rho + 2t_w)}$$

$$= \frac{230 \times 5}{(230 \times 0.01727 + 2 \times 5)} = 82.31 \text{ mm} > d_s + t_f = 75 \text{ mm} \quad \text{OK}$$

$$d_w = d_c - (d_s + t_f) = 82.31 - 75 = 7.31 \text{ mm}$$

$$M_{ux} = 0.91 f_y \left[A_s \frac{(h - d_c)}{2} - b_f t_f (d_s - d_w) - t_w d_w (d_c - d_w) \right] + 0.87 f_y \frac{A_r}{2} d_r$$

Material partial safety factors taken as unity for comparison purpose with experimental results ($\gamma_{ms}, \gamma_{mr}, \gamma_{mc} = 1$)

$$= 337 \left[2120 \frac{(230 - 82.31)}{2} - 100 \times 8(67 - 7.31) - 8 \times 7.3(82.31 - 7.31) \right] + 459 \frac{464.53}{2} 160$$

$$M_{ux} = 52.8 \text{ kN.m}$$

A.5.2.2 Plastic neutral axis in flange/minor axis bending (Fig. 3.8)

This condition arises when:

$$\rho b d_s < A_s = 0.01727 \times 230 \times 65 = 258 \text{ mm}^2 < 2120 \quad \text{OK, then}$$

$$d_c = \frac{A_s + 4t_f d_s}{b\rho + 4t_f} = \frac{2120 + 4 \times 8 \times 65}{230 \times 0.0173 + 4 \times 8} = 116.8 \text{ mm, and}$$

$$M_{wy} = 0.91f_y \left[A_s \frac{(h - d_c)}{2} - 2t_f d_s (d_c - d_s) \right] + 0.87f_y \frac{A_r}{2} d_r$$

$$\begin{aligned} M_{wy} &= 337 \left[2120 \frac{(230 - 116.8)}{2} - 2 \times 8 \times 65(116.8 - 65) \right] + 459 \frac{464.53}{2} 160 \\ &= 39.37 \text{ kN.m} \end{aligned}$$

A.5.3 Calculation of the ultimate load carrying capacity

A.5.3.1 Major axis bending

- Design parameters

- k_{1x} :

$$\lambda_x = \frac{l_{ex}}{l_E}$$

$$l_E = \pi \sqrt{\frac{E_c I_{c+} + E_s I_{s+} + E_r I_r}{N_u}}$$

$$l_E = \pi \sqrt{\frac{6499 \times 2.27 \times 10^8 + 200 \times 10^3 \times 3.49 \times 10^6 + 200 \times 10^3 \times 2.973 \times 10^6}{1254.66 \times 10^3}}$$

$$l_E = 4664.73 \text{ mm}$$

$$\lambda_x = \frac{l_{ex}}{l_E} = \frac{2080}{4664.73} = 0.4459$$

From column buckling curve selection chart

$$d/b_f = 96/100 = 0.96 < 1.2, \text{ Use curve b (Table 13.2 BS 5400)}$$

$$\text{For } \lambda_x = 0.4459, \quad k_{1x} = 0.9066$$

$$\beta = 1 \quad C_4 = 120$$

▪ k_{20x} , k_{2x} , and k_{3x} :

$$k_{20x} = 0.9\alpha_c^2 + 0.2 = 0.9(0.2606)^2 + 0.2 = 0.2611 < 0.75 \quad \text{OK}$$

$$k_{2x} = k_{20} \left[\frac{90 - 25(2\beta - 1)(1.8 - \alpha_c) - C_4 \lambda_x}{30(2.5 - \beta)} \right]$$

$$k_{2x} = 0.2611 \left[\frac{90 - 25(2 \times 1 - 1)(1.8 - 0.2606) - 120 \times 0.4459}{30(2.5 - 1)} \right]$$

$$k_{2x} = -0.01156 \quad \text{and} \quad 0 < k_{2x} < k_{20x}, \text{ hence, } k_{2x} = 0$$

Since bending about the strong axis is being considered ($\lambda_x < \lambda_y$; see λ_y

below), hence, $k_{3x} = 0$

$$N_x = \frac{k_{1x} N_u}{[1 + (k_{1x} - k_{2x})(N_u \cdot e_x / M_{ux})]}$$

$$N_x = \frac{0.9066 \times 1254.66}{[1 + (0.9066 - 0)(1254.66 \times .04 / 52.78)]} = 610.98 \text{ kN}$$

Note: For column subjected to uniaxial bending about the major axis and not restrained against failure about the minor axis, the ultimate load-carrying capacity should be taken as equal to that of a column subjected to biaxial bending with the minimum applied moment about the minor axis, i.e.: $M_y = 0.03 b N_u$.

A.5.3.2 Minor axis bending

- Design parameters

- k_{ly} :

$$\lambda_y = \frac{l_{ey}}{l_E}$$

$$l_E = \pi \sqrt{\frac{E_c I_{ct} + E_s I_{st} + E_r I_r}{N_u}}$$

$$l_E = \pi \sqrt{\frac{6499 \times 2.289 \times 10^8 + 200 \times 10^3 \times 1.34 \times 10^6 + 200 \times 10^3 \times 2.973 \times 10^6}{1254.66 \times 10^3}}$$

$$l_E = 4300.3 \text{ mm}$$

$$\lambda_y = \frac{l_{ey}}{l_E} = \frac{2080}{4300.3} = 0.4837$$

From column buckling curve selection chart

$$d/b_f = 96/100 = 0.96 < 1.2, \text{ Use curve c (Table 13.3 BS 5400)}$$

$$\text{For } \lambda_y = 0.4837, \quad k_{ly} = 0.8536$$

$$\beta = 1 \quad C_4 = 140$$

- $k_{20y}, k_{2y}, k_{3y}, \text{ and } k_{4y}$:

$$k_{20y} = 0.9\alpha_c^2 + 0.2 = 0.9(0.2606)^2 + 0.2 = 0.2611 < 0.75 \quad \text{OK}$$

$$k_{2y} = k_{20y} \left[\frac{90 - 25(2\beta - 1)(1.8 - \alpha_c) - C_4 \lambda_x}{30(2.5 - \beta)} \right] \quad \mathbf{557056}$$

$$k_{2y} = 0.2611 \left[\frac{90 - 25(2 \times 1 - 1)(1.8 - 0.2606) - 140 \times 0.484}{30(2.5 - 1)} \right]$$

$$k_{2y} = -0.0941 \quad \text{and} \quad 0 < k_{2y} < k_{20y}, \text{ hence, } k_{2y} = 0$$

$$k_{3y} = 0.425 - 0.075 \beta_y - 0.005 C_4 \lambda_y$$

$$= 0.425 - 0.075 \times 1 - 0.005 \times 140 \times 0.4837 = 0.0114$$

and should be taken between the limits:

$$(0.2 - 0.25 \alpha_c) \geq k_{3y} \geq -0.03 (1 + \beta_y)$$

$$(0.2 - 0.25 \times 0.2606) \geq k_{3y} \geq -0.03 (1 + 1)$$

$$0.135 \geq k_{3y} \geq -0.06$$

hence, $k_{3y} = 0.0114$

$$k_4 = 1 + (k_{1y} - k_{2y} - 4k_{3y})(N_u \cdot e_y / M_{uy})$$

$$= 1 + (0.8536 - 0 - 4 \times 0.0114)(1254.66 \times 0.03 \times 0.230 / 39.37)$$

$$= 1.1777$$

$$N_y = \frac{-k_4 + \sqrt{k_4^2 + 16k_{1y}k_{3y}(N_u \cdot e_y / M_{uy})^2}}{8k_{3y}(N_u \cdot e_y / M_{uy})^2} N_u$$

$$N_y = \frac{-1.1777 + \sqrt{1.1777^2 + 16 \times 0.8536 \times 0.0114 (1254.66 \times 0.03 \times 0.23 / 39.37)^2}}{8 \times 0.0114 (1254.66 \times 0.03 \times 0.23 / 39.37)^2} N_u$$

$$= 0.72383 \times 1254.66$$

$$= 908.16 \text{ kN}$$

$$N_{ax} = k_{1x} N_u = 0.9066 \times 1254.66 = 1137.48$$

A.5.3.3 Biaxial bending

$$\frac{1}{N_{xy}} = \frac{1}{N_x} + \frac{1}{N_y} - \frac{1}{N_{ax}}$$

$$\frac{1}{N_{xy}} = \frac{1}{610.98} + \frac{1}{908.16} + \frac{1}{1137.48}$$

$$N_{xy} = 538. \text{ kN}$$

Hence, the ultimate load of the column, $N_{xy} = 538 \text{ kN}$

The experimental failure load of the column, $N_e = 680 \text{ kN}$

The ratio of the calculated ultimate load to the experimental load

$$(N_{xy})_{BS} / N_e = 538/680 = 0.79.$$

سلوك الأعمدة الفولاذية المركبة المغلفة بالخرسانة الخفيفة

إعداد

عبّاس محمد علي الشّهاري

إشراف

الأستاذ الدكتور بسّام أبوغزالة

ملخص

الأعمدة الفولاذية المغلفة هي أحد الأنماط الشائعة للأعمدة المركبة. هذا النظام يجمع بين الصلابة وقابلية التشكيل للخرسانة المسلحة و بين القوة وسرعة الإنشاء للفولاذ الإنشائي للوصول إلى منشأ إقتصادي. هذه الأعمدة المركبة المغلفة بالخرسانة لم تتلقَ نفس مستوى الاهتمام الذي لقيته الأعمدة الفولاذية أو الخرسانية المسلحة. وعلى الرغم من شيوع هذا النمط، فإن الدراسات التجريبية التي أجريت على الأعمدة المركبة المغلفة بالخرسانة الخفيفة قليلة جداً. علاوة على ذلك، فإن بعض الكودات لها اشتراطات خاصة على استخدام الخرسانة الخفيفة.

لقد تم إجراء دراسة تجريبية على أعمدة فولاذية مغلفة بالخرسانة الخفيفة لدراسة سلوكها وتصرفها تحت تأثير الأحمال اللامركزية. هذه الدراسة تهدف إلى التحقق من صلاحية هذا النوع من الخرسانة في الإنشاءات المركبة وكذلك التأكد من كفاية وملاءمة كود المعهد الأمريكي للإنشاءات الفولاذية AISC-LRFD وكذلك كود الجسور البريطاني BS-5400 في احتساب مقاومة هذه الأعمدة. ولتحقيق هذا الهدف فقد أجريت تجارب عملية على ستة عشر عموداً مفصلية النهايات (Pin-ended)، ذات مقاسات طبيعية (Full-scale)، عُرضت لحمل محوري ضاغط وعزم حول المحور الرئيسي حتى الإنهيار. تسعة من هذه الأعمدة عُلفت بخرسانة خفيفة الركام و ثلاثة عُلفت بخرسانة عادية بينما أربعة اختبرت كأعمدة فولاذية مجردة لأغراض المقارنة. تم اختبار تأثير نسبة النحافة، لامركزية الحمل المسلط، خواص الخرسانة، وكذلك نسبة مساحة فولاذ الإنشاء على سلوك و قدرة تحمل الأعمدة. وتم دراسة علاقة الحمل بالترخيم وعلاقة العزم بالتقوس وخاصية التماسك بين الخرسانة والفولاذ إضافة إلى أنماط الإنهيار وكذلك تشقق الخرسانة.

أظهرت نتائج الاختبارات أنّ تغليف أعمدة الفولاذ بالخرسانة الخفيفة قد زاد قدرة تحمل أعمدة الفولاذ زيادة كبيرة ولكن قلت مرونتها. كما أن قدرة تحمل الخرسانة الخفيفة نوع (A) يصل إلى 73% بينما نوع (B) يصل إلى 63% من تحمل الخرسانة العادية بالنسبة للأعمدة منخفضة اللامركزية، أما الأعمدة عالية اللامركزية، فإن قدرة تحمل الخرسانة الخفيفة والعادية متساوية تقريباً. علاوة على ذلك، فقد تبين أن الخرسانة خفيفة الركام ذات ترابط مثالي مع مقاطع الفولاذ حتى مرحلة الإنهيار. كما أن

نسبة مساحة الفولاذ الإنشائي إلى المساحة الإجمالية للعمود لها تأثير مهم أيضاً على قدرة تحمل الأعمدة المركبة. حيث أن زيادة 2% من نسبة الفولاذ أدت إلى زيادة في قدرة التحمل تصل إلى 47%. كذلك تبين أن شروط وخطوات التصميم لكود المعهد الأمريكي للإنشاءات الفولاذية AISC-LRFD وكذلك لكود الجسور البريطاني BS-5400 المتوفرة حالياً كافية لاحتساب مقاومة الأعمدة المركبة المغلفة بالخرسانة خفيفة الركام. كما تبين أيضاً أن مقاومة الأعمدة المحسوبة بالطريقتين كانت إلى جانب الأمان وبتوافق معقول مع نتائج الاختبارات. لذلك على الرغم من أن السيطرة على جودة الخرسانة الخفيفة صعبة إلى حد ما، فإنه من المفيد استبدال الخرسانة العادية المغلفة للأعمدة الفولاذية بالخرسانة الخفيفة في بعض الحالات لأدائها الجيد وفوائدها المتميزة.